AD-A156 139 TARGET OBSERVABILITY FOR SATELLITE-BASED SENSORS(U) 1/2
NAVAL POSTGRADUATE SCHOOL MONTEREY CA R E BOND MAR 85

UNCLASSIFIED F/G 17/7 NL

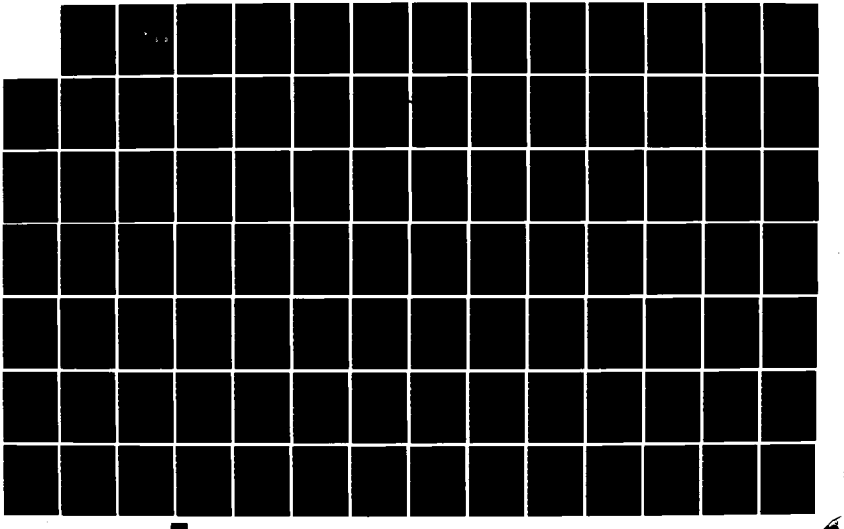

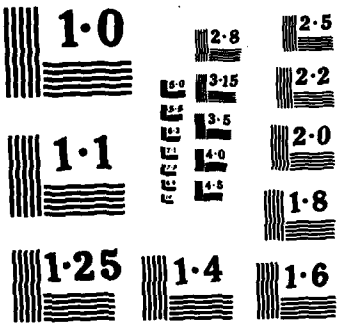

NATIONAL BUREAU OF STANDARDS
MICROCOPY RESOLUTION TEST CHART

(2)

NAVAL POSTGRADUATE SCHOOL
Monterey, California

THESIS

TARGET OBSERVABILITY
FOR
SATELLITE-BASED SENSORS

by

Robert E. Lee Bond

March 1985

Thesis Advisor: R. R. Mohler

Approved for public release; distribution unlimited.

SECURITY CLASSIFICATION OF THIS PAGE (When Data Entered)

REPORT DOCUMENTATION PAGE		READ INSTRUCTIONS BEFORE COMPLETING FORM
1. REPORT NUMBER	2. GOVT ACCESSION NO. AD-A156 139	3. RECIPIENT'S CATALOG NUMBER
4. TITLE (and Subtitle) Target Observability for Satellite-Based Sensors		5. TYPE OF REPORT & PERIOD COVERED Master's Thesis; March 1985
		6. PERFORMING ORG. REPORT NUMBER
7. AUTHOR(s) Robert E. Lee Bond		8. CONTRACT OR GRANT NUMBER(s)
9. PERFORMING ORGANIZATION NAME AND ADDRESS Naval Postgraduate School Monterey, California 93943		10. PROGRAM ELEMENT, PROJECT, TASK AREA & WORK UNIT NUMBERS
11. CONTROLLING OFFICE NAME AND ADDRESS Naval Postgraduate School Monterey, California 93943		12. REPORT DATE March 1985
		13. NUMBER OF PAGES 129
14. MONITORING AGENCY NAME & ADDRESS(if different from Controlling Office)		15. SECURITY CLASS. (of this report) UNCLASSIFIED
		15a. DECLASSIFICATION/DOWNGRADING SCHEDULE

16. DISTRIBUTION STATEMENT (of this Report)

Approved for public release; distribution unlimited.

17. DISTRIBUTION STATEMENT (of the abstract entered in Block 20, if different from Report)

18. SUPPLEMENTARY NOTES

19. KEY WORDS (Continue on reverse side if necessary and identify by block number)

Nonlinear Observability; Satellite-Based Sensors; Extended Kalman Filter

20. ABSTRACT (Continue on reverse side if necessary and identify by block number)

The purpose of this thesis is to discuss the observability of targets moving on or near the Earth's surface when viewed from space by an orbiting satellite. A simplified derivation of the satellite's orbital mechanics is undertaken, which taken in conjunction with a description of the target's motion allows for the derivation of a system of relative coordinates. An observability analysis is then

DD FORM 1 JAN 73 1473 EDITION OF 1 NOV 65 IS OBSOLETE

S/N 0102-LF-014-6601

SECURITY CLASSIFICATION OF THIS PAGE (When Data Entered)

performed on the resulting series of nonlinear equations, which in turn forms the basis for the design of a deterministic nonlinear observer and an Extended Kalman Filter to track the target.

Accession For	
NTIS GRA&I	X
DTIC TAB	☐
Unannounced	☐
Justification	
By	
Distribution/	
Availability Codes	
Dist	Avail and/or Special
A/1	

Approved for public release; distribution is unlimited.

Target Observability for Satellite-Based Sensors

by

Robert E. Lee Bond
Lieutenant, United States Navy
B.S. Systems Engineering, U.S. Naval Academy, 1979

Submitted in partial fulfillment of the requirements for the degree of

MASTER OF SCIENCE IN ELECTRICAL ENGINEERING

from the

NAVAL POSTGRADUATE SCHOOL
March 1985

Author: _____
Robert E. Lee Bond

Approved by: _____
R. R. Mohler, Thesis Advisor

_____
P. H. Moose, Second Reader

_____
Harriett Rigas, Chairman, Department of Electrical and Computer Engineering

_____
J. N. Dyer,
Dean of Science and Engineering

ABSTRACT

The purpose of this thesis is to discuss the observability of targets moving on or near the earth's surface when viewed from space by an orbiting satellite. A simplified derivation of the satellite's orbital mechanics is undertaken, which taken in conjunction with a description of the target's motion allows for the derivation of a system of relative coordinates. An observability analysis is then performed on the resulting series of nonlinear equations, which in turn forms the basis for the design of a deterministic nonlinear observer and an Extended Kalman Filter to track the target. -> cont. keywords include: see 1473

TABLE OF CCNTENTS

LIST OF TABLES

LIST OF FIGURES

ACKNOWLEDGEMENT

tc Jackie and Beth

TABLE II

GSW as a Function of Altitude

h	Θ	GSW
150 nm	33.2°	1995 nm
600 nm	63.4°	3796 nm
2250 nm	105.6°	6338 nm
5600 nm	135.3°	8118 nm
10900 nm	152.3°	9136 nm
19322 nm	162.7°	9760 nm
∞	180°	10800 nm

The second aspect of swath width is minimum swath width (MSW) required for coverage, as a function of the number of revolutions per day. Because the swaths cut by a satellite in a circular orbit are most widely spread as it crosses the equator, this simply means computing n, the number of equator crossings per day, and then swath angle is defined as

$$\Theta_s = 360^\circ / n \qquad (2.11)$$

where

$$n = \frac{(24\ \text{HRS})\,GM}{2\pi (r_e + h)^{3/2}} = \frac{344\,0000\ \text{nm}^{3/2}}{(r_e + h)^{3/2}}$$

so

$$\Theta_s = (1.05 \times 10^{-4})^\circ \left[\frac{r_e + h}{\text{nm}}\right]^{3/2} \qquad (2.12)$$

Taking into account both the ascending and descending trajectories, the typical satellite orbit can actually be considered to cross the equator twice per revolution (see Figures 2.3 and 2.4), and so $\Theta_s/2$ is a sufficient swath width to ensure coverage along the entire equator, which is of course a worst-case approach for achieving coverage of

satellites, are the related concepts of swath width and revisit time interval. Swath width relates directly to that area viewed by the satellite as it passes overhead; revisit time is the measure of how frequently a particular point on the ground is in view from a passing satellite.

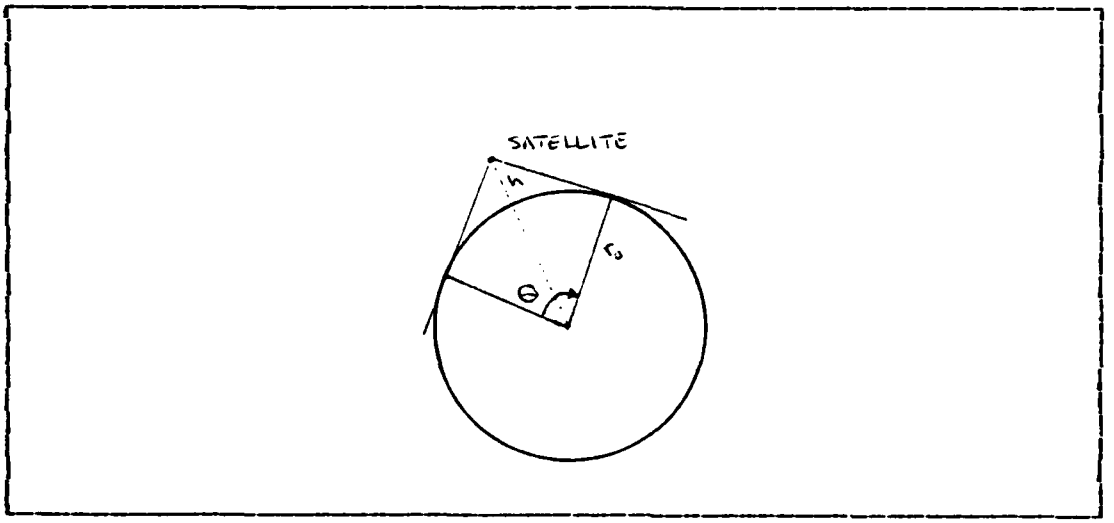

Figure 2.6 Geometric Swath Width

The first aspect of swath width to be considered is the maximum viewing angle, or Geometric Swath Width (GSW). As shown in Figure 2.6, this is the maximum viewable area by the satellite, and is related to the altitude as follows:

$$\cos\frac{\Theta}{2} = \frac{r_o}{r_o + h},$$

or

$$\Theta = 2\cos^{-1}\left[\frac{r_o}{r_o + h}\right], \qquad (2.9)$$

or, in terms of distance,

$$GSW = 2 r_o \cos^{-1}\left[\frac{r_o}{r_o + h}\right]. \qquad (2.10)$$

Some typical values for GSW are shown in Table II .

which appears to be a potentially large number, but as Figure 2.5 indicates, is actually only a few degrees per day. When one considers that the typical tracking satellite makes a dozen or more revolutions of the Earth daily, the change in the ground tracks of Figures 2.3 and 2.4 would be quite small for each revolution; further, as long as the satellite's ground station is aware of the precession and makes compensation for it, there is no discernable error introduced into the target tracking problem.

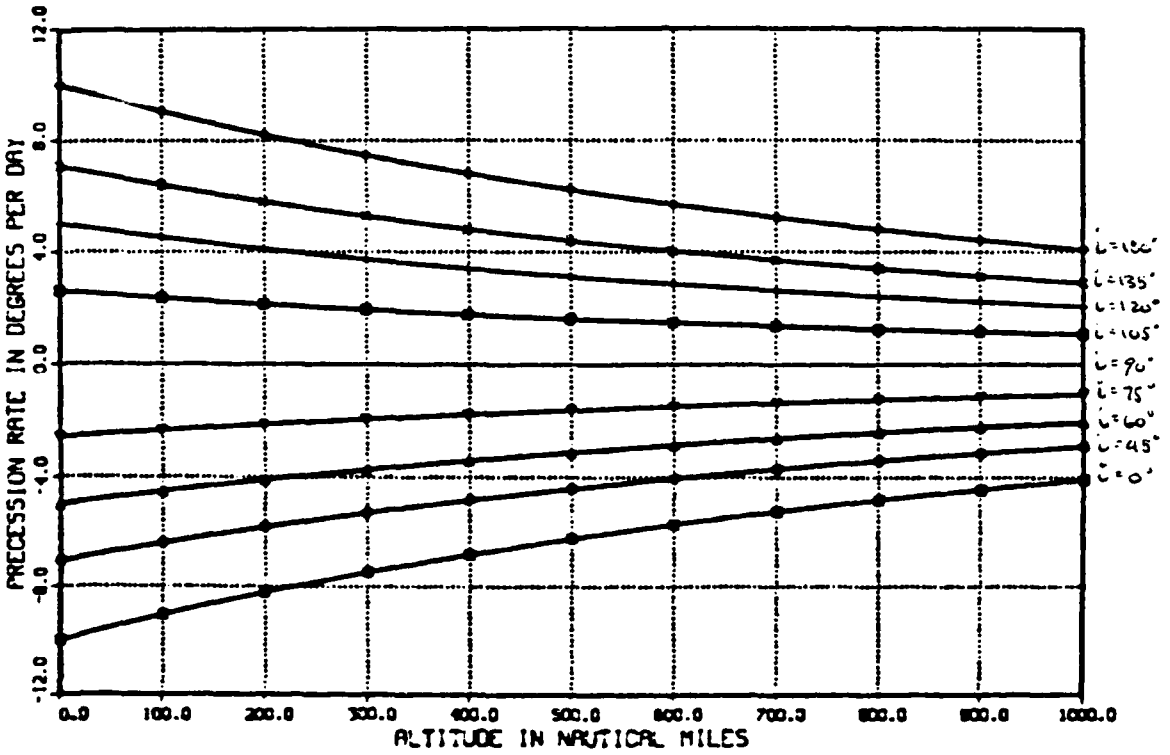

Figure 2.5 Precession Rates
For Various Altitudes and Inclinations

C. EARTH COVERAGE

The key quantities to consider when discussing Earth coverage for either a single satellite, or an array of

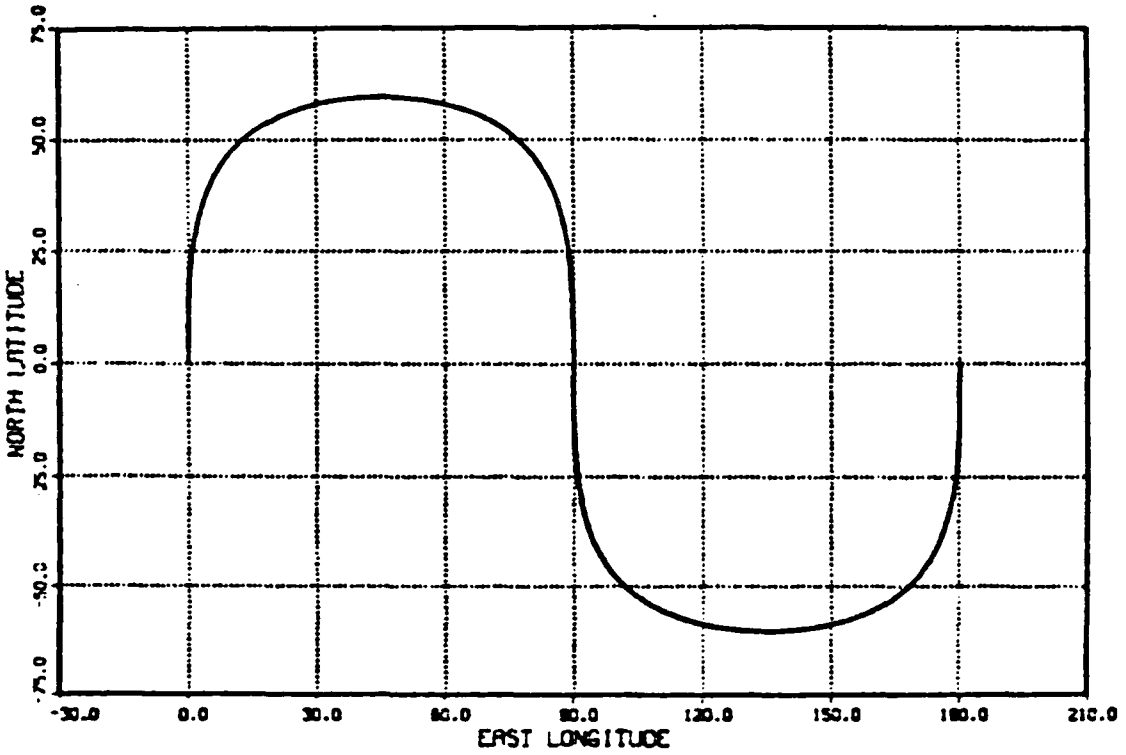

Figure 2.4 Satellite Ground Track
For a Nominal Period of Twelve Hours

The last factor that must be considered to achieve absolute accuracy in predicting the satellite's orbital path is the non-spherical shape of the Earth; to wit, the Earth is actually a slightly oblate ellipsoid, which causes a slow drift, or precession, of the satellite's orbital plane around the Earth with respect to the fixed stars. [Ref. 5] includes a detailed discussion of the effects of precession on the orbital plane, including the derivation of a formula for precession rate, which is offered here without proof; for a circular orbit,

$$\dot{\Omega} = \frac{-2.386 \cdot 10^{13} \cdot \cos i}{(r_e + h_s)^{7/2}} \quad {}^{\circ}/_{\text{DAY}},$$

Consider now that the Earth is rotating in an easterly direction; the rate at which east longitude is traversed by the satellite is now decreased by the Earth's rotational speed, or

$$\dot{\lambda} = \frac{\cos i\,\dot{\phi}}{\cos^2\phi + \sin^2\phi\cos^2 i} - \omega_e \,. \tag{2.8}$$

Employing equations 2.7 and 2.8 for the generation of latitude and longitude respectively led to the computer-generated ground tracks shown in Figures 2.3 and 2.4 for two typical orbital periods (note that the inclination angle is 60 degrees in both cases).

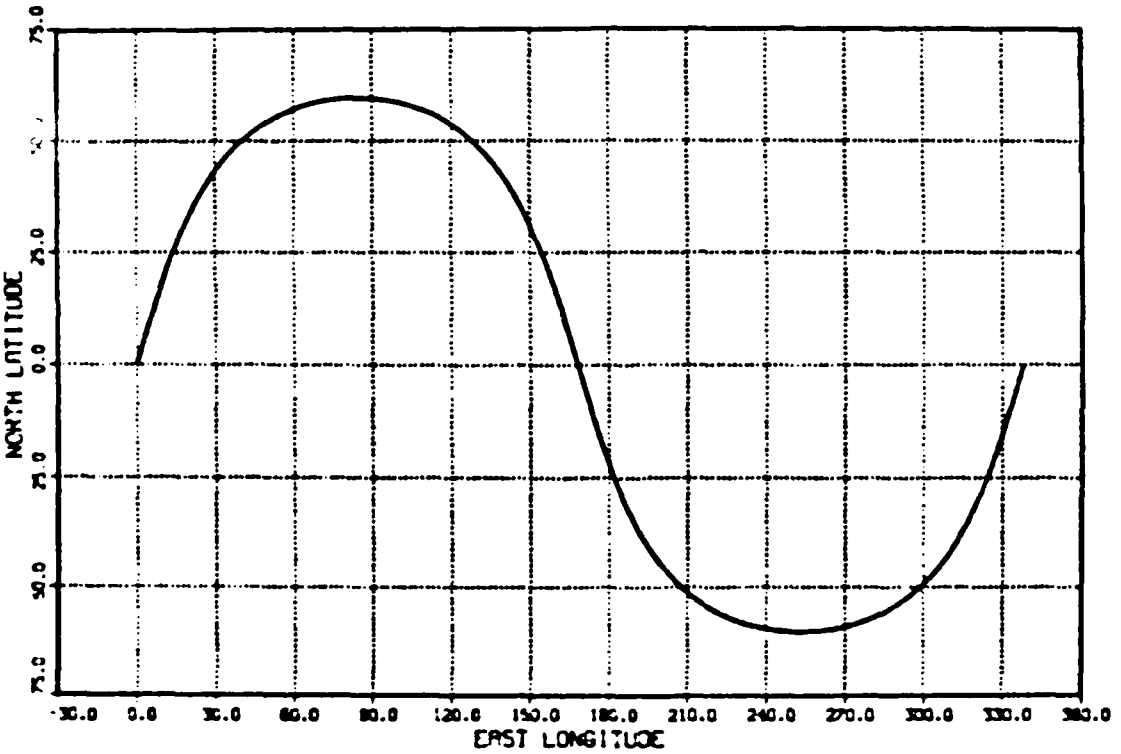

Figure 2.3 Satellite Ground Track
For a Nominal Period of Ninety Minutes

$$L = \tan^{-1} Z/\sqrt{X^2+Y^2},$$

$$\lambda = \tan^{-1} Y/X. \qquad (2.4)$$

If the Earth were truly a stationary sphere, these equations would be sufficient to describe the satellite's motion. Because the Earth is actually spinning under the satellite, however, angular rates must be considered, so that the Earth's rotational speed (shown as ω_E in Figure 2.2) may likewise be considered. Therefore equations 2.3 and 2.4 above must be differentiated with respect to time as follows (note that i is time-independent):

$$\dot{X} = -r\sin\phi\,\dot{\phi},$$

$$\dot{Y} = r\cos\phi\cos i\,\dot{\phi}, \qquad (2.5)$$

$$\dot{Z} = r\cos\phi\sin i\,\dot{\phi},$$

$$\dot{L} = \frac{\left[X^2+Y^2\right]\dot{Z} - Z\left[X\dot{X}+Y\dot{Y}\right]}{\sqrt{X^2+Y^2}},$$

$$\dot{\lambda} = \frac{X\dot{Y}-Y\dot{X}}{X^2+Y^2}. \qquad (2.6)$$

Substitute equations 2.5 into equations 2.6,

$$\dot{L} = \frac{\cos\phi\cos i\,\dot{\phi}}{\sqrt{\cos^2\phi + \sin^2\phi\cos^2 i}}, \qquad (2.7)$$

$$\dot{\lambda} = \frac{\cos i\,\dot{\phi}}{\cos^2\phi + \sin^2\phi\cos^2 i}.$$

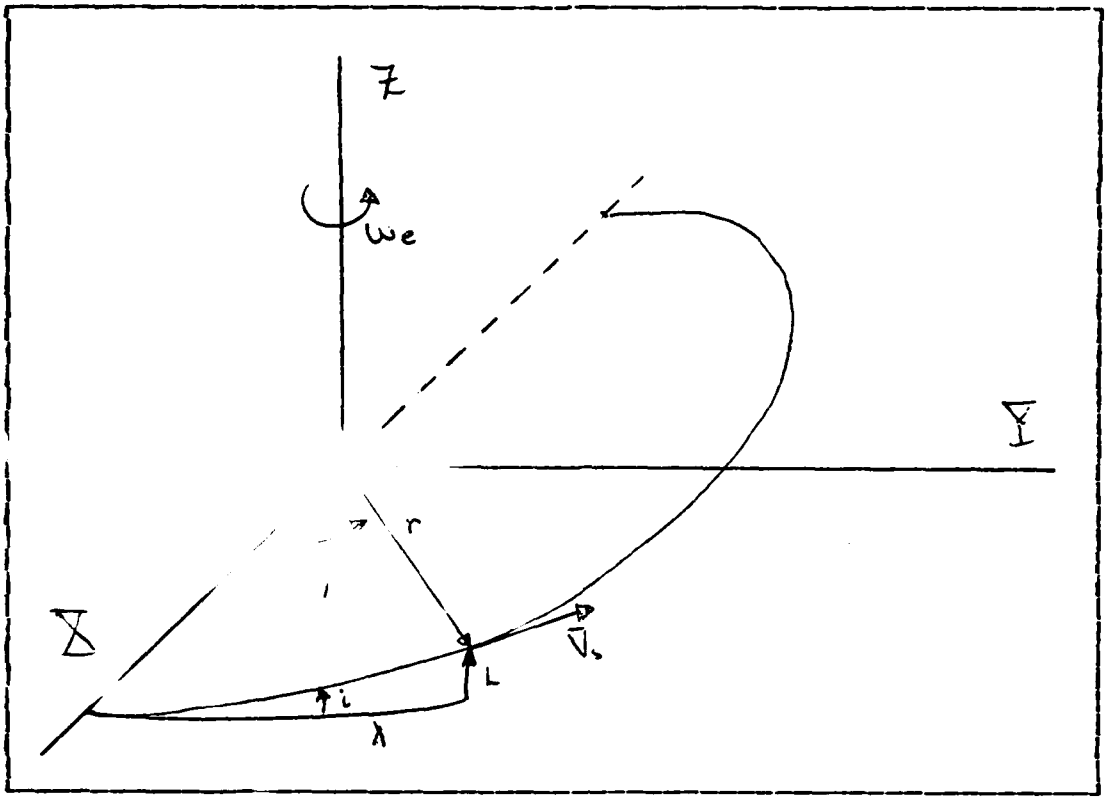

Figure 2.2 Inclination of the Orbital Plane

If the orbital plane is then rotated about the X axis through i degrees, then the coordinates are transformed by

$$\mathbb{T} = \begin{bmatrix} 1 & 0 & 0 \\ 0 & \cos i & -\sin i \\ 0 & \sin i & \cos i \end{bmatrix};$$

that is, now

$$\begin{aligned} X &= r\cos\phi, \\ Y &= r\sin\phi\cos i, \\ Z &= r\sin\phi\sin i, \end{aligned} \tag{2.3}$$

and the latitude and longitude are described by

disturbances will produce oscillations about the reference orbit with its same period, i.e.

$$T_{osc} = T_{SAT} = \left[\frac{4\pi^2 r^3}{GM}\right]^{1/2}.$$

B. SATELLITE GROUND TRACK

The earth-satellite model as developed in Section A is obviously over-simplified for the purposes of target tracking; thus far, the Earth has been represented only as a point mass rather than as a spinning globe, which would make it extremely difficult to describe any motion across the Earth's surface.

One intrinsic feature of a satellite's orbit used in measuring its flight path is the inclination angle i, which represents the positive angle between the orbital plane and the equatorial plane. This angle can be used, together with earth's surface coordinates, to describe the path over ground, or ground track, of the satellite.

In Figure 2.2, the Z axis coincides with the Earth's polar axis; L and Λ measure north latitude and east longitude respectively; and r, ϕ, and $\bar{V}_s$ describe the satellite's motion in its orbital plane as before.

If the satellite is considered to have originally orbited in the equatorial plane, its position would have been described by

$$X = r\cos\phi,$$
$$Y = r\sin\phi,$$
$$Z = 0.$$

must be subtracted, i.e.

$$h = r - r_o \ .$$

Of special interest is the satellite at zero altitude, also known as a Herget satellite, with a period of 84.5 minutes. As [Ref. 5] indicates, this gives a value for the lower bound of a satellite's period. Some other periods and altitudes of interest are summarized in Table I :

TABLE I

Typical Periods, Altitudes, and Orbital Velocities

Period T	Altitude h	Orbital Velocity
90 min	150 nm	15030 knots
3 hr	2250 nm	11930 knots
6 hr	5600 nm	9470 knots
12 hr	10900 nm	7510 knots
23 hr 56 min	19322 nm	5970 knots

This last orbit, with a period of one solar day, is the geosynchronous orbit frequently adopted in satellite communications applications; for tracking of surface-bound targets, however, low-altitude orbits will be of much greater interest. Typical altitudes will generally be less than 1000 nautical miles, depending on the sensitivity and accuracy of the tracking sensor: this corresponds to periods of two hours or less.

Finally, it can be shown by the method of the potential energy well [Ref. 6], and also by the application of the theory of perturbations [Ref. 4], that this reference orbit will be stable in the presence of small disturbances in either the orbital plane or the third dimension, and these

$$\frac{d}{dt}\left(\frac{\partial \mathcal{L}}{\partial \dot{\phi}}\right) = \frac{\partial \mathcal{L}}{\partial \phi},$$

or

$$\frac{d}{dt}\left(mr^2\dot{\phi}\right) = 0. \qquad (2.2)$$

Equation 2.2 indicates that angular momentum is conserved (i.e. its derivative is zero), and that $\dot{\phi}$ will be constant for a given orbital radius. Further, if the angular momentum vector is interpreted as

$$\bar{J} = m(\bar{r}\times\bar{v}) = mr^2\dot{\phi}\hat{i},$$

then the fact of its conservation indicates that the orbit will remain stable in its original plane. The introduction of a third coordinate, which ultimately becomes the angle of inclination i, and which remains arbitrary throughout the Lagrangian derivation, proves this conclusively.

Solving equation 2.1 for the the physical constants reveals that

$$r^3\dot{\phi}^2 = GM.$$

Considering that $\dot{\phi} = 2\pi/T,$

where T is the satellite's period, then

$$\frac{r^3}{T^2} = \frac{GM}{4\pi^2}$$

for a satellite in an earth orbit; this is Kepler's Second Law of Orbital Motion.

The radius in this equation is the distance of the satellite from the Earth's center; for altitude above the Earth, the Earth's radius, here represented as

$$r_o = 3438\text{nm} = 6366\text{km}$$

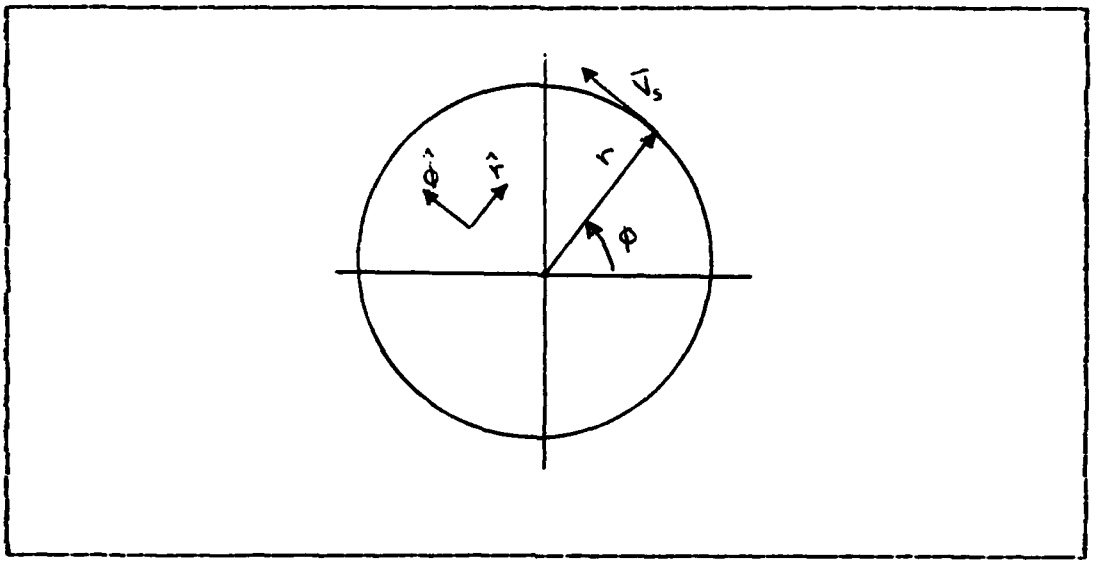

Figure 2.1 Satellite Orbit in its Plane

The circular orbit is the simplest case, such that the velocity is purely tangential and can be characterized as

$$\bar{V}_s = r\dot{\phi}\hat{\phi}.$$

The kinetic energy T is then

$$T = \tfrac{1}{2} m \bar{V}_s \cdot \bar{V}_s = \tfrac{1}{2} m r^2 \dot{\phi}^2,$$

and in the absence of any external disturbances, the Lagrangian function is written as follows:

$$\mathcal{L} = T - V = \tfrac{1}{2} m r^2 \dot{\phi}^2 + GMm/r.$$

By the rules of Lagrangian mechanics,

$$\frac{d}{dt}\left(\frac{\partial \mathcal{L}}{\partial \dot{r}}\right) = \frac{\partial \mathcal{L}}{\partial r},$$

or

$$0 = mr\dot{\phi}^2 - GMm/r^2; \qquad (2.1)$$

II. SATELLITE DYNAMICS AND OBSERVATION OF TARGETS

In considering the tracking of a surface or air target by a satellite hurtling through space at speeds approaching 15000 knots, it is obviously imperative to understand the dynamics of the motion of the satellite. Only then can a relative coordinate system be established, with the ultimate goal of describing the target's motion over the Earth's surface; first, however , the satellite's own motion must be similarly described.

In the following derivations, the Earth will be approximated by a uniformly-dense, perfect sphere. This approximation has often been characterized qualitatively as being twice as good as that of a "spherical" basketball; its quantitative implications will be discussed in Sections B and C below.

A. SATELLITE REFERENCE ORBIT

Lagrangian Mechanics, as developed in [Ref. 4] offers the easiest method for analyzing the satellite's motion. The Earth and the satellite can each be represented by point masses; in the absence of external disturbances, it can be shown that the satellite's orbit will remain planar. The gravitational potential of the satellite is inversely proportional to its distance from the Earth; using circular polar coordinates as shown in Figure 2.1, this potential energy V is then described by

$$V = -GMm/r \quad ,$$

where G is Newton's constant of universal gravitation, M is the mass of the Earth, and m is the mass of the satellite.

Chapter IV finally tackles the problem of state observability. Observability, as defined here and in [Ref. 1], is the capability, given the observations and knowledge of the control input to the system over time, to reconstruct the entire system state back to the initial condition. Testing for this condition on a linear system is perfectly straightforward; the method is fully developed in [Ref. 2] and elsewhere. The observability of the nonlinear system is by far the more interesting problem, as the problem is more realistic, and the methodology for testing of nonlinear observability is far less well developed and/or documented. To that end, the method which is newly developed in [Ref. 1] is herein employed, and the analysis ultimately becomes as much of a test of the method as the observability of the system.

Based on the results of the analysis in Chapter IV, Chapter V is then an admittedly imperfect, first-cut attempt at designing a deterministic nonlinear observer, and then tracking the target with an EKF. The comments in [Ref. 3] concerning filter initialization and measurement covariance estimation become pertinent.

Finally, Chapter VI summarizes the thesis' results, and makes some suggestions for further analysis, specifically in the area of multiple targets and observers. The real-world significance of the report is also discussed.

I. INTRODUCTION

In pursuit of an interest in the problems and potential of satellite tracking of earth's surface or low altitude targets, the interested student quickly discovers a plethora of information available on the subject, but little in the way of analysis of the entire problem, start-to-finish. The purpose of this report then is to provide that analysis, beginning with the mechanics of the orbiting satellite; next developing a model to represent the target motion; and continuing through an observability analysis of the problem. Finally, a first-cut attempt is made, based on the observability study, to design a deterministic nonlinear observer and an Extended Kalman Filter (hereafter referred to as an EKF) to observe and track the target.

Chapter II of this report examines in depth the physical dynamics of a satellite orbiting the Earth, and then the target moving on or just above its surface. A working model is developed for the satellite, including a look at its ground track; its rotation about its own axes as it moves through space; and the translation of its raw observed data into earth's surface coordinates. Both position and rate data are considered, and specific formulae are developed along the lines of a computer algorithm for coordinate transformation.

Chapter III deals more specifically with the model for the target itself. Actually, two models are considered: first, a realistic model, necessarily nonlinear, due to the non-synchronous motion of the target and satellite on concentric spheres; and then secondly a slightly nonrealistic linearized version. Both surface and air targets are considered, but for brevity's sake, only the surface target is discussed fully in the various examples.

the entire globe. This leads to the information summarized in Table III; the last (geosynchronous) case is obviously unrealistic for tracking applications, as MSW is greater than GSW.

TABLE III

MSW as a Function of Altitude

h	n	Θ_s	MSW
150 nm	16	11.25°	675 nm
600 nm	13.41	13.47°	808 nm
2250 nm	8	22.5°	1350 nm
5600 nm	4	45°	2700 nm
10900 nm	2	90°	5400 nm
19322 nm	1	180°	10800 nm

The overlap, or difference between Tables II and III, determines the maximum number of times a single satellite can possibly view a stationary target on the equator during successive orbits. This number N can be calculated by dividing twice equation 2.10 by equation 2.12, or

$$N = \frac{4\cos^{-1}\left[\frac{r_e}{r_e+h}\right]}{1.05\times10^{-4}} \left[\frac{nm}{r_e+h}\right]^{3/2}$$

Unfortunately, average time between revisits cannot be characterized as 24 hrs/N, as successive swaths will overlap on consecutive orbits, and then the target will not be illuminated for several orbits. At this point it is necessary to place additional satellites in the orbital pattern, or constellation, to ensure coverage during every orbit, i.e. a minimum of 360/GSW (rounded up) is required. This will then provide n visits per day to the equatorial target, where n

is again as defined in equation 2.11 . Once this has been achieved, insertion of additional satellites will only continue to increase the revisit frequency while correspondingly decreasing the revisit time.

The last factor in this revisit time problem is the consideration of horizon-to-horizon coverage along the path, that is, until now the discussion has only dealt with measuring the time between successive CPA's (Closest Point of Approach) of the satellite to the target. As Figure 2.7 indicates, however, the target is actually in view long before the satellite passes overhead, and remains in view until the satellite passes over the far horizon.

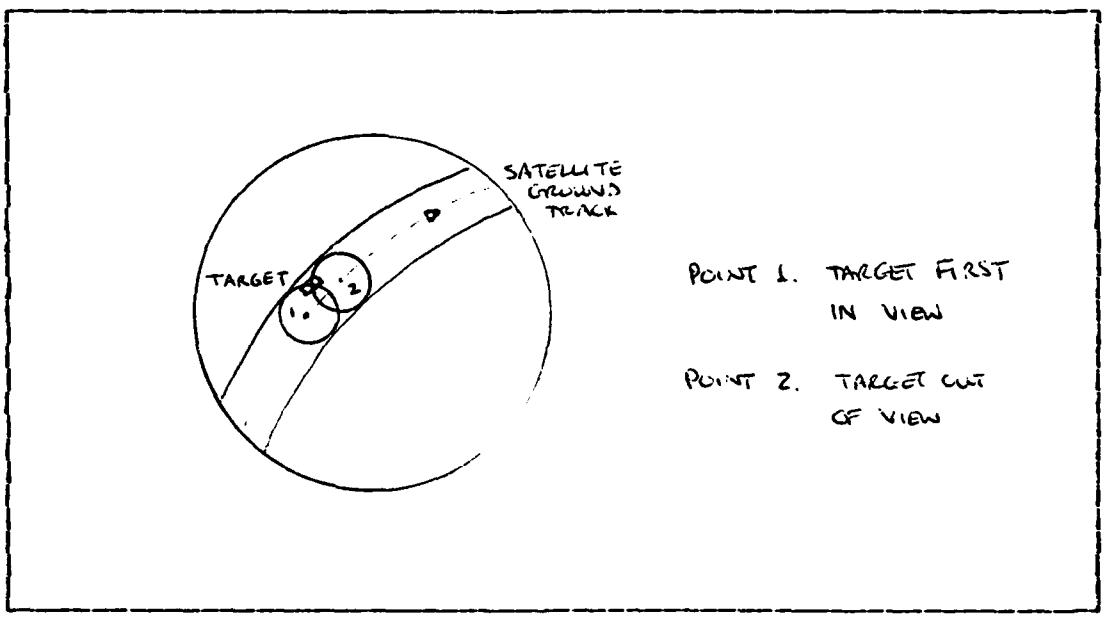

Figure 2.7 Target Time-in-View for a Single Pass

If the target lies directly on the satellite's path, then the maximum viewing angle Θ_v is defined in Figure 2.8 as

$$\Theta_v = 2\left[\cos^{-1}\left[\frac{r_e}{r_e + h_s}\right] + \cos^{-1}\left[\frac{r_e}{r_e + h_t}\right]\right].$$

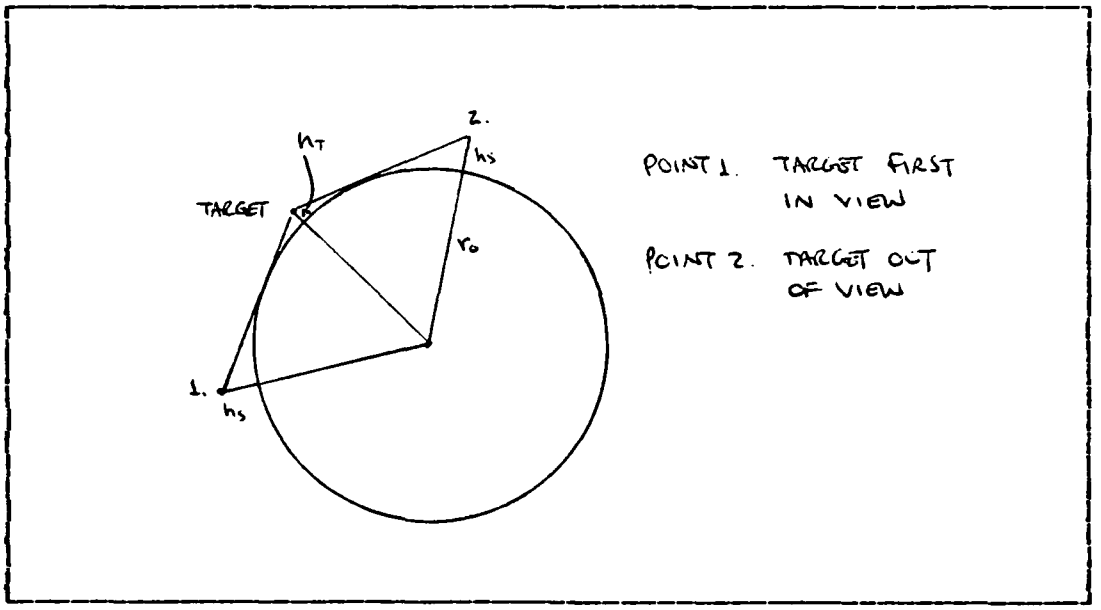

Figure 2.8 Viewing Angle

This translates to a viewing time of

$$T_v = T_s \frac{\Theta_v}{360} = \frac{2\pi (r_0+h)^{3/2}}{\sqrt{GM}} \left[\frac{\cos^{-1}\left[\frac{r_0}{r_0+h_s}\right] + \cos^{-1}\left[\frac{r_0}{r_0+h_T}\right]}{180} \right].$$

For a surface target and a satellite at 150 nm elevation, this translates to a time-in-view of 8.3 minutes. This viewing time will increase as satellite altitude increases, and decrease as the target moves toward the outside of the swath. Regardless, the revisit time between target observations is always decreased by this viewing time.

The final facet of ground coverage to be considered is coverage at the poles. Having used the Equator as the worst case for swath spreading, one might then expect the swaths to converge at the poles. Actually, the convergence of the

ground track occurs about the latitude lines of the angle of inclination because they are the circles of smallest circumference to be viewed from directly above; hopefully the swath width of the satellite is then great enough to overlap the poles. Thus for an orbital inclination of 60 degrees, the most closely grouped locus of points observed from directly overhead are the latitude circles 60° N and 60° S. To see if the swath overlap will at least cover the poles, Figure 2.9 must be considered. $\Theta/2$ is the half-angle from equation 2.9, so

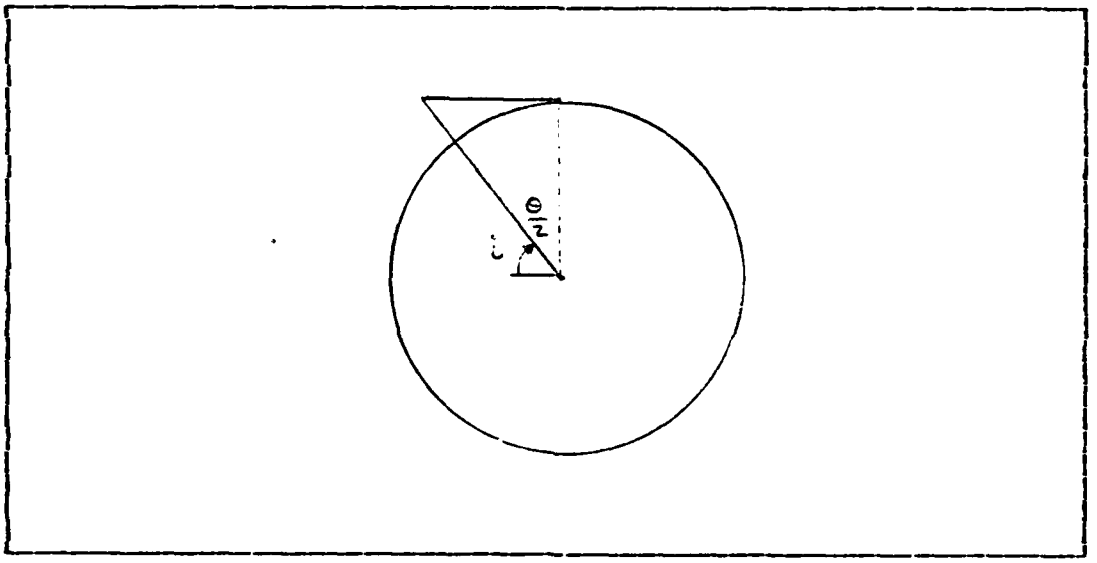

Figure 2.9 Minimum Inclination for Polar Coverage

$$90^\circ - i = \cos^{-1}\left[\frac{r_o}{r_o+h}\right],$$

or

$$i = 90^\circ - \cos^{-1}\left[\frac{r_o}{r_o+h}\right].$$

Table IV summarizes these results for typical orbital heights.

TABLE IV

Minimum Inclination for Polar Coverage

h	i
150 nm	73.4°
600 nm	58.4°
2250 nm	37.2°
5600 nm	22.4°
10900 nm	13.9°
19322 nm	8.7°

To summarize thus far, a satellite placed at an altitude of 600 nm would be useful for tracking purposes; its GSW of 63.4° and MSW of 13.47° ensure that a target would be viewed on at least four (and probably five) consecutive passes, and its orbital period of 107.4 minutes indicates that the target would be viewed frequently enough to acquire timely and significant information about its location, course, and speed. Inclining it a minimum of 58.4 degrees would ensure coverage of both poles, and its precession rate of -3 degrees per day (or about -0.2 degrees per orbit) would not deter its ability to maintain track on the target. Realistically, a single satellite would not be used; the placement of a minimum of six in the constellation would ensure that no target would go more than one period without being observed, and the placement of additional satellites would only then increase the frequency of target observation.

D. SATELLITE ORIENTATION IN SPACE

Having developed a working model for the orbiting satellite, the next phase of the problem will consider the satellite's observation of its target, either by passive (i.e.

IR) or active (i.e. search radar) means. First, however, a coordinate frame of reference for that observation is required. Thus far the assumption that the satellite can be represented by a point mass has sufficed; now, however, it must be realized that the satellite has dimension, is irregularly shaped, and quite possibly undergoes radical attitude changes throughout the course of its orbit. It is therefore imperative that the satellite be able to orient itself with reference to its ground point, that is, the point on the Earth's surface directly between the satellite and the Earth's center. This is because, realistically, the satellite will be measuring (at best) a line-of-sight range and a series of angles (probably altitude and azimuth) to the target: it is these angles that must be oriented with respect to the reference directions, in order that the data fed to the tracking computer be consistent.

In considering Figure 2.10, Figures 2.10 (a) and 2.10 (e) show the space reference orientation and the satellite aligned in that orientation; Figures 2.10 (b), (c), and (d) show the initial position and intermediate rotations of the satellite axes required to achieve that orientation. It should be emphasized that these rotations are computational rather that mechanical; as long as the target falls within the sensor's coverage area, there is no need to actually physically rotate the satellite into any new position. Rather the target coordinates are transformed mathematically as follows:

Step 1. Rotate around the x axis by Π_1 to get y axis into "NE" plane.

$$\Pi_1 = \begin{bmatrix} 1 & 0 & 0 \\ 0 & \cos\delta_1 & \sin\delta_1 \\ 0 & -\sin\delta_1 & \cos\delta_1 \end{bmatrix}.$$

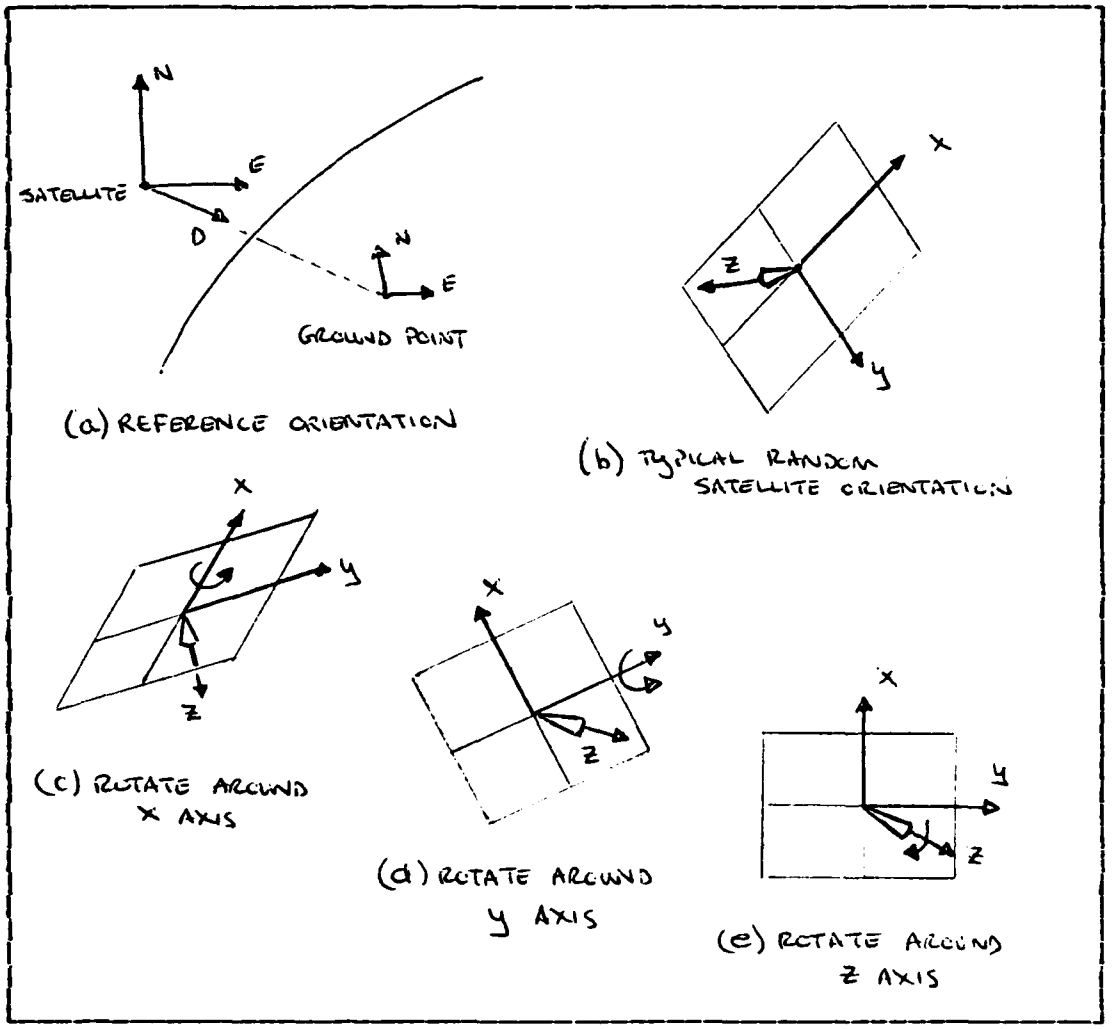

Figure 2.10 Translation of the Satellite To the Reference Orientation

Step 2. Rotate around the y axis by Π_2 to get the z axis in the "D" direction.

$$\Pi_2 = \begin{bmatrix} \cos\delta_2 & 0 & -\sin\delta_2 \\ 0 & 1 & 0 \\ \sin\delta_2 & 0 & \cos\delta_2 \end{bmatrix}.$$

Step 3. Rotate around the z axis by Π_3 to get the x and y axes aligned in the "N" and "E" directions.

$$\Pi_3 = \begin{bmatrix} \cos\delta_3 & \sin\delta_3 & 0 \\ -\sin\delta_3 & \cos\delta_3 & 0 \\ 0 & 0 & 1 \end{bmatrix}.$$

Thus to get from x-y-z coordinates to N-E-D coordinates, the transformation is

$$\begin{bmatrix} N \\ E \\ D \end{bmatrix} = \Pi_3 \cdot \Pi_2 \cdot \Pi_1 \begin{bmatrix} x \\ y \\ z \end{bmatrix}. \qquad (2.13)$$

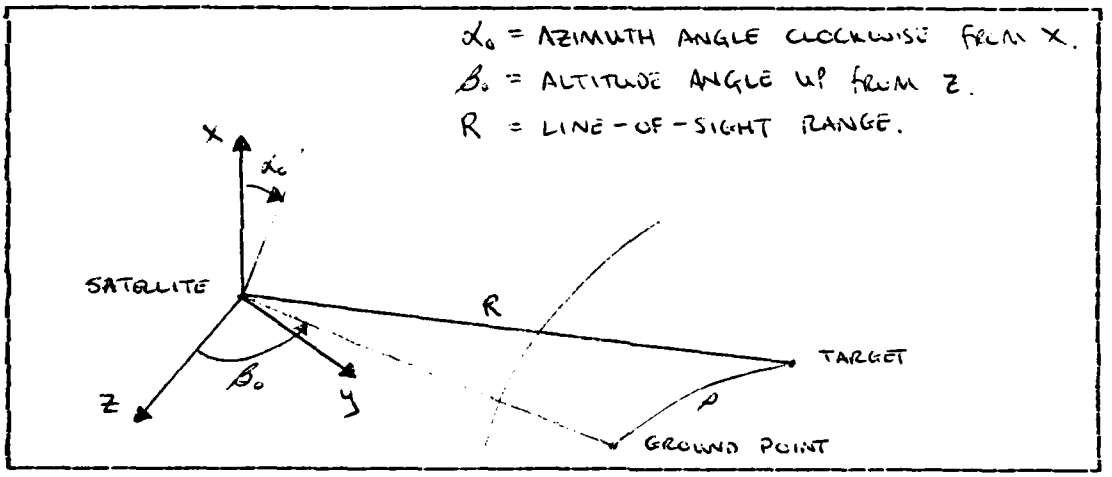

Figure 2.11 Angles Transformed to Rectangular Coordinates

There is actually another step involved both before and after the transformation of equation 2.13, that of transforming from the angles to the rectangular coordinates and back. The translation from an initial set of raw angular measurements to the satellite's x-y-z rectangular coordinates is shown in Figure 2.11 . The corresponding equations are

$$x = R \sin\beta_o \cos\alpha_o,$$
$$y = R \sin\beta_o \sin\alpha_o,$$
$$z = R \cos\beta_o . \qquad (2.14)$$

Meanwhile, the transformation from the N-E-D reference rectangular coordinates to the observed angular coordinates is depicted in Figure 2.12, and described mathematically by

$$R = \sqrt{N^2 + E^2 + D^2},$$
$$\alpha = \tan^{-1} E/N,$$
$$\beta = \cos^{-1} D/R . \qquad (2.15)$$

It is worthy of note that R remains unchanged by all the transformations; only α and β change. Thus the complete transformation from angles-referenced-to-satellite to angles-referenced-to-ground is

$$\begin{bmatrix} N \\ E \\ D \end{bmatrix} = \mathbb{T}_3 \mathbb{T}_2 \mathbb{T}_1 \begin{bmatrix} R \sin\beta_o \cos\alpha_o \\ R \sin\beta_o \sin\alpha_o \\ R \cos\beta_o \end{bmatrix}, \qquad (2.16)$$

and

$$R = \sqrt{N^2 + E^2 + D^2},$$
$$\alpha = \tan^{-1} E/N,$$
$$\beta = \cos^{-1} D/R .$$

Step 3. Rotate around the z axis by $\mathbb{T}_3$ to get the x and y axes aligned in the "N" and "E" directions.

$$\mathbb{T}_3 = \begin{bmatrix} \cos\delta_3 & \sin\delta_3 & 0 \\ -\sin\delta_3 & \cos\delta_3 & 0 \\ 0 & 0 & 1 \end{bmatrix}.$$

Thus to get from x-y-z coordinates to N-E-D coordinates, the transformation is

$$\begin{bmatrix} N \\ E \\ D \end{bmatrix} = \mathbb{T}_3 \cdot \mathbb{T}_2 \cdot \mathbb{T}_1 \begin{bmatrix} x \\ y \\ z \end{bmatrix}. \qquad (2.13)$$

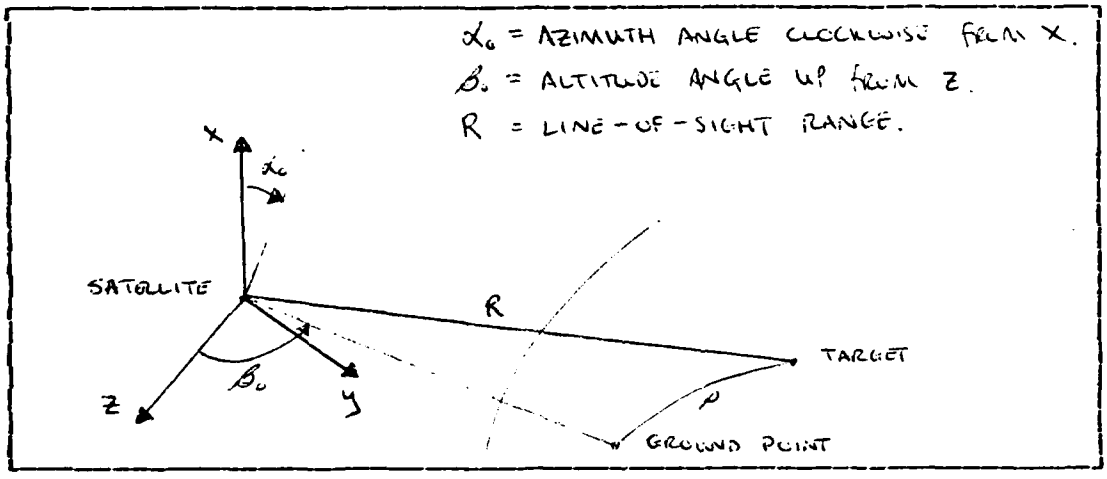

Figure 2.11 Angles Transformed to Rectangular Coordinates

There is actually another step involved both before and after the transformation of equation 2.13, that of transforming from the angles to the rectangular coordinates and back. The translation from an initial set of raw angular measurements to the satellite's x-y-z rectangular coordinates is shown in Figure 2.11 . The corresponding equations are

$$x = R \sin\beta_c \cos\alpha_c,$$
$$y = R \sin\beta_c \sin\alpha_c,$$
$$z = R \cos\beta_c. \qquad (2.14)$$

Meanwhile, the transformation from the N-E-D reference rectangular coordinates to the observed angular coordinates is depicted in Figure 2.12, and described mathematically by

$$R = \sqrt{N^2+E^2+D^2},$$
$$\alpha = \tan^{-1} E/N,$$
$$\beta = \cos^{-1} D/R. \qquad (2.15)$$

It is worthy of note that R remains unchanged by all the transformations; only α and β change. Thus the complete transformation from angles-referenced-to-satellite to angles-referenced-to-ground is

$$\begin{bmatrix} N \\ E \\ D \end{bmatrix} = \mathbb{T}_3 \mathbb{T}_2 \mathbb{T}_1 \begin{bmatrix} R \sin\beta_c \cos\alpha_c \\ R \sin\beta_c \sin\alpha_c \\ R \cos\beta_c \end{bmatrix}, \qquad (2.16)$$

and

$$R = \sqrt{N^2+E^2+D^2},$$
$$\alpha = \tan^{-1} E/N,$$
$$\beta = \cos^{-1} D/R.$$

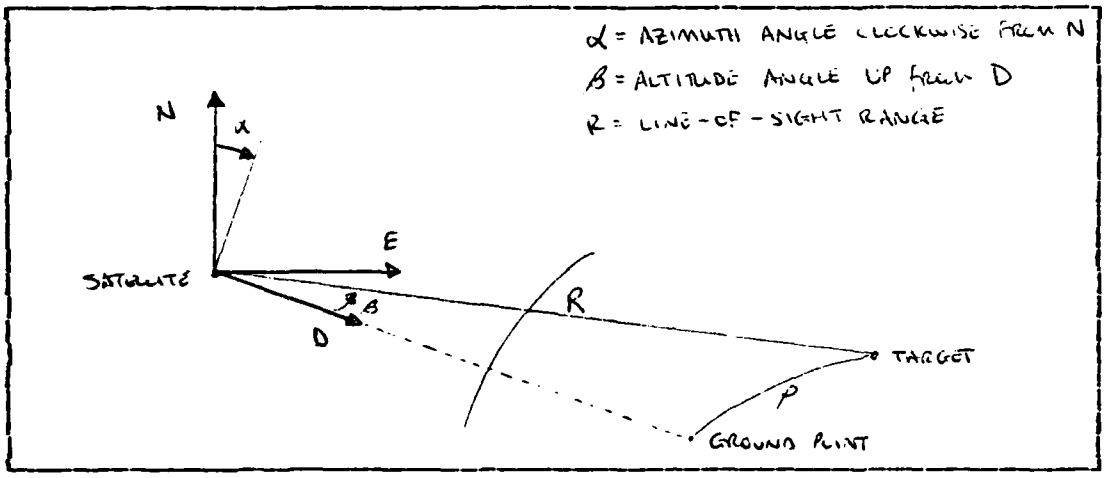

Figure 2.12 Rectangular Coordinates Transformed to Angles

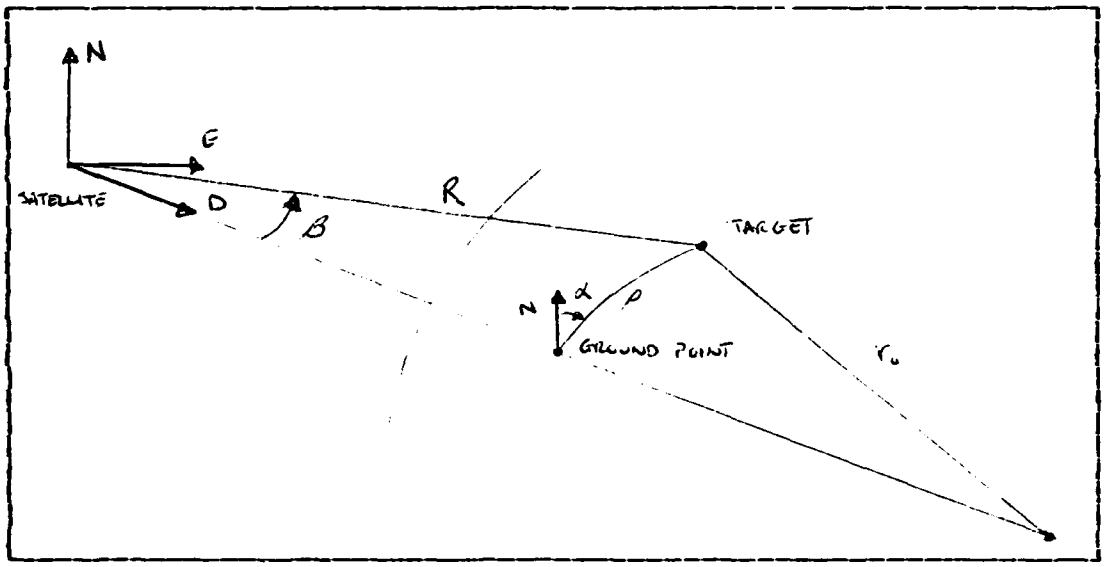

Figure 2.13 Observing the Target from Space

E. SATELLITE OBSERVATION OF A NEAR-SURFACE TARGET

Equations 2.16 detail the realignment of raw target information along the space reference axes, N-E-D; the

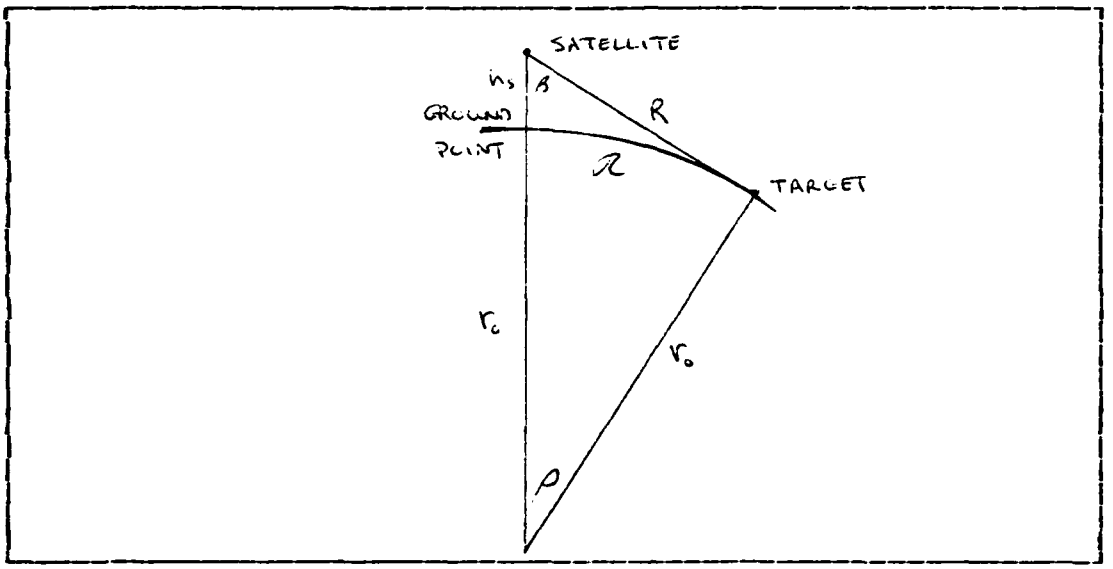

Figure 2.14 Satellite-Target-Earth Center Triangle

final step in calculating target position and velocity on the Earth's surface is to translate the range and the space angles into earth's surface coordinates, i.e. latitude and longitude. Figure 2.13 shows the pertinent variables, while Figure 2.14 shows the triangle formed by the satellite, the target, and the earth's center. The latter figure presumes a surface target; the case of an air target will be discussed momentarily.

To find the earth's surface distance along a great circle passing through the ground point and the target's position, one need only find the earth-central angle ρ with the law of cosines, as shown in Figure 2.14 ,

$$\rho = \cos^{-1} \frac{r_o^2 + (r_o + h_s)^2 - R^2}{2 r_o (r_o + h_s)} , \qquad (2.17)$$

and then the arc length, or surface distance

$$\mathcal{A} = r_o \rho .$$

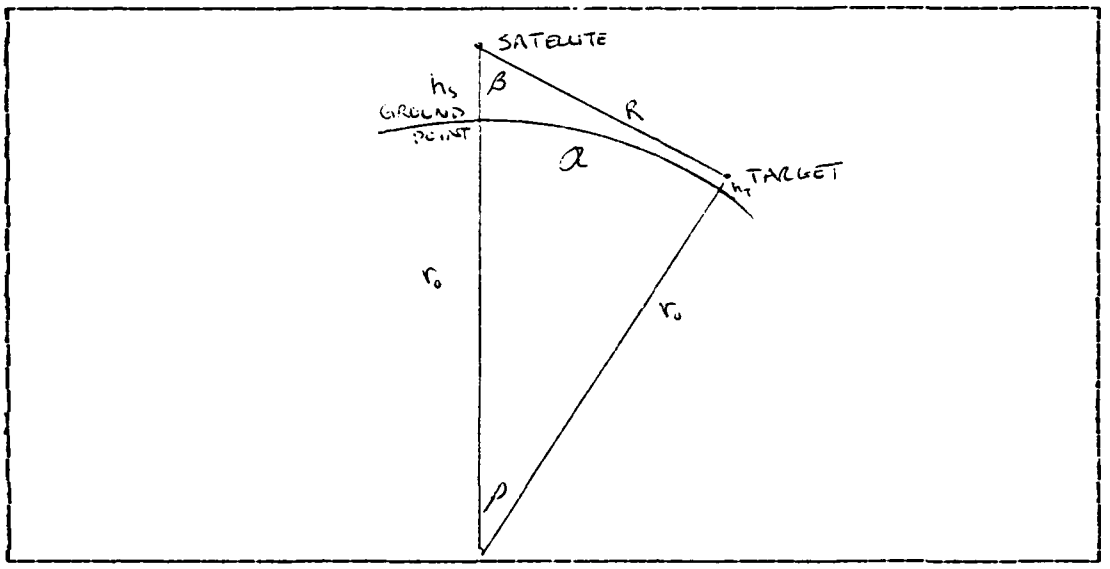

Figure 2.15 Same Triangle for an Air Target

Note that the angle β was not required in this calculation; it is required, however, for calculations involving an air target of unknown altitude, as shown in Figure 2.15 Solving for the target height requires applying the law of cosines again:

$$h_T = \left[(r_o + h_s)^2 + R^2 - 2R(r_o + h_s)\cos\beta \right]^{1/2} - r_o , \qquad (2.18)$$

and then φ follows from the law of sines:

$$\varphi = \sin^{-1} \frac{R \sin\beta}{r_o + h_T} , \qquad (2.19)$$

and once again, $\alpha = r_o \varphi$

In either case, once the great circle distance from the ground point to the target is known, the target's latitude

so

$$\alpha = \sin^{-1}\left[\frac{\cos L_T \sin\chi}{\sin\rho}\right] \tag{3.13}$$

To obtain $\dot{\alpha}$, consider

$$\cos\alpha\,\dot{\alpha} = \frac{1}{\sin^2\rho}\left[\sin\rho\left(\dot{\chi}\cos L_T\cos\chi - \dot{L}_T\sin L_T\sin\chi\right) - \dot{\rho}\cos L_T\sin\chi\cos\rho\right]$$

or

$$\dot{\alpha} = \frac{1}{\sin^2\rho\cos\alpha}\left[\sin\rho\left(\dot{\chi}\cos L_T\cos\chi - \dot{L}_T\sin L_T\sin\chi\right) - \dot{\rho}\cos L_T\sin\chi\cos\rho\right] \tag{3.14}$$

To obtain β, the law of cosines is again applied to Figure 2.15, this time yielding

$$\cos\beta = \frac{R^2 + (r_e+h_s)^2 - (r_e+h_T)^2}{2R(r_e+h_s)}$$

so

$$\beta = \cos^{-1}\left[\frac{R^2 + (r_e+h_s)^2 - (r_e+h_T)^2}{2R(r_e+h_s)}\right] \tag{3.15}$$

To obtain $\dot{\beta}$, consider

$$-\sin\beta\,\dot{\beta} = \frac{1}{4R^2(r_e+h_s)^2}\left[2R(r_e+h_s)\left[2R\dot{R} - 2(r_e+h_T)\dot{h}_T\right] - \left[R^2 + (r_e+h_s)^2 - (r_e+h_T)^2\right]2\dot{R}(r_e+h_s)\right]$$

or

$$\dot{\beta} = \frac{2R(r_e+h_T)\dot{h}_T - \dot{R}\left[R^2 - (r_e+h_s)^2 + (r_e+h_T)^2\right]}{2R^2(r_e+h_s)\sin\beta} \tag{3.16}$$

The observation model is summarized in Figure 3.3 . Any realistic computational procedure would of course use the intermediate variables L, λ , χ , ρ , and their derivatives; for the sake of completeness, however, it should be noted that the observer functions could be written as functions of the original state vector.

To solve for ρ and $\dot{\rho}$, equation 2.21 is rewritten as follows:

$$\cos\rho = \sin L_T \sin L_S + \cos L_T \cos L_S \cos\chi, \tag{3.9}$$

and then $-\sin\rho\dot{\rho} = \dot{L}_T(\cos L_T \sin L_S - \sin L_T \cos L_S \cos\chi)$

$$+\dot{L}_S(\sin L_T \cos L_S - \cos L_T \sin L_S \cos\chi) - \dot{\chi}\cos L_T \cos L_S \sin\chi,$$

or

$$\dot{\rho} = \frac{1}{\sin\rho}\left[\dot{L}_T(\sin L_T \cos L_S \cos\chi - \cos L_T \sin L_S)\right.$$

$$\left.+\dot{L}_S(\cos L_T \sin L_S \cos\chi - \sin L_T \cos L_S) + \dot{\chi}\cos L_T \cos L_S \sin\chi\right]. \tag{3.10}$$

Enough information is now available to solve for the space coordinates R, α, β, and their derivatives. To obtain R, the law of cosines is applied to Figure 2.15 as follows:

$$R^2 = (r_0 + h_T)^2 + (r_0 + h_S)^2 - 2(r_0 + h_S)(r_0 + h_T)\cos\rho,$$

so

$$R = \left[(r_0 + h_T)^2 + (r_0 + h_S)^2 - 2(r_0 + h_S)(r_0 + h_T)\cos\rho\right]^{1/2}. \tag{3.11}$$

To obtain $\dot{R}$, consider

$$R\dot{R} = \left[(r_0 + h_T) - (r_0 + h_S)\cos\rho\right]\dot{h}_T + \dot{\rho}(r_0 + h_T)(r_0 + h_S)\sin\rho,$$

or

$$\dot{R} = \frac{1}{R}\left[\left[(r_0 + h_T) - (r_0 + h_S)\cos\rho\right]\dot{h}_T + \dot{\rho}(r_0 + h_T)(r_0 + h_S)\sin\rho\right]. \tag{3.12}$$

To obtain α, the law of sines for spherical triangles is applied to Figure 2.16 as follows:

$$\frac{\sin\alpha}{\sin(90 - L_T)} = \frac{\sin\chi}{\sin\rho},$$

or

$$\frac{\sin\alpha}{\cos L_T} = \frac{\sin\chi}{\sin\rho},$$

Assuming that external nonlinear forces such as wind or sea drag are either negligible and/or unpredictable, this completes the target model.

2. Satellite Observation

The observer matrix $\underset{\sim}{H}$ will obviously be a nonlinear operator on the state vector. To begin its derivation, the n-e-h_T coordinates must be transformed to latitude-longitude-altitude coordinates by solving equations 3.1 in reverse, and then differentiating as follows:

$$L_T = \frac{n}{r_o} \quad , \quad L_T^{\circ} = \frac{n^{\circ}}{r_o}$$

$$\lambda_T = \frac{e}{r_o \cos L_T} \quad , \quad \lambda_T^{\circ} = \frac{\dot{e}\cos L_T + e L_T^{\circ} \sin L_T}{r_o \cos^2 L_T} \tag{3.6}$$

The ultimate goal of this transformation will be to express the space observations in terms of the state vector, i.e.

$$\underset{\sim}{y} = \begin{bmatrix} y_1 \\ y_2 \\ y_3 \\ y_4 \\ y_5 \\ y_6 \end{bmatrix} = \begin{bmatrix} R \\ \dot{R} \\ \alpha \\ \dot{\alpha} \\ \beta \\ \dot{\beta} \end{bmatrix} = \begin{bmatrix} H_1(\underset{\sim}{x}) \\ H_2(\underset{\sim}{x}) \\ H_3(\underset{\sim}{x}) \\ H_4(\underset{\sim}{x}) \\ H_5(\underset{\sim}{x}) \\ H_6(\underset{\sim}{x}) \end{bmatrix} = \underset{\sim}{H}(\underset{\sim}{x}) \tag{3.7}$$

First, however, it is useful to calculate in terms of the state vector the intermediate variables χ and ρ, as they were defined in Figure 2.16. Solutions for χ are trivial:

$$\chi = \lambda_T - \lambda_S \, ,$$
$$\dot{\chi} = \lambda_T^{\circ} - \lambda_S^{\circ} \, . \tag{3.8}$$

have six state variables, defined by the quantities developed in Part A of this chapter as follows:

$x_1 = n$ = northerly distance traveled (nm),
$x_2 = \dot{n} = V_n = V\cos\phi$ = northerly velocity (kts),
$x_3 = e$ = easterly distance traveled (nm),
$x_4 = \dot{e} = V_e = V\sin\phi$ = easterly velocity (kts),
$x_5 = h_T$ = altitude above earth's surface (nm),
$x_6 = \dot{h}_T$ = rate of climb (kts);

and negative values for these variables represent southerly distance, southerly velocity, westerly distance, westerly velocity, (no negative altitude), and rate of descent, respectively. For a surface target, x_5 and x_6 are zero; for a constant-altitude air target, x_6 is zero. The target is thus modeled continuously by

$$\dot{\underline{x}}(t) = \begin{bmatrix} 0 & 1 & 0 & 0 & 0 & 0 \\ 0 & 0 & 0 & 0 & 0 & 0 \\ 0 & 0 & 0 & 1 & 0 & 0 \\ 0 & 0 & 0 & 0 & 0 & 0 \\ 0 & 0 & 0 & 0 & 0 & 1 \\ 0 & 0 & 0 & 0 & 0 & 0 \end{bmatrix} \underline{x}(t) + \begin{bmatrix} 0 & 0 & 0 \\ 1 & 0 & 0 \\ 0 & 0 & 0 \\ 0 & 1 & 0 \\ 0 & 0 & 0 \\ 0 & 0 & 1 \end{bmatrix} \underline{u}(t), \tag{3.4}$$

where u(t) represents either noise in the n-e-h_T system, or else acceleration in the three directions. Realistically, because computation requires a finite time and one satellite cannot normally be dedicated solely to observing a single target, the observations will necessarily be discrete, and hopefully periodic in time T. The discrete model analogous to that of equation 3.4 is

$$\underline{x}(k+1) = \begin{bmatrix} 1 & T & 0 & 0 & 0 & 0 \\ 0 & 1 & 0 & 0 & 0 & 0 \\ 0 & 0 & 1 & T & 0 & 0 \\ 0 & 0 & 0 & 1 & 0 & 0 \\ 0 & 0 & 0 & 0 & 1 & T \\ 0 & 0 & 0 & 0 & 0 & 1 \end{bmatrix} \underline{x}(k) + \begin{bmatrix} T^2/2 & 0 & 0 \\ T & 0 & 0 \\ 0 & T^2/2 & 0 \\ 0 & T & 0 \\ 0 & 0 & T^2/2 \\ 0 & 0 & T \end{bmatrix} \underline{u}(k). \tag{3.5}$$

Now, the discussion of Chapter II essentially derives the system equations for describing a target's motion in terms of space coordinates; however, to have a near-earth target described in terms of R, α, β, and their derivatives would not necessarily be useful, as it would require all the coordinate transformations of Chapter II to be performed over again to relay any useful information to the ground. In addition, the presumption of a constant (in the absence of control input) course, speed, and/or rate of climb (air target) would be mathematically impossible, since these coordinates would not be available; therefore, since assuming constant $\dot{R}$, $\dot{\alpha}$, and $\dot{\beta}$ would still not achieve constant V_N, V_E, and $\dot{h}_T$, the second derivatives of R, α, and β would be required, i.e. the differentiation of equations 2.24 through 2.31. To avoid this unnecessary complication, the reverse derivation will be performed here, i.e. a description of both target motion and space observation in terms of earth's surface coordinates. The model will be derived for the most general case, i.e. all variables non-zero. The constant altitude aircraft or surface target will be considered simply to be special cases of this.

1. Target Model

If the target is presumed to maintain a constant course and speed in the absence of a control input (acceleration), a simple one-dimensional model might take the form of

$$\dot{\underline{x}}(t) = \begin{bmatrix} 0 & 1 \\ 0 & 0 \end{bmatrix} \underline{x}(t) + \begin{bmatrix} 0 \\ 1 \end{bmatrix} u(t),$$

where u(t) can actually be either system noise or an acceleration. Since three mutually perpendicular coordinates are required to describe the target position, the system should

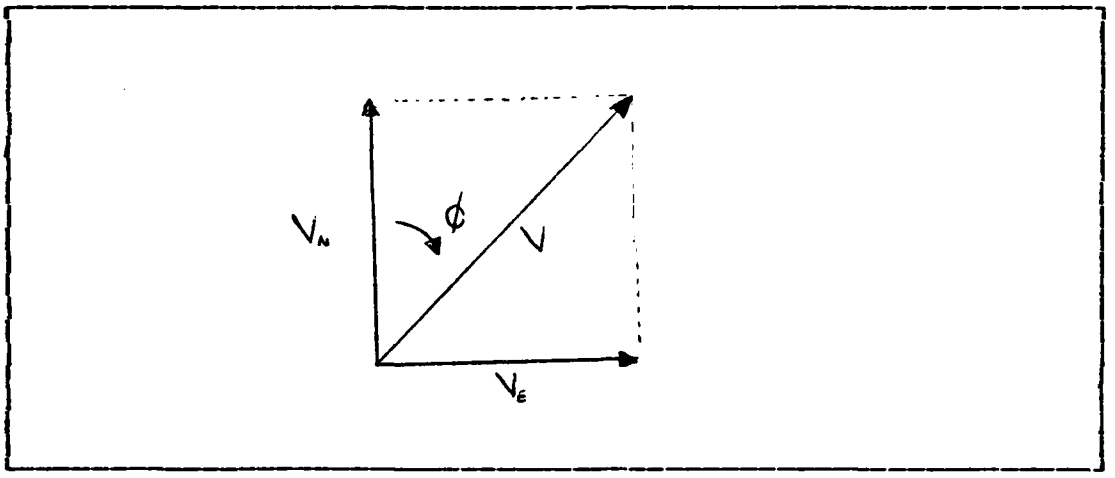

Figure 3.2 Resolution of the Velocity Components

becomes necessary effectively tc work backwards through the equations of those three previous sections and develop a system of equations that feature the target as the plant and the satellite as the observer. It would of course greatly facilitate the observability analysis if both the plant and observer for the system could be linear, and take the form

$$\dot{\underset{\sim}{x}}(t) = \underset{\sim}{A}\underline{x}(t) + \underset{\sim}{B}\underline{u}(t),$$
$$\underline{y}(t) = \underset{\sim}{C}\underline{x}(t).$$

In that case, the observability study of Chapter IV would become straightforward, and this aspect of this problem would no doubt have been fully explored years ago. Unfortunately, as the complicated angular rotations and spherical geometry of Chapter II portend, there is no realistic way to pick variables sc that the problem will be fully linear. It remains then to experiment with either a linear plant and nonlinear observer, or vice versa; it would ultimately be advantageous to avoid if possible the completely nonlinear system described by

$$\dot{\underset{\sim}{x}}(t) = \underset{\sim}{F}(\underline{x}(t),\underline{u}(t),t),$$
$$\underline{y}(t) = \underset{\sim}{H}(\underline{x}(t),t).$$

On the other hand, if rate data is not immediately available, the next position observation is required, and the velocities at time k are approximated by

$$V_N(k) = \dot{n}(k) = \frac{n(k)-n(k-1)}{T},$$

$$V_E(k) = \dot{e}(k) = \frac{e(k)-e(k-1)}{T},$$

$$\dot{h}_T(k) = \frac{h_T(k)-h_T(k-1)}{T}. \tag{3.3}$$

in either case, then velocity $V = \left[V_N^2 + V_E^2\right]^{1/2}$,

and course $\phi = \tan^{-1} V_E/V_N$

as shown in Figure 3.2 . For an aircraft flying at constant altitude, h_T will be zero; for a surface target, both h_T and $\dot{h}_T$ will be zero. Otherwise, this first-order model allows for nonzero velocities in the n, e, and h_T directions. To avoid the necessity to include any higher order variables in the target description, the model will represent acceleration as the control vector $\underline{u}(t)$ in all further discussion of the target's performance.

B. SATELLITE DATA OBSERVED FROM TARGET MOTION

Thus far, the result of the discussion in Sections IID, IIE, and IIIA of this report effectively has been to develop an algorithm for describing the motion of a near-earth target, given the parameters of the orbit of the tracking satellite and the observed target data. No matter what method of analysis is employed, however, any observability study requires first a target model, and then some series of observations based on target behavior; therefore it now

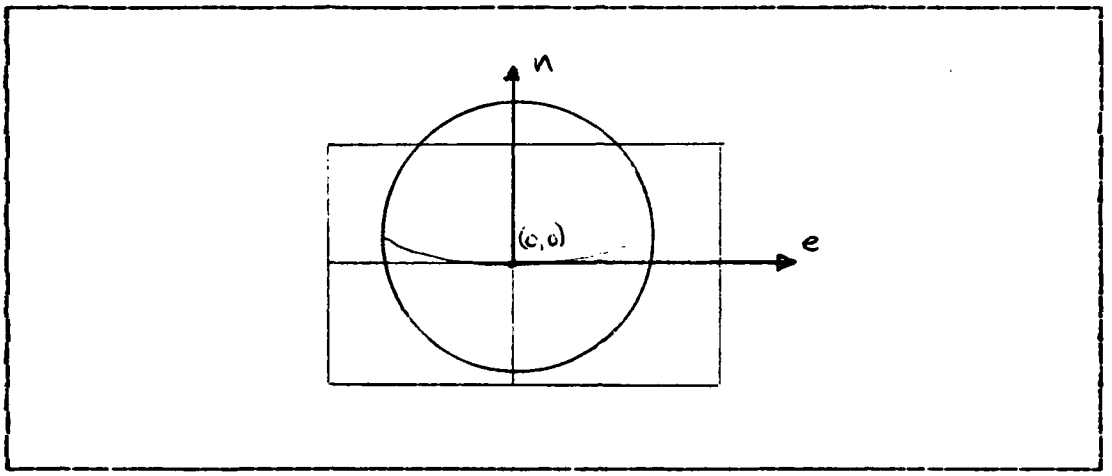

Figure 3.1 Earth's Surface Projected onto Cartesian Grid

compute the velocity components if they are not readily available. If the earth's surface is projected upward onto a Cartesian Grid with its origin at $(L, \lambda) = (0,0)$ as in Figure 3.1, then a position (n,e,h_T) would be described by equations 3.1, with h_T unchanged from Chapter II.

$$n = r_o L_T$$

$$e = r_o \lambda_T \cos L_T \tag{3.1}$$

If rate data is available from the satellite, then the northerly and easterly velocity components are computed simply by differentiating equations 3.1 with respect to time; obviously, $\dot{h}_T$ is once again as in Chapter II.

$$V_N = \dot{n} = r_o \dot{L}_T$$

$$V_E = \dot{e} = r_o \left[\dot{\lambda}_T \cos L_T - \lambda_T \dot{L}_T \sin L_T \right] \tag{3.2}$$

III. TARGET MOTION

It is henceforth assumed that the satellite's position and orientation in space are known, and thus observed target data can be translated into ground coordinates in accordance with the discussion presented in the last two sections of Chapter II. This leaves the problem of reconstructing the target's motion from the observed data. With an eye toward the observability analysis upcoming in Chapter IV, an effort will be made to employ a linear target model, while the observations will be necessarily highly nonlinear. The alternatives would be nonlinear equations describing both the target's motion and the observation, or a nonlinear plant with a linear observation achieved by another coordinate transformation, both of which would only further complicate the problem at this point. They do present viable possibilities, however, which might be investigated as part of a search for convenient coordinates conducive to appropriate nonlinear observability analysis and tracking design.

A. TARGET MOTION RECONSTRUCTED FROM SATELLITE DATA

In Chapter II, algorithms were developed for transforming raw satellite sensor information into ground coordinate data; given range and bearings, the computational result is target latitude and longitude. If range and bearing rate information is also available, the result is then latitude and longitude rates.

To reconstruct the target's motion from this information is fairly straightforward. The first step is to translate the latitude and longitude into linear distances, and then

This completes the description of the recorded data available from the orbiting satellite and its observation of a near-surface target. The next chapter is devoted to reconstructing the target's motion from this information; this will then lead to the observability analysis of Chapter IV.

Having transformed the raw rate data to the reference coordinate rates with equations 2.24 through 2.26, these rates are then translated to earth's surface coordinates by differentiating equations 2.17 through 2.23 .

Then, from 2.17 (surface target),

$$\dot{\rho} = \frac{2R\dot{R}}{r_o(r_o+h_s)\sin\rho} ; \qquad (2.27)$$

from 2.18 ,

$$\dot{h}_T = \frac{\dot{R}\left(R-(r_o+h_s)\cos\beta\right) + R(r_o+h_s)\dot{\beta}\sin\beta}{r_o+h_T} ; \qquad (2.28)$$

from 2.19 (air target),

$$\dot{\rho} = \frac{(r_o+h_T)\left[\dot{R}\sin\beta + R\dot{\beta}\cos\beta\right] - R\dot{h}_T\sin\beta}{(r_o+h_T)^2\cos\rho} ; \qquad (2.29)$$

and in either case, $\dot{x} = r_o\dot{\rho}$.

From 2.20 ,

$$\dot{L}_T = \frac{1}{\cos L_T}\left[\dot{L}_S\left[\cos L_S\cos\rho - \sin L_S\sin\rho\cos\alpha\right] - \dot{\alpha}\cos L_S\sin\rho\sin\alpha + \dot{\rho}\left[\cos L_S\cos\rho\cos\alpha - \sin L_S\sin\rho\right]\right] , \qquad (2.30)$$

and from 2.21 through 2.23 ,

$$\dot{\lambda}_T = \dot{x} + \dot{\lambda}_S = \frac{1}{\cos L_T\cos L_S\sin x}\left[\dot{\rho}\sin\rho + \dot{L}_T\left[\cos L_T\sin L_S - \sin L_T\cos L_S\cos x\right] - \dot{L}_S\left[\sin L_T\cos L_S - \cos L_T\sin L_S\cos x\right]\right] + \dot{\lambda}_S . \qquad (2.31)$$

These equations 2.24 through 2.31 completely define the derivation of target latitude and longitude rates based on raw angular and range rate data available at the satellite. If applied sequentially by a computer, the target's rate of travel could easily be calculated.

This gives rate of change of the target's coordinates referenced to the satellite's axes and based on the target's motion; if the satellite can instantly fix its position in space, then x-y-z can be transformed to N-E-D by applying the transformation equation 2.13 to correct for satellite attitude. If the satellite's own rate of rotation around its three axes is taken into account, however--i.e. the satellite is tumbling fast enough to affect significantly the observed angular rates--then that transformation 2.13 must also be differentiated, i.e.

$$\begin{bmatrix} \dot{N} \\ \dot{E} \\ \dot{D} \end{bmatrix} = \left[\dot{\mathbb{T}}_3 \mathbb{T}_2 \mathbb{T}_1 + \mathbb{T}_3 \dot{\mathbb{T}}_2 \mathbb{T}_1 + \mathbb{T}_3 \mathbb{T}_2 \dot{\mathbb{T}}_1 \right] \begin{bmatrix} \dot{x} \\ \dot{y} \\ \dot{z} \end{bmatrix},$$

$$\dot{\mathbb{T}}_1 = \begin{bmatrix} 0 & 0 & 0 \\ 0 & -\sin\delta_1 & \cos\delta_1 \\ 0 & -\cos\delta_1 & -\sin\delta_1 \end{bmatrix} \dot{\delta}_1, \qquad (2.25)$$

where

$$\dot{\mathbb{T}}_2 = \begin{bmatrix} -\sin\delta_2 & 0 & -\cos\delta_2 \\ 0 & 0 & 0 \\ \cos\delta_2 & 0 & -\sin\delta_2 \end{bmatrix} \dot{\delta}_2, \quad \dot{\mathbb{T}}_3 = \begin{bmatrix} -\sin\delta_3 & \cos\delta_3 & 0 \\ -\cos\delta_3 & -\sin\delta_3 & 0 \\ 0 & 0 & 0 \end{bmatrix} \dot{\delta}_3$$

In the next step, equations 2.15 are differentiated to obtain

$$\dot{R} = \frac{N\dot{N} + E\dot{E} + D\dot{D}}{R},$$

$$\dot{\alpha} = \frac{N\dot{E} - E\dot{N}}{N^2 + E^2},$$

$$\dot{\beta} = \frac{R\dot{D} - D\dot{R}}{R\sqrt{N^2 + E^2}}. \qquad (2.26)$$

and finally

$$\lambda_T = \lambda_s + \pi. \tag{2.23}$$

It should be emphasized that both latitudes are referenced North here, and both longitudes East. To switch to south latitude and/or west longitude, one need only know

For N Lat < 0, S Lat = -N Lat;
For E Long < 0, W Long = -E Long;
For E Long > 180, W Long = 360 - E Long.

Sample calculations using these equations reveal that it takes a significant amount of target elevation to generate an appreciable change in β, i.e. at a range of 1000 nm from a satellite at elevation 600nm, a target flying at 25000 ft would have a β angle only 0.2° different from that of a surface target. Therefore, depending on its sensitivity, the satellite sensor may or may not distinguish betwen target types, if dependent on a single look at position only. The necessarily greater speed of the air target, however, will ultimately become obvious if the satellite system is either capable of calculating range and bearing rates based on multiple observations, or else rate information is an intrinsic part of the single observation. Therefore, this model must provide for the satellite's ability to observe $\dot{R}$, $\dot{\alpha}$, and $\dot{\beta}$ in addition or as opposed to R, α, and β. The transformation equations 2.14 through 2.23 must then be differentiated with respect to time to get the range and bearing rates referenced to N-E-D, and then the target's latitude, longitude, and altitude rates.

Differentiating equations 2.14,

$$\begin{aligned}
\dot{x} &= \dot{R}\sin\beta_c\cos\alpha_o + R\dot{\beta}_c\cos\beta_c\cos\alpha - R\dot{\alpha}_o\sin\beta_c\sin\alpha_o, \\
\dot{y} &= \dot{R}\sin\beta_c\sin\alpha_o + R\dot{\beta}_c\cos\beta_c\sin\alpha_o + R\dot{\alpha}_o\sin\beta_c\cos\alpha_o, \\
\dot{z} &= \dot{R}\cos\beta_c - R\dot{\beta}_o\sin\beta_c.
\end{aligned} \tag{2.24}$$

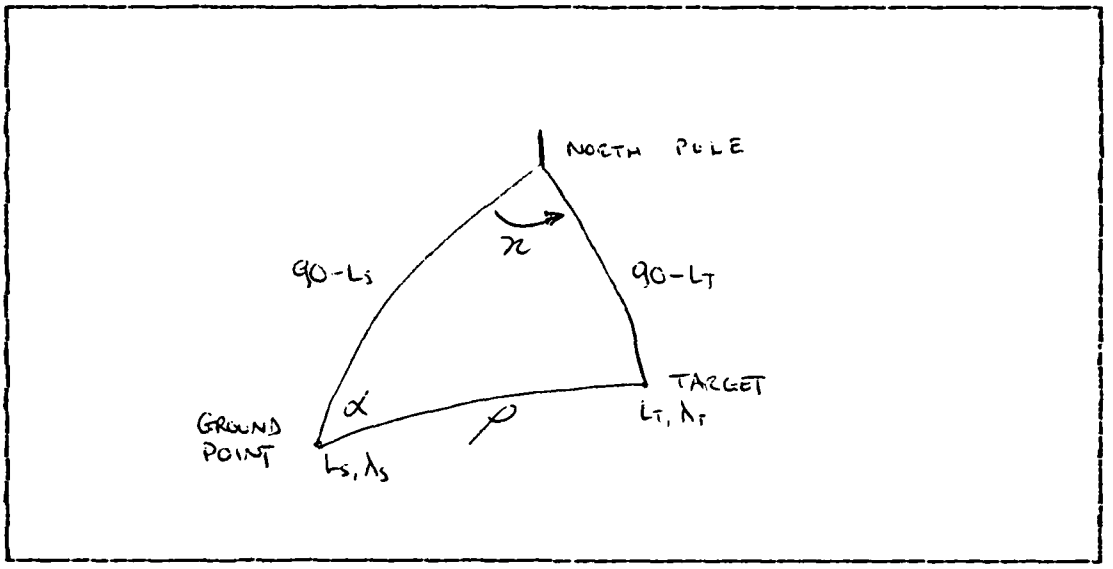

Figure 2.16 Surface Triangle for Target Position

and longitude may be calculated by using the spherical triangle shown in Figure 2.16 . Using the law of cosines for spherical triangles, and realizing now that it is actually more convenient to work with earth-central angles rather than great circle distances, then

$$\cos(90-L_T) = \cos(90-L_S)\cos\rho + \sin(90-L_S)\sin\rho\cos\alpha,$$

or, equivalently,

$$L_T = \sin^{-1}\left[\sin L_S \cos\rho + \cos L_S \sin\rho \cos\alpha\right]. \qquad (2.20)$$

Similarly,

$$\cos\rho = \cos(90-L_T)\cos(90-L_S) + \sin(90-L_T)\sin(90-L_S)\cos\chi, \qquad (2.21)$$

or, solving for χ ,

$$\chi = \cos^{-1}\left[\frac{\cos\rho - \sin L_T \sin L_S}{\cos L_T \cos L_S}\right], \qquad (2.22)$$

$$\dot{\underline{x}}(t) = \begin{bmatrix} 0&1&0&0&0&0 \\ 0&0&0&0&0&0 \\ 0&0&0&1&0&0 \\ 0&0&0&0&0&0 \\ 0&0&0&0&0&1 \\ 0&0&0&0&0&0 \end{bmatrix} \underline{x}(t) + \begin{bmatrix} 0&0&0 \\ 1&0&0 \\ 0&0&0 \\ 0&1&0 \\ 0&0&0 \\ 0&0&1 \end{bmatrix} \underline{u}(t); \quad \underline{y}(t) = \underline{H}(\underline{x}(t)) = \begin{bmatrix} R(\underline{x}(t)) \\ \dot{R}(\underline{x}(t)) \\ \alpha(\underline{x}(t)) \\ \dot{\alpha}(\underline{x}(t)) \\ \beta(\underline{x}(t)) \\ \dot{\beta}(\underline{x}(t)) \end{bmatrix}$$

WHERE

$$L_T = \frac{n}{r_0}, \quad \dot{L}_T = \frac{\dot{n}}{r_0}$$

$$\lambda_T = \frac{e}{r_0 \cos L_T}, \quad \dot{\lambda}_T = \frac{\dot{e}\cos L_T + \dot{L}_T e \sin L_T}{r_0 \cos^2 L_T}$$

$$\chi = \lambda_T - \lambda_S, \quad \dot{\chi} = \dot{\lambda}_T - \dot{\lambda}_S$$

$$\rho = \cos^{-1}\left[\sin L_T \sin L_S + \cos L_T \cos L_S \cos\chi\right]$$

$$\dot{\rho} = \frac{1}{\sin\rho}\left[\dot{L}_T\left(\sin L_T \cos L_S \cos\chi - \cos L_T \sin L_S\right) + \dot{\chi}\cos L_T \cos L_S \sin\chi + \dot{L}_S\left(\cos L_T \sin L_S \cos\chi - \sin L_T \cos L_S\right)\right]$$

$$H_1 = R = \left[(r_0+h_T)^2 + (r_0+h_S)^2 - 2(r_0+h_T)(r_0+h_S)\cos\rho\right]^{1/2}$$

$$H_2 = \dot{R} = \frac{1}{R}\left[\dot{h}_T\left[(r_0+h) - (r_0+h_S)\cos\rho\right] + \dot{\rho}(r_0+h_T)(r_0+h_S)\sin\rho\right]$$

$$H_3 = \alpha = \sin^{-1}\left[\frac{\cos L_T \sin\chi}{\sin\rho}\right]$$

$$H_4 = \dot{\alpha} = \frac{\sin\rho\left[\dot{\chi}\cos L_T \cos\chi - \dot{L}_T \sin L_T \sin\chi\right] - \dot{\rho}\cos L_T \sin\chi\cos\rho}{\cos\alpha \sin^2\rho}$$

$$H_5 = \beta = \cos^{-1}\left[\frac{R^2 + (r_0+h_S)^2 - (r_0+h_T)^2}{2R(r_0+h_S)}\right]$$

$$H_6 = \dot{\beta} = \frac{2R(r_0+h_T)\dot{h}_T - \dot{R}\left(R^2 - (r_0+h_S)^2 + (r_0+h_T)^2\right)}{2R^2(r_0+h_S)\sin\beta}$$

Figure 3.3 Summary of State and Observer Equations Including Intermediate Variables

3. Two Simpler Cases

The significant complexity of these equations suggests that some simpler representation of the system might be useful in the observability analysis, if only to test the method prior to its employment on the system of Figure 3.3 . One approximation might be to presume for the moment that the satellite is directly overhead the target, and that relative motion between them is arbitrarily small enough that the Earth is approximately planar beneath it; for the trigonometric functions,

$$\tan\beta \doteq \sin\beta \doteq \beta \qquad \text{and} \qquad \cos\beta \doteq 1.$$

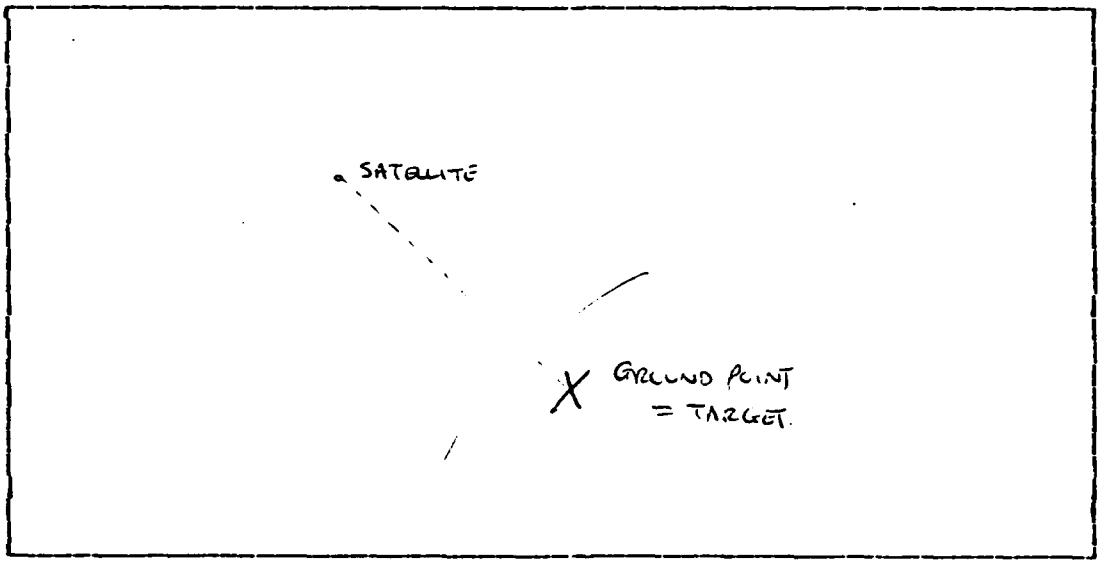

Figure 3.4 Satellite Directly Overhead the Target

If one considers that for a satellite directly overhead the target as shown in Figure 3.4,

$$L_T = L_S, \quad \lambda_T = \lambda_S, \qquad \text{and} \qquad h_T = h_S - R.$$

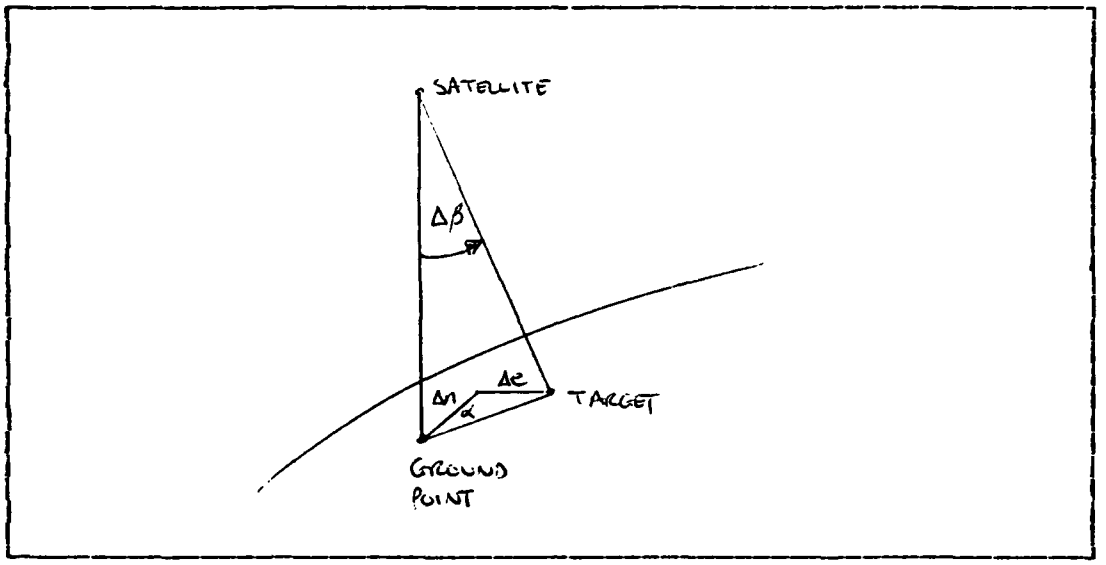

Figure 3.5 Perturbation About the Observation From Directly Overhead

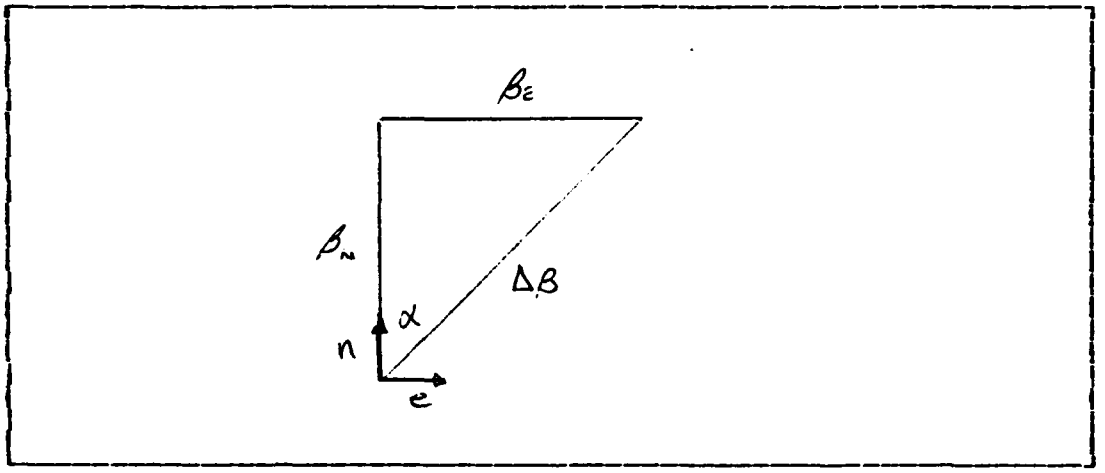

Figure 3.6 Resolution of Beta Along the N-E Axes

then for a satellite nearly overhead the target, the problem can be considered as a perturbation about the directly overhead case. In Figure 3.5, let

$$
\begin{aligned}
X_1 &= \Delta n \doteq r_0 (L_T - L_S), \\
X_2 &= \Delta \dot{n} \doteq V_N - r_0 \dot{L}_S, \\
X_3 &= \Delta e \doteq r_0 \cos L_S (\lambda_T - \lambda_S), \\
X_4 &= \Delta \dot{e} \doteq V_E - r_0 \cos L_S \dot{\lambda}_S, \\
X_5 &= \Delta h \doteq h_S - h_T, \\
X_6 &= \Delta \dot{h} = -\dot{h}_T .
\end{aligned}
\tag{3.17}
$$

To fully linearize the problem, it turns out that β must be eliminated; this can be done (in this special case only) as shown in Figure 3.6:

$$
\begin{aligned}
\beta_N &= \Delta\beta \cos\alpha, \\
\beta_E &= \Delta\beta \sin\alpha .
\end{aligned}
\tag{3.18}
$$

Now the observation may be defined by

$$
\underline{y} = \begin{bmatrix} H_1 \\ H_2 \\ H_3 \\ H_4 \\ H_5 \\ H_6 \end{bmatrix} = \begin{bmatrix} X_5 \\ X_6 \\ X_1/h_S \\ X_2/h_S \\ X_3/h_S \\ X_4/h_S \end{bmatrix} . \tag{3.19}
$$

Thus the continuous system is described by

$$
\dot{\underline{x}}(t) = \begin{bmatrix} 0&1&0&0&0&0 \\ 0&0&0&0&0&0 \\ 0&0&0&1&0&0 \\ 0&0&0&0&0&0 \\ 0&0&0&0&0&1 \\ 0&0&0&0&0&0 \end{bmatrix} \underline{x}(t) + \begin{bmatrix} 0&0&0 \\ 1&0&0 \\ 0&0&0 \\ 0&1&0 \\ 0&0&0 \\ 0&0&1 \end{bmatrix} \underline{u}(t),
$$

$$
\underline{y}(t) = \begin{bmatrix} 0&0&0&0&1&0 \\ 0&0&0&0&0&1 \\ 1/h_S&0&0&0&0&0 \\ 0&1/h_S&0&0&0&0 \\ 0&0&1/h_S&0&0&0 \\ 0&0&0&1/h_S&0&0 \end{bmatrix} \underline{x}(t). \tag{3.20}
$$

and the corresponding discrete system plant is

$$\underline{X}(K+1) = \begin{bmatrix} 1 & T & 0 & 0 & 0 & 0 \\ 0 & 1 & 0 & 0 & 0 & 0 \\ 0 & 0 & 1 & T & 0 & 0 \\ 0 & 0 & 0 & 1 & 0 & 0 \\ 0 & 0 & 0 & 0 & 1 & T \\ 0 & 0 & 0 & 0 & 0 & 1 \end{bmatrix} \underline{X}(K) + \begin{bmatrix} T^2/2 & 0 & 0 \\ T & 0 & 0 \\ 0 & T^2/2 & 0 \\ 0 & T & 0 \\ 0 & 0 & T^2/2 \\ 0 & 0 & T \end{bmatrix} \underline{U}(K), \tag{3.21}$$

with the same observer matrix as above but with values taken only at discrete points in time.

Experimental computations show that for a satellite at altitude 600nm and a target at less than 60° latitude, these approximations yield about one percent error or less for β less than 5°; however, the maximum possible overhead time during which this model applies is about 20 seconds. It follows then that this sort of observation could only be made a very few times during the satellite's revolution, severely limiting the real-world usefulness of this linear model. For the purpose of examining the observability of the target under these conditions, however, the model should still prove quite useful.

The other simplified model that might be instrumental in gaining some insight into the method of the observability analysis is the simplest nonlinear case, i.e. the satellite tracking a fixed point on the earth's surface. Simplifying the equations 3.5 through 3.16 yields the system depicted by the equations in Figure 3.7

This completes the various derivations for all the target models.

$$\underline{x} = \begin{bmatrix} n \\ e \end{bmatrix}, \quad \dot{\underline{x}}(t) = \underline{0}, \quad \underline{y} = \underline{H}(\underline{x}(t)) \text{ AS IN FIGURE 3.3}$$

$$L_T = \frac{n}{r_c}, \quad \dot{L}_T = 0$$

$$\lambda_T = \frac{e}{r_c \cos L_T}, \quad \dot{\lambda}_T = 0$$

$$\alpha = \lambda_T - \lambda_S, \quad \dot{\alpha} = \dot{\lambda}_T - \dot{\lambda}_S$$

$$\rho = \cos^{-1}\left[\sin L_T \sin L_S + \cos L_T \cos L_S \cos\alpha\right]$$

$$\dot{\rho} = \frac{1}{\sin\rho}\left[\dot{L}_S\left(\cos L_T \sin L_S \cos\alpha - \sin L_T \cos L_S\right) + \dot{\alpha}\cos L_T \cos L_S \sin\alpha\right]$$

$$H_1 = R = \left[r_c^2 + (r_c + h_S)^2 - 2 r_c (r_c + h_S)\cos\rho\right]^{1/2}$$

$$H_2 = \dot{R} = \frac{\dot{\rho}\, r_c (r_c + h_S)\sin\rho}{R}$$

$$H_3 = \alpha = \sin^{-1}\left[\frac{\cos L_T \sin\alpha}{\sin\rho}\right]$$

$$H_4 = \dot{\alpha} = \frac{\dot{\alpha}\sin\rho\cos L_T \cos\alpha - \dot{\rho}\cos L_T \sin\alpha\cos\rho}{\cos\alpha \sin^2\rho}$$

$$H_5 = \beta = \cos^{-1}\left[\frac{R^2 + (r_c + h_S)^2 - r_c^2}{2R(r_c + h_S)}\right]$$

$$H_6 = \dot{\beta} = \frac{-\dot{R}\left[R^2 + r_c^2 - (r_c + h_S)^2\right]}{2R^2 (r_c + h_S)\sin\beta}$$

Figure 3.7 Equations for Tracking a Fixed Target

IV. TARGET OBSERVABILITY

This Chapter is subdivided into three major sections, specifically the observability analyses of the three different target models developed in Chapter III. First, the linearized model will be analyzed by the method of [Ref. 2], and then the stationary target and the general-case, nonlinear, moving target will be analyzed by the method developed in [Ref. 1].

A. OBSERVABILITY OF THE LINEARIZED MODEL

For convenience' sake, the linearized model has been subdivided into four cases, namely surface and air targets with discrete and continuous modeling for each. The method of [Ref. 2] is the formation of the observability matrix $\underset{\sim}{G}$ from the system

$$\dot{\underset{\sim}{x}} = \underset{\sim}{A}\underset{\sim}{x} + \underset{\sim}{B}\underset{\sim}{u}$$
$$\underset{\sim}{y} = \underset{\sim}{C}\underset{\sim}{x}$$

such that $$\underset{\sim}{G} = \left[\underset{\sim}{C}^T \mid \underset{\sim}{A}^T\underset{\sim}{C}^T \mid \underset{\sim}{A}^{T^2}\underset{\sim}{C}^T \mid \cdots \underset{\sim}{A}^{T^{n-1}}\underset{\sim}{C}^T\right]$$

for n observations, and for system observability, $\underset{\sim}{G}$ must be nonsingular. In the following derivations, the minimum amount of information necessary for observability is considered.

1. Surface Target Continuous Model

The system model is

$$\dot{\underset{\sim}{x}}(t) = \begin{bmatrix} 0 & 1 & 0 & 0 \\ 0 & 0 & 0 & 0 \\ 0 & 0 & 0 & 1 \\ 0 & 0 & 0 & 0 \end{bmatrix} \underset{\sim}{x}(t) + \begin{bmatrix} 0 & 0 \\ 1 & 0 \\ 0 & 0 \\ 0 & 1 \end{bmatrix} \underset{\sim}{u}(t)$$

For a single look,

$$\underline{y}(t) = \begin{bmatrix} \beta_N \\ \dot{\beta}_N \\ \beta_E \\ \dot{\beta}_E \end{bmatrix} = 1/h_s \begin{bmatrix} 1 & 0 & 0 & 0 \\ 0 & 1 & 0 & 0 \\ 0 & 0 & 1 & 0 \\ 0 & 0 & 0 & 0 \end{bmatrix} \underline{x}(t)$$

is required; then $\underset{\sim}{G} = \left[\underline{C}^T \mid \underline{A}^T\underline{C}^T \cdots\right] = \underline{C}^T = \underline{C}$.

For two or more looks,

$$\underline{y}(t) = \begin{bmatrix} \beta_N \\ \beta_E \end{bmatrix} = 1/h_s \begin{bmatrix} 1 & 0 & 0 & 0 \\ 0 & 0 & 1 & 0 \end{bmatrix} \underline{x}(t)$$

is required, and

$$\underset{\sim}{G} = \left[\underline{C}^T \mid \underline{A}^T\underline{C}^T\right] = 1/h_s \left[\begin{array}{cc|cc} 1 & 0 & 0 & 0 \\ 0 & 0 & 1 & 0 \\ \hline 0 & 1 & 0 & 0 \\ 0 & 0 & 0 & 1 \end{array}\right].$$

For the next observation, $\underline{A}^{T^2} = \underline{0}$, so there is no need to take the process any further. If only position observability is desired, rather then full state observability, then

$$\underline{y} = \begin{bmatrix} \beta_N \\ \beta_E \end{bmatrix}$$

is enough even for only a single observation.

2. Surface Target Discrete Model

Now the system model is

$$\underline{x}(K+1) = \begin{bmatrix} 1 & T & 0 & 0 \\ 0 & 1 & 0 & 0 \\ 0 & 0 & 1 & T \\ 0 & 0 & 0 & 1 \end{bmatrix} \underline{x}(K) + \begin{bmatrix} T^2/2 & 0 \\ T & 0 \\ 0 & T^2/2 \\ 0 & T \end{bmatrix} \underline{u}(K).$$

For a single look,

$$\underline{y}(K) = \begin{bmatrix} \beta_N \\ \dot{\beta}_N \\ \beta_E \\ \dot{\beta}_E \end{bmatrix} = 1/h_s \begin{bmatrix} 1 & 0 & 0 & 0 \\ 0 & 1 & 0 & 0 \\ 0 & 0 & 1 & 0 \\ 0 & 0 & 0 & 1 \end{bmatrix} \underline{x}(K)$$

is required, and $\underline{G} = \underline{C}^T$ just as before. For two or more looks,

$$\underline{y}(K) = 1/n_s \begin{bmatrix} 1 & 0 & 0 & 0 \\ 0 & 0 & 1 & 0 \end{bmatrix} \underline{x}(K)$$

is required, and

$$\underline{G} = 1/n_s \begin{bmatrix} 1 & 0 & T & 0 \\ 0 & 0 & T & 0 \\ 0 & 1 & 0 & 1 \\ 0 & 0 & 0 & T \end{bmatrix}.$$

which simplifies easily to the same nonsingular matrix obtained in the analogous continuous case.

Obviously for this simplified case, the transition from continuous to discrete modeling made no difference; it has been implicitly assumed that the discrete samples are taken often enough that all maneuvers (i.e. accelerations) are observed, in accordance with the Sampling (or Shannon Information) Theorem familiar from communications applications. Otherwise, observability will decrease significantly as information about the target is lost.

3. Air Target Continuous Model

The system is now modeled by

$$\dot{\underline{x}}(t) = \begin{bmatrix} 0 & 1 & 0 & 0 & 0 & 0 \\ 0 & 0 & 0 & 0 & 0 & 0 \\ 0 & 0 & 0 & 1 & 0 & 0 \\ 0 & 0 & 0 & 0 & 0 & 0 \\ 0 & 0 & 0 & 0 & 0 & 1 \\ 0 & 0 & 0 & 0 & 0 & 0 \end{bmatrix} \underline{x}(t) + \begin{bmatrix} 0 & 0 & 0 \\ 1 & 0 & 0 \\ 0 & 0 & 0 \\ 0 & 1 & 0 \\ 0 & 0 & 0 \\ 0 & 0 & 1 \end{bmatrix} \underline{u}(t).$$

For a single look,

$$\underline{y}(t) = \begin{bmatrix} 0 & 0 & 0 & 0 & 1 & 0 \\ 0 & 0 & 0 & 0 & 0 & 1 \\ 1/n_s & 0 & 0 & 0 & 0 & 0 \\ 0 & 1/n_s & 0 & 0 & 0 & 0 \\ 0 & 0 & 1/n_s & 0 & 0 & 0 \\ 0 & 0 & 0 & 1/n_s & 0 & 0 \end{bmatrix} \underline{x}(t)$$

is required, and $\underline{G} = \underline{C}^T$ as in the surface target cases. For two or more looks,

$$\underline{y}(t) = \begin{bmatrix} R \\ \beta_m \\ \beta_e \end{bmatrix} = \begin{bmatrix} 0 & 0 & 0 & 0 & 1 & 0 \\ 1/h_s & 0 & 0 & 0 & 0 & 0 \\ 0 & 0 & 1/h_s & 0 & 0 & 0 \end{bmatrix} \underline{x}(t)$$

is required, and

$$\underline{G} = \begin{bmatrix} 0 & 1/h_s & 0 & 0 & 0 & 0 \\ 0 & 0 & 0 & 0 & 1/h_s & 0 \\ 0 & 0 & 1/h_s & 0 & 0 & 0 \\ 0 & 0 & 0 & 0 & 0 & 1/h_s \\ 1 & 0 & 0 & 0 & 0 & 0 \\ 0 & 0 & 0 & 1 & 0 & 0 \end{bmatrix}$$

for complete observability. As in the surface case, if only position observability is desired, then

$$\underline{y}(t) = \begin{bmatrix} R \\ \beta_m \\ \beta_e \end{bmatrix}$$

is adequate even with only the single observation.

4. Air Target Discrete Model

The model has now become

$$\underline{x}(KH) = \begin{bmatrix} 1 & T & 0 & 0 & 0 & 0 \\ 0 & 1 & 0 & 0 & 0 & 0 \\ 0 & 0 & 1 & T & 0 & 0 \\ 0 & 0 & 0 & 1 & 0 & 0 \\ 0 & 0 & 0 & 0 & 1 & T \\ 0 & 0 & 0 & 0 & 0 & 1 \end{bmatrix} \underline{x}(K) + \begin{bmatrix} T^2/2 & 0 & 0 \\ T & 0 & 0 \\ 0 & T^2/2 & 0 \\ 0 & T & 0 \\ 0 & 0 & T^2/2 \\ 0 & 0 & T \end{bmatrix} \underline{u}(K).$$

For a single look,

$$\underline{y}(K) = \begin{bmatrix} 0 & 0 & 0 & 0 & 1 & 0 \\ 0 & 0 & 0 & 0 & 0 & 1 \\ 1/h_s & 0 & 0 & 0 & 0 & 0 \\ 0 & 1/h_s & 0 & 0 & 0 & 0 \\ 0 & 0 & 1/h_s & 0 & 0 & 0 \\ 0 & 0 & 0 & 1/h_s & 0 & 0 \end{bmatrix} \underline{x}(K)$$

is required, and as expected, $\underset{\sim}{G} = \underset{\sim}{C}^T$ again. For two or more looks,

$$\underline{y}(K) = \begin{bmatrix} R \\ \beta_w \\ \beta_s \end{bmatrix} = \begin{bmatrix} 0 & 0 & 0 & 0 & 1 & 0 \\ 1/h_s & 0 & 0 & 0 & 0 & 0 \\ 0 & 0 & 1/h_s & 0 & 0 & 0 \end{bmatrix} \underline{x}(K)$$

is needed, and

$$\underset{\sim}{G} = \left[\begin{array}{cc|cc|cc} 0 & 1/h_s & 0 & 0 & 1/h_s & 0 \\ 0 & 0 & 0 & 0 & T/h_s & 0 \\ 0 & 0 & 1/h_s & 0 & 0 & 1/h_s \\ 0 & 0 & 0 & 0 & 0 & T/h_s \\ 1 & 0 & 0 & 1 & 0 & 0 \\ 0 & 0 & 0 & T & 0 & 0 \end{array}\right]$$

which simplifies to the same nonsingular matrix as in the continuous case. Again, the assumption has been made that information is sampled at the minimum (i.e. Nyquist) rate, which is twice as often as the target's highest frequency of maneuver.

B. NONLINEAR MODEL OF THE STATIONARY TARGET

Applying the method of [Ref. 1], summarized here briefly, concerns primarily the analysis of a Jacobian matrix defined by

$$\underset{\sim}{J} = \begin{bmatrix} \frac{\partial y}{\partial x_1} & \frac{\partial y}{\partial x_2} & \cdots & \frac{\partial y}{\partial x_n} \\ \frac{\partial \dot{y}}{\partial x_1} & \frac{\partial \dot{y}}{\partial x_2} & \cdots & \frac{\partial \dot{y}}{\partial x_n} \\ \frac{\partial \ddot{y}}{\partial x_1} & \frac{\partial \ddot{y}}{\partial x_2} & \cdots & \frac{\partial \ddot{y}}{\partial x_n} \\ \vdots & \vdots & & \vdots \\ \frac{\partial y^{(n-1)}}{\partial x_1} & \frac{\partial y^{(n-1)}}{\partial x_2} & \cdots & \frac{\partial y^{(n-1)}}{\partial x_n} \end{bmatrix}$$

for each observation of an n-system. A nonzero determinant will show that all the states in $\underline{x}$ are connected to at least one of the measurements $\underline{y}$, and so an inverse function exists such that

$$\underset{\sim}{x} = \underset{\sim}{H}^{-1}(\underset{\sim}{y}).$$

For observability, however, this mapping of $\underset{\sim}{y}$ back into $\underset{\sim}{x}$ must be one-to-one, so that a particular series of measurements $\underset{\sim}{y}$ will always determine a unique initial state $\underset{\sim}{x}(t_o)$. This requirement is satisfied if a second condition is met, i.e. $\underset{\sim}{J}$ must be positive or negative definite, and the mapping unique with finite covering. The complete proof of these concepts is presented in [Ref. 1] and [Ref. 7]. For multiple observation variables (i.e. numbering m), an n x mn matrix is formed; if any n x n matrix can be extracted that satisfies these conditions, the system will be observable. For the six-variable, six-observation case upcoming in Section C of this chapter, this will lead to a great many possibilities and problems, but for the two-variable case of this section, the method should prove very useful. The approach will be to first consider each observation separately, and then in combination.

Starting from the equations for the observation of the stationary target depicted in Figure 3.7, derivation of the Jacobian matrix for y = R is accomplished by means of implicit differentiation along the lines of functional dependency depicted in Figure 4.1 . Consider

$$\frac{\partial y_1}{\partial x_1} = \frac{\partial R}{\partial n} = \frac{\partial R}{\partial \rho}\left[\frac{\partial \rho}{\partial L_T} + \frac{\partial \rho}{\partial \kappa}\frac{\partial \kappa}{\partial \lambda_T}\frac{\partial \lambda_T}{\partial L_T}\right]\frac{\partial L_T}{\partial n},$$

$$\frac{\partial y_1}{\partial x_2} = \frac{\partial R}{\partial e} = \frac{\partial R}{\partial \rho}\frac{\partial \rho}{\partial \kappa}\frac{\partial \kappa}{\partial \lambda_T}\frac{\partial \lambda_T}{\partial e},$$

$$\frac{\partial \dot{y}_1}{\partial x_1} = \frac{\partial \dot{R}}{\partial n} = \left[\left[\frac{\partial \dot{R}}{\partial R}\frac{\partial R}{\partial \rho} + \frac{\partial \dot{R}}{\partial \rho} + \frac{\partial \dot{R}}{\partial \dot{\rho}}\frac{\partial \dot{\rho}}{\partial \rho}\right]\left[\frac{\partial \rho}{\partial L_T} + \frac{\partial \rho}{\partial \kappa}\frac{\partial \kappa}{\partial \lambda_T}\frac{\partial \lambda_T}{\partial L_T}\right] + \frac{\partial \dot{R}}{\partial \dot{\rho}}\left[\frac{\partial \dot{\rho}}{\partial L_T} + \frac{\partial \dot{\rho}}{\partial \kappa}\frac{\partial \kappa}{\partial \lambda_T}\frac{\partial \lambda_T}{\partial L_T}\right]\right]\frac{\partial L_T}{\partial n},$$

$$\frac{\partial \dot{y}_1}{\partial x_2} = \frac{\partial \dot{R}}{\partial e} = \left[\left[\frac{\partial \dot{R}}{\partial R}\frac{\partial R}{\partial \rho} + \frac{\partial \dot{R}}{\partial \rho} + \frac{\partial \dot{R}}{\partial \dot{\rho}}\frac{\partial \dot{\rho}}{\partial \rho}\right]\frac{\partial \rho}{\partial \kappa} + \frac{\partial \dot{R}}{\partial \dot{\rho}}\frac{\partial \dot{\rho}}{\partial \kappa}\right]\frac{\partial \kappa}{\partial \lambda_T}\frac{\partial \lambda_T}{\partial e}.$$

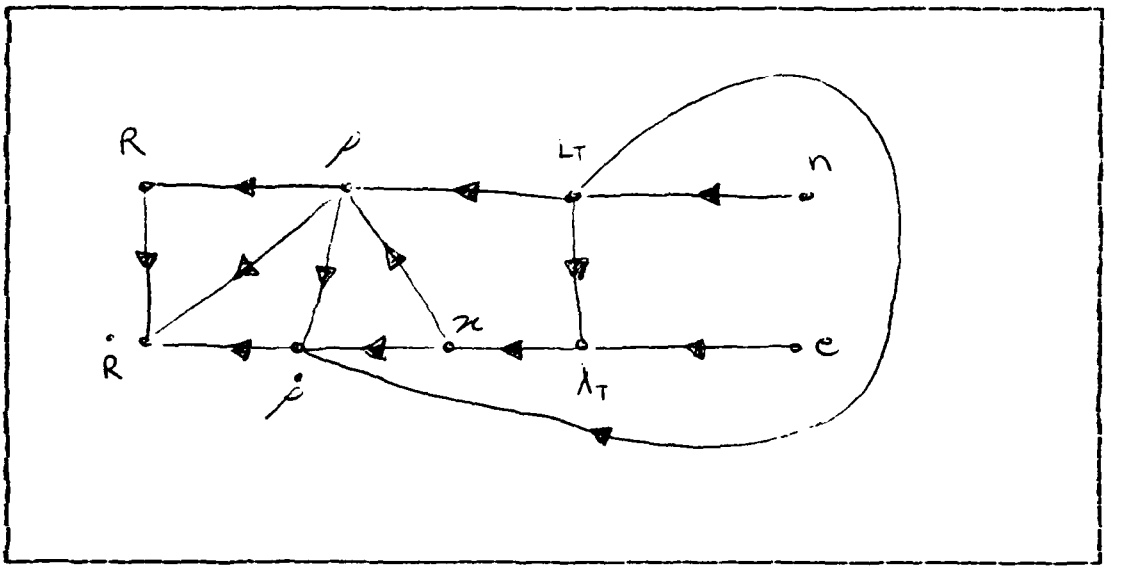

Figure 4.1 Functional Relaticnship of R and R to n and e

Thus the Jacobian matrix for R is written

$$\underset{\sim}{J}_1 = \begin{bmatrix} \frac{\partial R}{\partial n} & \frac{\partial R}{\partial e} \\ \frac{\partial \dot{R}}{\partial n} & \frac{\partial \dot{R}}{\partial e} \end{bmatrix}.$$

Simplification of the determinant results in

$$|\underset{\sim}{J}_1| = \frac{\partial R}{\partial \rho}\frac{\partial \dot{R}}{\partial \dot{\rho}}\frac{\partial L_T}{\partial n}\frac{\partial \kappa}{\partial \lambda_T}\frac{\partial \lambda_T}{\partial e}\left[\frac{\partial \rho}{\partial L_T}\frac{\partial \dot{\rho}}{\partial \kappa} - \frac{\partial \rho}{\partial \kappa}\frac{\partial \dot{\rho}}{\partial L_T}\right].$$

Substitute for the quantity in brackets:

$$|\underset{\sim}{J}_1| = \frac{\partial R}{\partial \rho}\frac{\partial \dot{R}}{\partial \dot{\rho}}\frac{\partial L_T}{\partial n}\frac{\partial \kappa}{\partial \lambda_T}\frac{\partial \lambda_T}{\partial e}\frac{1}{\sin^2\rho}\cdot$$

$$\left[2\dot{L}_T\cos^2 L_T \sin\kappa + \dot{\lambda}_T \cos L_T \cos\iota_T \left(\cos L_T \sin\iota_T \cos\kappa - \sin L_T \cos\iota_T\right)\right] \qquad (4.1)$$

which is obviously nonzero in the general case but may well have multiple solutions. Based on the criteria just defined, this indicates that both states in $\underline{x}$ are connected to the observation R, but the connection may very well not be one-to-one; some further analysis is obviously required.

The determinants of the $\underset{\sim}{J}$-matrices for each of the other observed variables may well prove similarly ambiguous; considering the observed variables in combination and attempting to establish nonsingularity and positive/negative definiteness of the resultant myriad of Jacobians may well prove difficult in the extreme, if only in the sense of requiring a copious amount of confusing algebra. While the basic geometry of the problem as developed in Chapter II leads one intuitively to the conclusion that a surface position can be uniquely established if either (α, β) or (R, α)--but not (R, β)--data are available, demonstrating it by this method proved a mammoth computational undertaking. Needless to say, when the problem is expanded to the four variables of the moving surface target and then the six variables of the air target, the algebra worsens several times over. The only alternative seemed to be a transformation of coordinates, specifically to a rectangular system, so that the differentiation could include some polynomials instead of only trigonometric functions. The transformation is accomplished as follows: establish a plane at a distance equal to $(h_s - h_t)$ below the satellite perpendicular to the vector connecting the satellite to the earth's center, determining in effect the target's horizon. For a surface target, the point of intersection is the satellite's ground point; for an air target, the intersection is h above the ground point. Then the target's position is projected up into the tangent plane, as shown in Figures 4.2 (a) and (b). It is now possible to establish the relative coordinates as follows:

$$\dot{\tilde{\underline{x}}} = \underset{\sim}{A}\tilde{\underline{x}} - \underset{\sim}{G}\left.\frac{\partial \underline{H}}{\partial \underline{x}}\right|_{\hat{\underline{x}}} \tilde{\underline{x}}$$

$$\text{or } \dot{\tilde{\underline{x}}} = \underset{\sim}{F}\tilde{\underline{x}} \text{ where } \underset{\sim}{F} = \underset{\sim}{A} - \underset{\sim}{G}\left.\frac{\partial \underline{H}}{\partial \underline{x}}\right|_{\hat{\underline{x}}} \tag{5.9}$$

The solution to equation 5.9 is

$$\hat{\underline{x}}(t) = e^{\underset{\sim}{F}t}\hat{\underline{x}}(o) \tag{5.10}$$

which converges for any $\underset{\sim}{F}$ with negative real eigenvalues.

For the time-invariant linear case where $\underset{\sim}{H}$ is a constant matrix, a unique $\underset{\sim}{G}$ matrix exists for any desired set of negative eigenvalues of $\underset{\sim}{F}$; however, for the general case, since $\left.\frac{\partial \underline{H}}{\partial \underline{x}}\right|_{\hat{\underline{x}}}$ obviously varies with state and time, $\underset{\sim}{G}$ must generally be a time-varying or state-varying function. Thus the problem remains, how to calculate $\underset{\sim}{G}$. Many methods have been demonstrated for the case of the time-varying linear observer which could be extended to cover this linearized case; the method of choice here, however, will be the EKF, which requires some preliminary discussion prior to its employment.

B. EXTENDED KALMAN FILTER--BACKGROUND

Both [Ref. 3] and [Ref. 8] discuss the analysis originally employed by Kalman and Bucy to develop the linear case and the so-called Extended Kalman (nonlinear case) filter. It suffices here to state that the theory applies to stochastic systems, rather than the perfectly deterministic system considered thus far, and involves perturbation about a linearized estimate of the target track in the same fashion as Section A above.

$$\underset{\sim}{y} = \underset{\sim}{H}(\hat{\underset{\sim}{x}}) + \left.\frac{\partial \underset{\sim}{H}}{\partial \underset{\sim}{x}}\right|_{\hat{\underset{\sim}{x}}} (\underset{\sim}{x} - \hat{\underset{\sim}{x}}) . \tag{5.4}$$

Now, since the method of [Ref. 8] assumes that only the measurements $\underset{\sim}{y}$ are available, the plant matrix must be simulated by the observer to generate successive estimates, i.e.

$$\dot{\hat{\underset{\sim}{x}}} = \underset{\sim}{A}\hat{\underset{\sim}{x}} , \tag{5.5}$$

However, unless the estimates are coincidentally initialized to values identical to the initial conditions of the actual system, there will be an inherent propogation error. Therefore a correction term must be added to equation 5.5 as follows:

$$\dot{\hat{\underset{\sim}{x}}} = \underset{\sim}{A}\hat{\underset{\sim}{x}} + \underset{\sim}{G}(\underset{\sim}{H}(\underset{\sim}{x}) - \underset{\sim}{H}(\hat{\underset{\sim}{x}})) , \tag{5.6}$$

where $\underset{\sim}{G}$ is the observer gain; the determination of $\underset{\sim}{G}$ will be discussed shortly. Equations 5.1 through 5.6 can be illustrated by the block diagram of Figure 5.1 .

To evaluate $\underset{\sim}{G}$, the first step is to substitute equation 5.4 into equation 5.6 so that

$$\dot{\hat{\underset{\sim}{x}}} = \underset{\sim}{A}\hat{\underset{\sim}{x}} + \underset{\sim}{G}\left.\frac{\partial \underset{\sim}{H}}{\partial \underset{\sim}{x}}\right|_{\hat{\underset{\sim}{x}}} (\underset{\sim}{x} - \hat{\underset{\sim}{x}}) . \tag{5.7}$$

It becomes useful to define the error in $\underset{\sim}{x}$ as

$$\tilde{\underset{\sim}{x}} = \underset{\sim}{x} - \hat{\underset{\sim}{x}} ; \tag{5.8}$$

$\dot{\tilde{\underset{\sim}{x}}}$ is defined by subtracting equation 5.7 from equation 5.3, i.e.

$$\dot{\tilde{\underset{\sim}{x}}} = \dot{\underset{\sim}{x}} - \dot{\hat{\underset{\sim}{x}}} = \underset{\sim}{A}\underset{\sim}{x} - \underset{\sim}{A}\hat{\underset{\sim}{x}} - \underset{\sim}{G}\left.\frac{\partial \underset{\sim}{H}}{\partial \underset{\sim}{x}}\right|_{\hat{\underset{\sim}{x}}} (\underset{\sim}{x} - \hat{\underset{\sim}{x}}) .$$

Substituting equation 5.8 where applicable,

$$\underset{\sim}{y} = \underset{\sim}{H}(\hat{\underset{\sim}{x}}) + \left.\frac{\partial \underset{\sim}{H}}{\partial \underset{\sim}{x}}\right|_{\hat{\underset{\sim}{x}}} (\underset{\sim}{x} - \hat{\underset{\sim}{x}}) + \begin{matrix}\text{HIGHER} \\ \text{ORDER} \\ \text{TERMS}\end{matrix} \quad . \qquad (5.2)$$

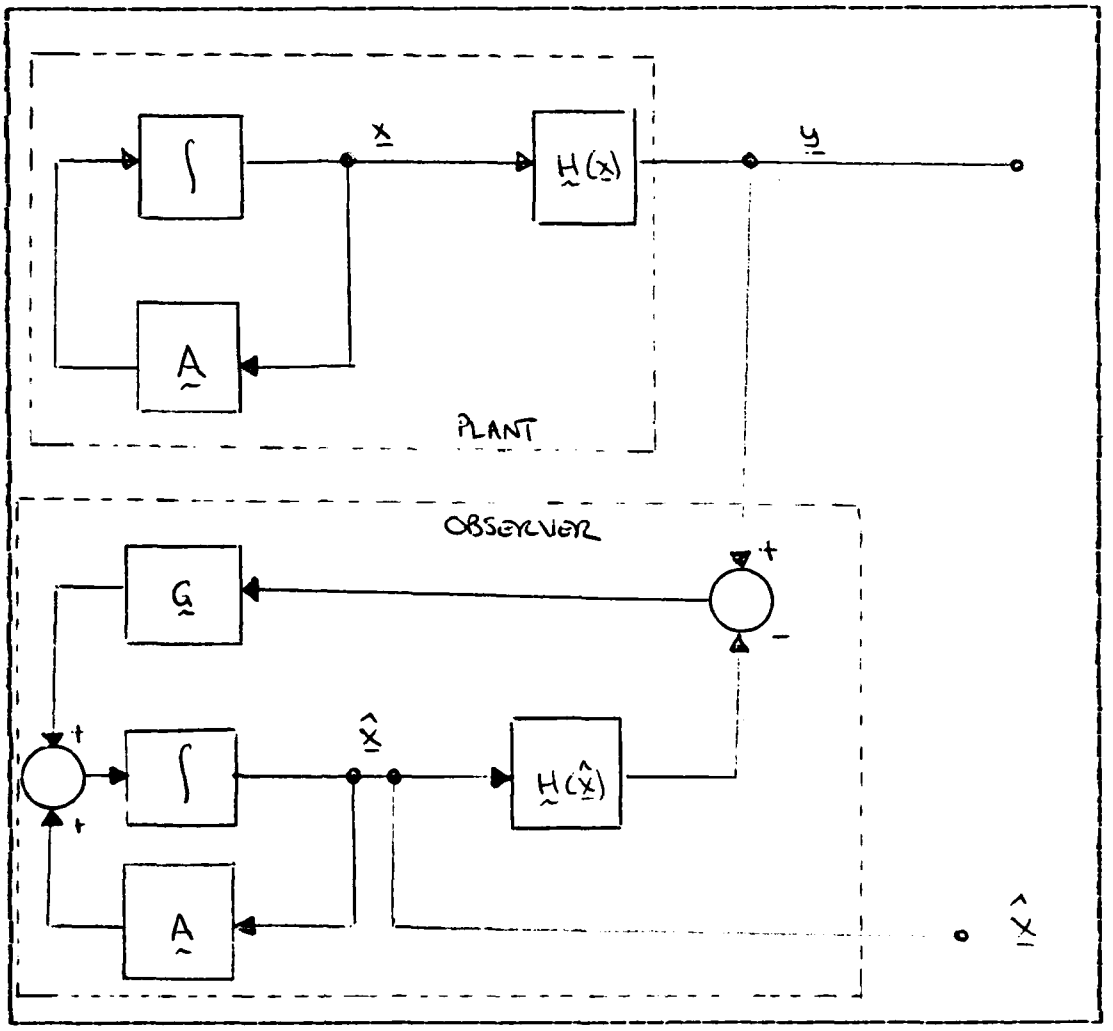

Figure 5.1 Plant and Observer for the General System

Ignoring the higher order terms and assuming for the moment a constant velocity target, the linearized system can now be described by

$$\dot{\underset{\sim}{x}} = \underset{\sim}{A}\underset{\sim}{x} \,, \qquad (5.3)$$

V. FILTERING AND TRACKING

The objective of this chapter is to apply the results of Chapter IV. Specifically, this will entail designing a deterministic nonlinear observer, and then an EKF, in accordance with the methods discussed in [Ref. 3] and [Ref. 8]. The original coordinates of the problem as developed in Chapters II and III will be employed, rather than the rectangular coordinates of Chapter IV.

A. DETERMINISTIC NONLINEAR OBSERVER

Actually, in [Ref. 8], Kirk only discusses the design of linear observers, but by employing the now-familiar technique of linearizing about an estimate with a first-order Taylor Series expansion, the technique can readily be extended to a nonlinear system. Some alternative methods of nonlinear observer design are discussed in [Ref. 9], [Ref. 10], [Ref. 11], and [Ref. 12].

For the system under consideration,

$$\underline{\dot{x}} = \underset{\sim}{A}\underline{x} + \underset{\sim}{B}\underline{u}\ , \quad \underline{y} = \underset{\sim}{H}(\underline{x}) \tag{5.1}$$

where

$$\underline{x} = \begin{bmatrix} n \\ \dot{n} \\ e \\ \dot{e} \\ h \\ \dot{h} \end{bmatrix},\ \underset{\sim}{A} = \begin{bmatrix} 0 & 1 & 0 & 0 & 0 & 0 \\ 0 & 0 & 0 & 0 & 0 & 0 \\ 0 & 0 & 0 & 1 & 0 & 0 \\ 0 & 0 & 0 & 0 & 0 & 0 \\ 0 & 0 & 0 & 0 & 0 & 1 \\ 0 & 0 & 0 & 0 & 0 & 0 \end{bmatrix},\ \underset{\sim}{B} = \begin{bmatrix} 0 & 0 & 0 \\ 1 & 0 & 0 \\ 0 & 0 & 0 \\ 0 & 1 & 0 \\ 0 & 0 & 0 \\ 0 & 0 & 1 \end{bmatrix},\ \underline{u} = \begin{bmatrix} a_N \\ a_E \\ a_H \end{bmatrix},\ \underline{y} = \begin{bmatrix} R \\ \alpha \\ \beta \end{bmatrix} = \underset{\sim}{H}(\underline{x}).$$

Assuming an observer-estimated trajectory $\hat{\underline{x}}$, the observation is linearized around it

insights; then the examination of the stationary surface target led to the coordinate transformation, and to the conclusion that any position variable of observation would suffice for observability of this type target. Consideration of the general target model showed it to be unobservable for any single variable of observation, and then a brief examination of the moving surface target led to the important conclusion that an α-only track is possible, at least if the target maneuvers. Further, it appears that the system is far more sensitive to fluctuations (i.e. noise) in the β measurements than R or α. In Chapter V some of these perceptions will be tested by the designing of a deterministic nonlinear observer and then tracking the target with an EKF.

some ambiguity in the observations and so the target is not observable. In the case of the α Jacobian, however, it is positive definite, i.e. the χ terms drop out and

$$|J_3| = (ea_N - na_E)^2 \qquad (4.5)$$

This indicates that a maneuvering surface target is observable when azimuthal bearings only are observed; this case corresponds very closely to the two-dimensional bearing-only tracking problem long familiar to submariners. If the target does not maneuver, then the α Jacobian becomes non-singular and the target is unobservable, and then more than one variable of observation, to include α or $\dot{\alpha}$, is required for observability.

It becomes obvious why the observability of nonlinear systems has long been considered a highly difficult problem. At least as much insight was gained into the problem from its mathematical derivation as from the application of this method of observability analysis. One area in which the method might also be useful is in evaluating the sensitivity of the system observability to fluctuations. Specifically, the terms in the β Jacobian are each smaller than the α or R terms by a factor of $1/\sqrt{n^2+e^2}$, which would, in the general case, mean a difference of three orders of magnitude. This would certainly lead one to presume that the system would be more sensitive to fluctuations in β than in R or α.

To summarize thus far, the geometric derivation of the coordinates in Chapter II leads one to believe that all three coordinates R, α, and β, or the derivatives of no more than two of them, are necessary to reconstruct the target motion in the most general (air target) case, while either the (R,α) or (α,β) combination is necessary and sufficient for the surface target. Examination of the linearized model in this chapter tended to validate those

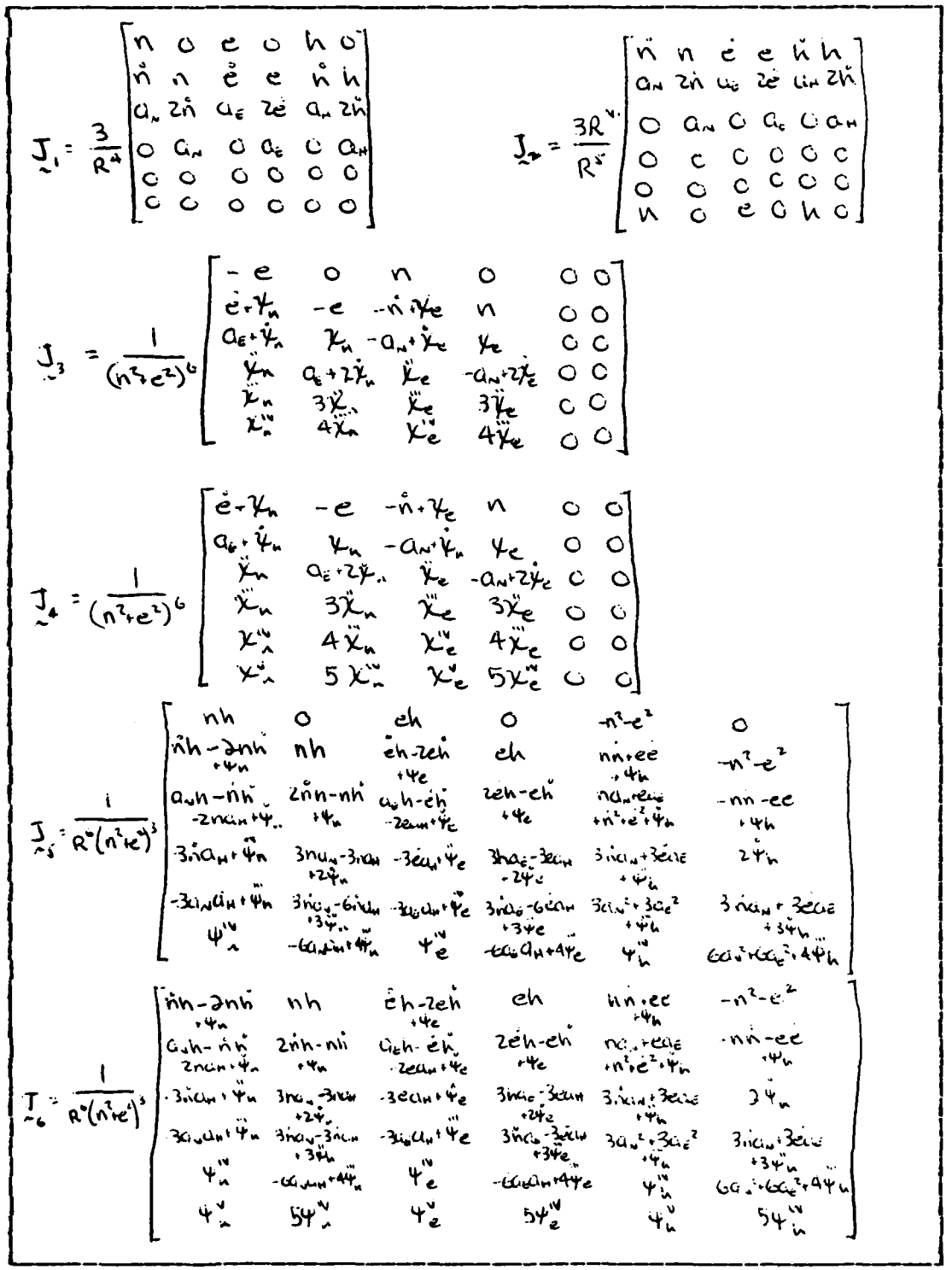

Figure 4.6 Jacobian Observer Matrices For the Six State Variables

well be possible, but these representations should suffice here. It is obvious from the occurence of the zero rows and columns that all the determinants excluding those of $\underset{\sim}{J}_4$ and $\underset{\sim}{J}_6$ are zero; computation of these last two determinants proves them to be zero also. Considering the observed variables in combination, it would seem that some variable in addition to R or $\dot{R}$ is always necessary for observability, as they have the only Jacobian matrices with zero rows. While the possible combinations of six columns out of the thirty-six are so numerous (approximately two million) that it is virtually impossible to explore them all, only one combination with a nonzero determinant and positive or negative definiteness is required for observability.

What one would expect, based on the insight gained in Chapters II and III from the mathematics of the derivation of the model, is that any combination including α or $\dot{\alpha}$ and at least one position variable (i.e. R and $\dot{\alpha}$, α and $\dot{\beta}$, etc.) should be observable, and that any determinant formed from a combination of columns from the appropriate $\underset{\sim}{J}$ matrices should prove it (excepting of course the zero columns in the α and $\dot{\alpha}$ matrices). The combinations of R, $\ddot{R}$, β, and $\dot{\beta}$ should however prove unobservable for the reason of a lack of positive/negative definiteness, that is, an ambiguity of target track resulting when reconstruction of the initial state is attempted from the measurements. To prove this condition true for each of the approximately 130,000 possible matrices is however obviously an unrealistic undertaking.

One slightly simpler case of particular interest might be that of the surface target, which involves the first four rows by four columns in each matrix. If the accelerations are nonzero, all the Jacobians except $\dot{R}$ have nonzero determinants. The R, $\ddot{\alpha}$, β, and $\dot{\beta}$ determinants are not positive or negative definite, indicating that there is still

$$|J_s| = \frac{\beta \cos\beta}{R \sin\beta} |J_1| \qquad (4.4)$$

So again the same form of determinant will be achieved, albeit with a different multiplicative constant. Thus for a target known to be stationary, the observation of any of the quantities R, α , or β is enough to fix its position. Presumably the same result could have been achieved in the original coordinate system had the algebra been carried through.

C. NONLINEAR MODEL OF THE GENERAL TARGET

Once the target is permitted to move, of course, the unique-intersection arguments just developed no longer apply. The equations shown in Figure 4.3 now are pertinent, but J_i is defined by

$$J_i = \begin{bmatrix} \frac{\partial y_i}{\partial x_1} & \frac{\partial y_i}{\partial x_2} & \cdots & \frac{\partial y_i}{\partial x_6} \\ \frac{\partial y_i'}{\partial x_1} & \frac{\partial y_i'}{\partial x_2} & \cdots & \frac{\partial y_i'}{\partial x_6} \\ \vdots & \vdots & & \vdots \\ \frac{\partial y_i^{v}}{\partial x_1} & \frac{\partial y_i^{v}}{\partial x_2} & \cdots & \frac{\partial y_i^{v}}{\partial x_6} \end{bmatrix} .$$

The derivation of the Jacobian matrices and their determinants is now a major project in itself, but it follows the same pattern previously established. In the interests of brevity, the requisite algebra is excluded from this discussion, but included in this report as Appendix A. After simplification by row reduction, the J matrices are as shown in Figure 4.6 , with the χ and Ψ terms as specified in the appendix. Further simplification of the determinants may

Consider first the α-only case:

$$\underset{\sim}{J}_3 = \begin{bmatrix} \frac{-e}{n^2+e^2} & \frac{n}{n^2+e^2} \\ \frac{\dot{e} - 2e\dot{\alpha}}{n^2+e^2} & \frac{\dot{n} - 2n\dot{\alpha}}{n^2+e^2} \end{bmatrix} ;$$

$$\left|\underset{\sim}{J}_3\right| = \frac{n\dot{e} - e\dot{n}}{-(n^2+e^2)^2} . \qquad (4.3)$$

The numerator is identical to that of the $\underset{\sim}{J}_1$ determinant; Figure 4.5 illustrates the situation here.

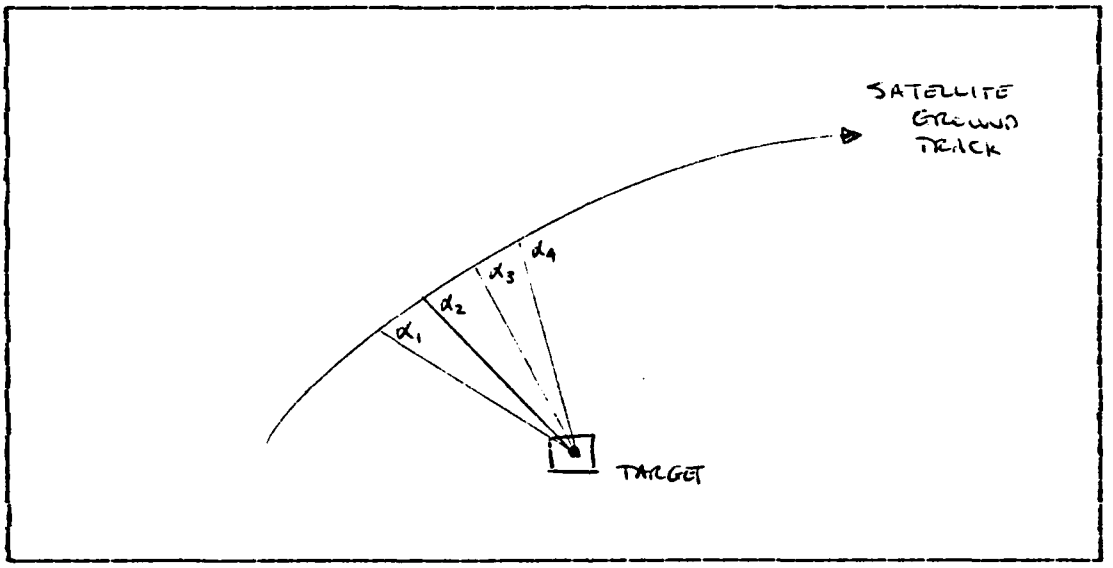

Figure 4.5 Azimuthal Bearing-Only Track Of the Stationary Target

For the record, in the β-only case,

$$\underset{\sim}{J}_5 = \begin{bmatrix} \frac{\partial R}{\partial n} \frac{\cos\beta}{R\sin\beta} & \frac{\partial R}{\partial e} \frac{\cos\beta}{R\sin\beta} \\ \beta \frac{\partial \dot{R}}{\partial n} - \frac{\dot{\beta}}{R}\left[1 + \frac{R^2}{n^2+e^2}\right]\frac{\partial R}{\partial n} & \beta \frac{\partial \dot{R}}{\partial e} - \frac{\dot{\beta}}{R}\left[1 + \frac{R^2}{n^2+e^2}\right]\frac{\partial R}{\partial e} \end{bmatrix} ;$$

one-to-one correspondence of the coordinates and the observability problems, but also due to the physical reasoning illustrated in Figure 4.4 .

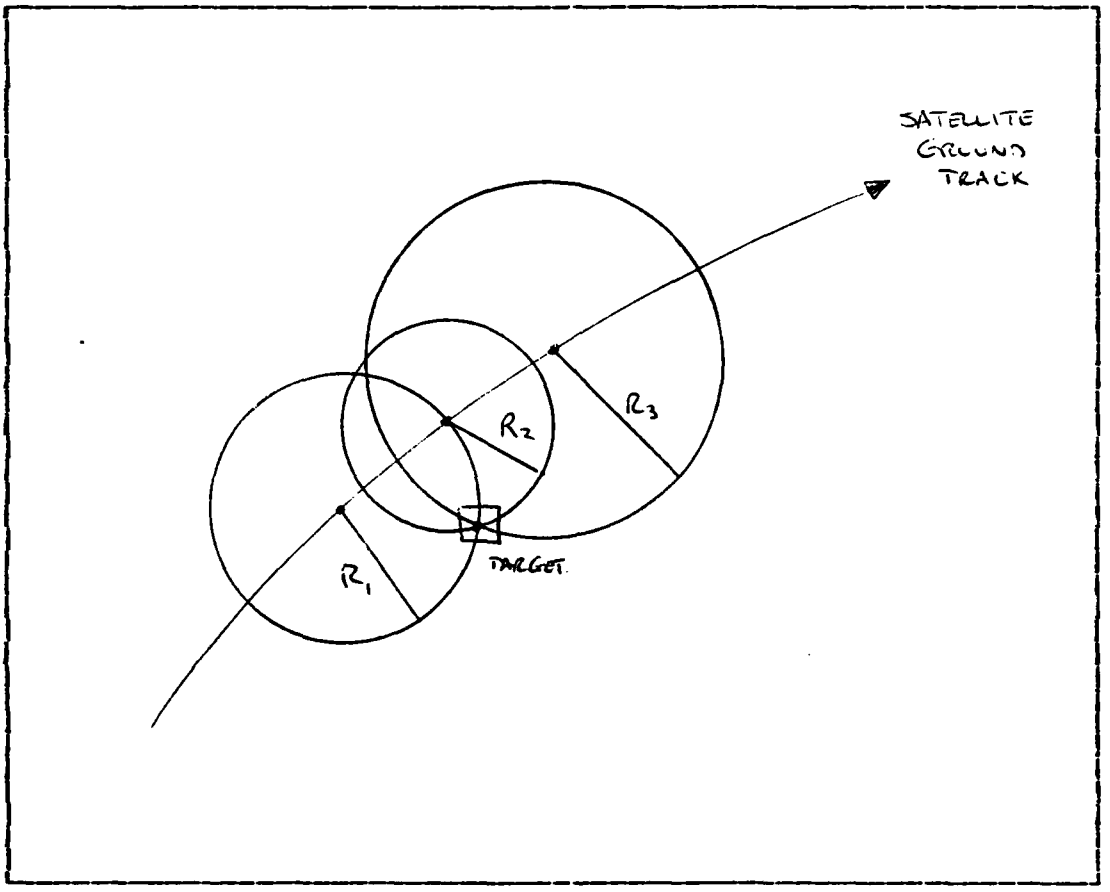

Figure 4.4 Tracking the Stationary Target

The satellite's ground track is a curve, and there is only one possible point of intersection of even three circles whose centers lie upon it. This observability will be more clearly demonstrated if the single observed variable to the stationary target is α ; obviously, the intersecting lines of bearing must define a single point. Further, since for a surface target every R defines a unique β and vice versa, the β -only case should be observable also.

$$\dot{\underline{X}} = \begin{bmatrix} 0 & 1 & 0 & 0 & 0 & 0 \\ 0 & 0 & 0 & 0 & 0 & 0 \\ 0 & 0 & 0 & 1 & 0 & 0 \\ 0 & 0 & 0 & 0 & 0 & 0 \\ 0 & 0 & 0 & 0 & 0 & 1 \\ 0 & 0 & 0 & 0 & 0 & 0 \end{bmatrix} \underline{X} + \begin{bmatrix} 0 & 0 & 0 \\ 1 & 0 & 0 \\ 0 & 0 & 0 \\ 0 & 1 & 0 \\ 0 & 0 & 0 \\ 0 & 0 & 1 \end{bmatrix} \underline{U}$$

$$y_1 = R = \left[n^2 + e^2 + h^2\right]^{1/2}$$

$$y_2 = \dot{R} = \left[n\dot{n} + e\dot{e} + h\dot{h}\right] / R$$

$$y_3 = \alpha = \text{TAN}^{-1}\, e/n$$

$$y_4 = \dot{\alpha} = \frac{n\dot{e} - e\dot{n}}{n^2 + e^2}$$

$$y_5 = \beta = \cos^{-1} h/R$$

$$y_6 = \dot{\beta} = \frac{h\dot{R} - R\dot{h}}{R\sqrt{n^2 + e^2}}$$

Figure 4.3 State and Observer Equations For the Cartesian Version of the Problem

$$|\underset{\sim}{J}_1| = \frac{1}{R^2}(n\dot{e} - e\dot{n})$$

$$= \frac{r_0^2}{R^2}\left[-\dot{\lambda}_S''(L_T - L_S)\cos i_S + L_S^{\circ}(\dot{\lambda}_T - \dot{\lambda}_S)\left[\cos i_S - (L_T - L_S)\sin i_S\right]\right], \qquad (4.2)$$

which is again nonzero in the general case, and which will, on reflection, lead to a unique solution for any particular target and a specified satellite; in fact, equation 4.1 should then also yield unique sclutions, not just due to the

$$\underline{X} = \begin{bmatrix} r_0 (L_T - L_S) \\ -r_0 \dot{L}_S \\ r_0 (\lambda_T - \lambda_S) \cos L_S \\ -r_0 \dot{\lambda}_S \cos L_S - \dot{L}_S r_0 (\lambda_T - \lambda_S) \sin L_S \\ h_S \\ 0 \end{bmatrix} .$$

The plant equation is unchanged, and the observations are

$$y_1 = R = \left[n^2 + e^2 + h^2\right]^{1/2} ,$$

$$y_2 = \dot{R} = \left[n\dot{n} + e\dot{e} + h\dot{h}\right] / R ,$$

$$y_3 = \alpha = \text{TAN}^{-1} e/n ,$$

$$y_4 = \dot{\alpha} = \frac{n\dot{e} - e\dot{n}}{n^2 + e^2} ,$$

$$y_5 = \beta = \cos^{-1} h/R ,$$

$$y_6 = \dot{\beta} = \frac{h\dot{R}}{R\sqrt{n^2+e^2}} .$$

Since only position is of interest, the Jacobian matrices will be

$$\underset{\sim}{J}_i = \begin{bmatrix} \frac{\partial y_i}{\partial x_1} & \frac{\partial y_i}{\partial x_3} \\ \frac{\partial \dot{y}_i}{\partial x_1} & \frac{\partial \dot{y}_i}{\partial x_3} \end{bmatrix} .$$

For i = 1, that is, the observation is the range R,

$$\underset{\sim}{J}_1 = \begin{bmatrix} n/R & e/R \\ \frac{\dot{n} - \dot{R} n/R}{R} & \frac{\dot{e} - \dot{R} e/R}{R} \end{bmatrix} .$$

After some simplification,

$$\underline{x} = \begin{bmatrix} n \\ \dot{n} \\ e \\ \dot{e} \\ h \\ \dot{h} \end{bmatrix} = \begin{bmatrix} (r_0+h_T)(L_T - L_S) \\ (r_0+h_T)(L_T^{\cdot} - L_S^{\cdot}) + h_T^{\cdot}(L_T - L_S) \\ (r_0+h_T)(\lambda_T - \lambda_S)\cos L_S \\ (r_0+h_T)(\lambda_T^{\cdot} - \lambda_S^{\cdot})\cos L_S + h_T^{\cdot}(\lambda_T - \lambda_S)\cos L_S - L_S^{\cdot}(r_0+h_T)(\lambda_T - \lambda_S)\sin L_S \\ h_S - h_T \\ -h_T^{\cdot} \end{bmatrix}$$

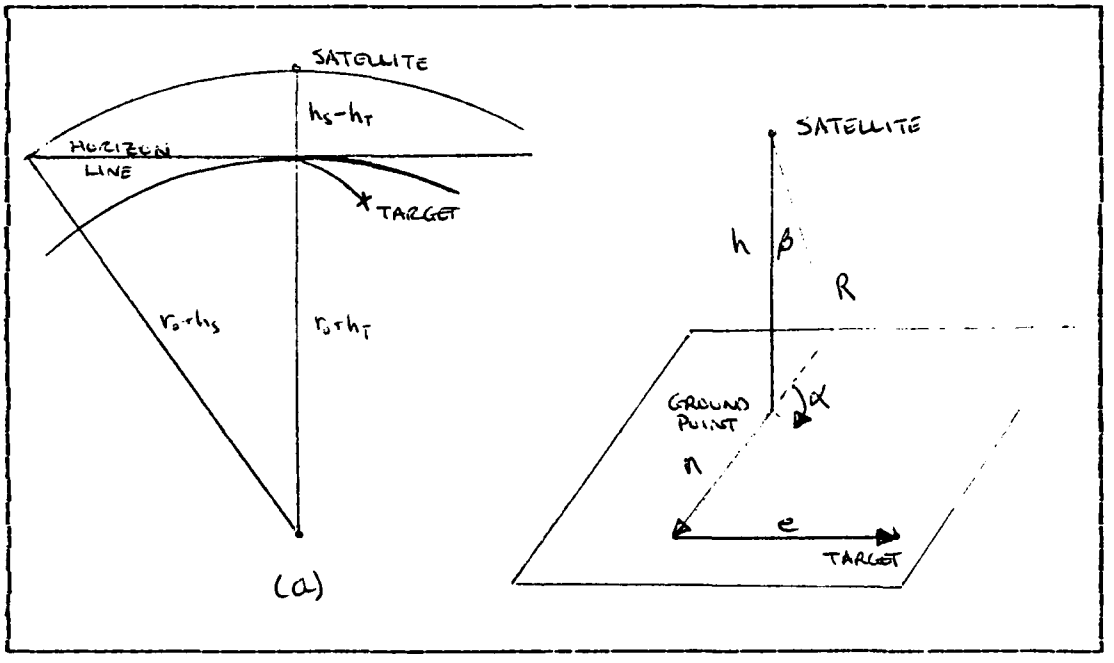

Figure 4.2 Projecting Target Position Into a Perpendicular Plane

As every set of true target cocrdinates yields a unique set of relative coordinates for a particular satellite, the mapping into the Cartesian coordinates is one-to-one, and an observable target in one system will be observable in the other. The complete set of state and observer equations in this coordinate system is as illustrated in Figure 4.2 (b) and summarized in Figure 4.3 . For the special case of the stationary surface target, the system simplifies as follows:

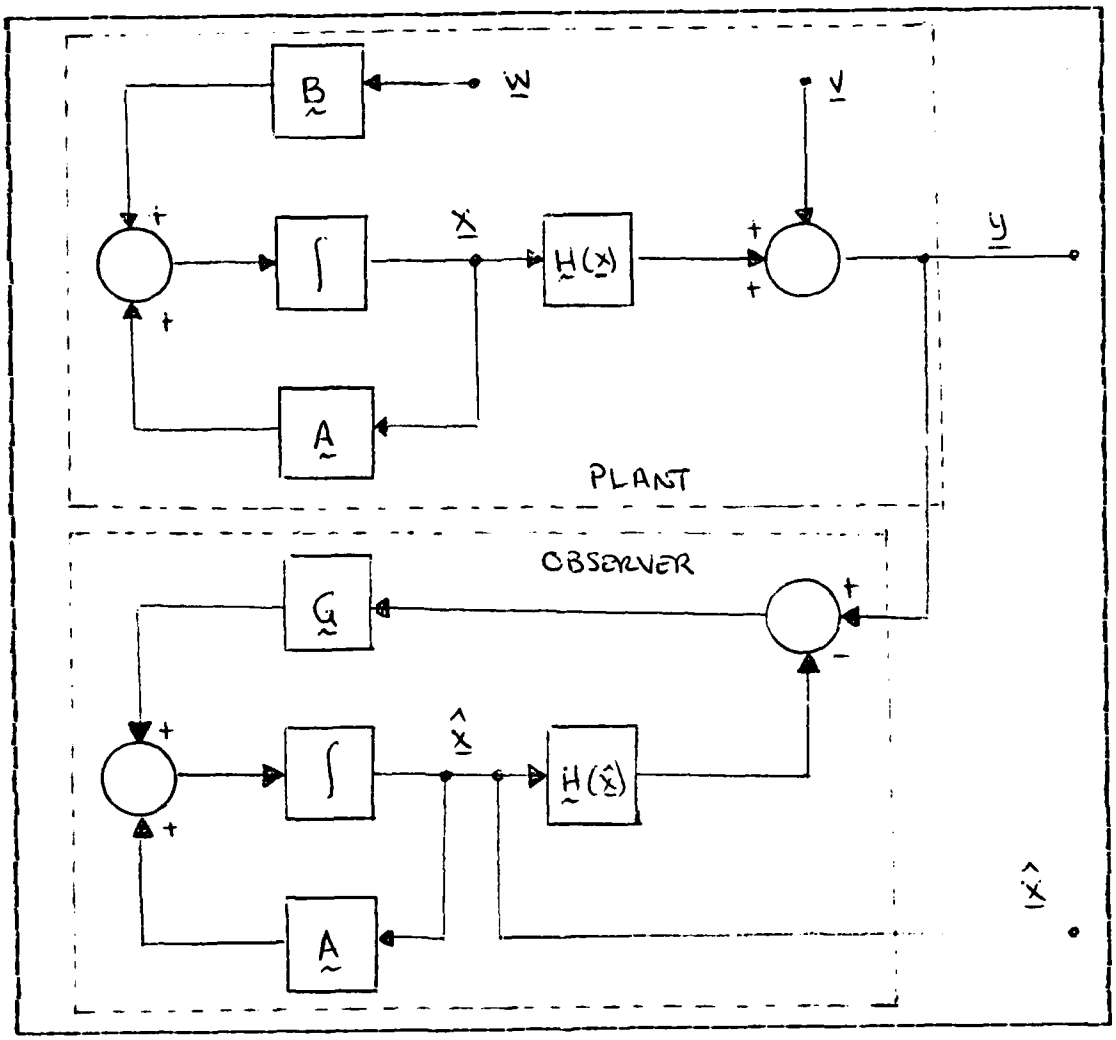

Figure 5.2 Plant and Observer for the Stochastic System

Figure 5.2 illustrates the addition of measurement and plant (or "system") noise to the problem. The describing equations of the plant are now

$$\dot{\underset{\sim}{x}} = \underset{\sim}{A}\underset{\sim}{x} + \underset{\sim}{B}\underset{\sim}{w} , \tag{5.11}$$

$$\underset{\sim}{y} = \underset{\sim}{H}(\underset{\sim}{x}) + \underset{\sim}{v} , \tag{5.12}$$

where $\underline{w}$ is system noise, and $\underline{v}$ is measurement noise. It is important to note that the form of the observer has not changed since the discussion in Section A of this chapter; now, however, the filter analysis provides a method for calculating the sequence of gain matrices $\underset{\sim}{G}$.

That last statement concerning a sequence of $\underset{\sim}{G}$'s suggests the convenience of a discrete (as opposed to continuous) representation of the system. Considering that the iterative calculations required to compute the successive estimates $\hat{\underline{x}}$ will require a measurably finite time-increment, it makes sense to work with the discrete system equivalent to the continuous system discussed thus far, i.e.

$$\underline{x}(k+1) = \underset{\sim}{\Phi}\,\underline{x}(k) + \underset{\sim}{\Gamma}\,\underline{w}(k), \tag{5.13}$$

$$\underline{y}(k) = \underset{\sim}{H}(\underline{x}(k)) + \underline{v}(k), \tag{5.14}$$

where

$$\underset{\sim}{\Phi} = e^{\underset{\sim}{A}t} = \begin{bmatrix} 1 & T & 0 & 0 & 0 & 0 \\ 0 & 1 & 0 & 0 & 0 & 0 \\ 0 & 0 & 1 & T & 0 & 0 \\ 0 & 0 & 0 & 1 & 0 & 0 \\ 0 & 0 & 0 & 0 & 1 & T \\ 0 & 0 & 0 & 0 & 0 & 1 \end{bmatrix}, \quad \underset{\sim}{\Gamma} = \int_T e^{\underset{\sim}{A}\zeta}\,d\zeta\,\underset{\sim}{B} = \begin{bmatrix} T^2/2 & 0 & 0 \\ T & 0 & 0 \\ 0 & T^2/2 & 0 \\ 0 & T & 0 \\ 0 & 0 & T^2/2 \\ 0 & 0 & T \end{bmatrix},$$

and $\underline{w}(k) = \begin{bmatrix} w_N(k) \\ w_E(k) \\ w_H(k) \end{bmatrix}$, $w_i(k) \sim N(0, \sigma_i^2)$; $\sigma_{NE}^2 = \sigma_{EH}^2 = \sigma_{NH}^2 = 0$,

$$\underline{v}(k) = \begin{bmatrix} v_R(k) \\ v_A(k) \\ v_B(k) \end{bmatrix}, \quad v_j(k) \sim N(0, \sigma_j^2), \quad \sigma_{RA}^2 = \sigma_{AB}^2 = \sigma_{RB}^2 = 0.$$

That is, both the system and observer noises are presumed to be white independently normally distributed with mean zero

and specified variances, which are independent of the Gaussian random variable $\underline{x}(0)$. The observer equation 5.6 will take the form

$$\hat{\underline{x}}(k+1) = \underset{\sim}{\Phi}\, \hat{\underline{x}}(k) + \underset{\sim}{G}(k)\left[\underset{\sim}{H}(\underline{x}(k)) - \underset{\sim}{H}(\hat{\underline{x}}(k))\right] \qquad (5.15)$$

It is now useful to introduce the double-subscripted notation required to compute the $\underset{\sim}{G}(k)$ matrices in the EKF algorithm, i.e.

$$\hat{\underline{x}}(k|k-1),$$

which signifies an estimate at time increment k based on information available at time increment k-1, as opposed to

$$\hat{\underline{x}}(k|k),$$

which represents the estimate at time k given the information available at time k.

The final element required to understand the EKF algorithm is the concept of the error covariance matrix $\underset{\sim}{P}(k)$, which can also be thought of as the expected value of the error vector squared, i.e.

$$\underset{\sim}{P}(k) = E((\tilde{\underline{x}})^2).$$

Its derivation and significance is fully explained in [Ref. 8], while [Ref. 3] discusses at length its initialization. Suffice it here to state that it is an intrinsic part of the EKF algorithm, which can now be summarized.

Given the state estimate and covariance matrix at time k-1 and the measurement at time k, the state and covariance at time k are estimated as follows:

$$\hat{\underline{x}}(k|k-1) = \underset{\sim}{\Phi}\, \hat{\underline{x}}(k-1|k-1), \qquad (5.16)$$

$$\underset{\sim}{P}(k|k-1) = \underset{\sim}{\Phi}\,\underset{\sim}{P}(k-1|k-1)\,\underset{\sim}{\Phi}^T + \underset{\sim}{\Gamma}\,\underset{\sim}{Q}\,\underset{\sim}{\Gamma}^T, \qquad (5.17)$$

where $$\underset{\sim}{Q} = \begin{bmatrix} \sigma_n^2 & 0 & 0 \\ 0 & \sigma_\varepsilon^2 & 0 \\ 0 & 0 & \sigma_u^2 \end{bmatrix}.$$

The EKF gain matrix is then calculated as follows:

$$\underset{\sim}{G}(k) = \underset{\sim}{P}(k|k-1)\,\underset{\sim}{h}^T(k)\left[\underset{\sim}{h}(k)\,\underset{\sim}{P}(k|k-1)\,\underset{\sim}{h}^T(k) + \underset{\sim}{R}\right]^{-1}, \qquad (5.18)$$

where $\underset{\sim}{h}(k) = \left.\dfrac{\partial \underset{\sim}{H}}{\partial \underset{\sim}{x}}\right|_{\hat{\underset{\sim}{x}}(k|k-1)}$ AND $\underset{\sim}{R} = \begin{bmatrix} \sigma_r^2 & 0 & 0 \\ 0 & \sigma_\lambda^2 & 0 \\ 0 & 0 & \sigma_\beta^2 \end{bmatrix}.$

Finally, the state vector and the covariance matrix are updated as follows:

$$\hat{\underset{\sim}{x}}(k|k) = \hat{\underset{\sim}{x}}(k|k-1) + \underset{\sim}{G}(k)\left[\underset{\sim}{y}(k) - \underset{\sim}{H}\left(\hat{\underset{\sim}{x}}(k|k-1)\right)\right] \qquad (5.19)$$

$$\underset{\sim}{P}(k|k) = \left[\underset{\sim}{I} - \underset{\sim}{G}(k)\,\underset{\sim}{h}(k)\right]\underset{\sim}{P}(k|k-1) \qquad (5.20)$$

All that remains is the question of initialization; [Ref. 3] develops fully the method used to initialize both the state vector and the covariance matrix, specifically the use of the first two target observations to generate initial estimates for both $\hat{\underset{\sim}{x}}$ and $\underset{\sim}{P}$. This method is illustrated in the specific example that follows immediately.

C. TARGET TRACKING WITH THE EKF

This section discusses the development of a computer program designed to implement the basic Kalman-Bucy filter algorithm discussed in Section B above. While admittedly crude, it serves as a first-cut tracking algorithm and can

be used in conjunction with the observability analysis of Chapter IV. The problem divides itself naturally into two parts, namely developing models for the satellite and the target; and then using the EKF algorithm, that is, equations 5.16 through 5.20, to see if the satellite can track the target.

1. Satellite and Target Models

This is the time when the various equations developed in Chapter II (satellite) and Chapter III (target) are necessary. For the purposes of this problem, a satellite with an altitude of 600 nm and an orbital inclination of 63.4° is used, as this is a typical orbital pattern used to ensure whole-earth coverage in a multi-satellite constellation. A surface target simplifies the problem slightly, as x need only be four-dimensional; thus the target chosen is a surface vessel on a heading of 315° at a speed of 28.3 knots, which equates to a northerly velocity of 20 knots and an easterly velocity of -20 knots. At time zero (i.e. k=0), the satellite is located overhead the point (0°N,0°E), while the target is located at (45° N,30°E), which is initially below the satellite's horizon; the program is designed to compute (R, α, β) as (0,0,0) until the target comes in view. The computer program listing appears in Appendix B; of perhaps greater interest is the data which appears in Table V, which shows the program run for 28 minutes with a time step of 30 seconds, i.e. k running from 0 to 56. For this single pass, the target was in view for 117 steps in time, or 19.5 minutes, a fairly representative viewing time.

2. EKF Operation

In the main, the EKF algorithm used in the computer program that appears as Appendix B is the direct application of the equations 5.16 through 5.20 to the particular

TABLE V

Target and Satellite Simulation with Observations

STEP	TIME	LAT	LONG	LAT	LONG	RANGE	ALPHA	BETA
0	0.0	0.00	0.00	45.00	30.00	0.0	0.00	0.00
1	0.5	1.50	0.63	45.00	30.00	0.0	0.00	0.00
2	1.0	3.00	1.25	45.01	29.99	0.0	0.00	0.00
3	1.5	4.49	1.88	45.01	29.99	0.0	0.00	0.00
4	2.0	5.99	2.52	45.01	29.99	0.0	0.00	0.00
5	2.5	7.48	3.15	45.01	29.99	0.0	0.00	0.00
6	3.0	8.98	3.80	45.02	29.98	0.0	0.00	0.00
7	3.5	10.47	4.45	45.02	29.98	0.0	0.00	0.00
8	4.0	11.96	5.11	45.02	29.98	0.0	0.00	0.00
9	4.5	13.44	5.78	45.02	29.98	0.0	0.00	0.00
10	5.0	14.93	6.45	45.03	29.97	0.0	0.00	0.00
11	5.5	16.41	7.14	45.03	29.97	0.0	0.00	0.00
12	6.0	17.89	7.85	45.03	29.97	0.0	0.00	0.00
13	6.5	19.36	8.56	45.04	29.97	2092.3	29.85	58.36
14	7.0	20.83	9.30	45.04	29.96	1995.2	30.33	58.31
15	7.5	22.30	10.05	45.04	29.96	1898.4	30.87	58.15
16	8.0	23.76	10.82	45.04	29.96	1801.8	31.45	57.90
17	8.5	25.21	11.61	45.05	29.96	1705.5	32.09	57.53
18	9.0	26.66	12.43	45.05	29.95	1609.8	32.80	57.01
19	9.5	28.11	13.27	45.05	29.95	1514.6	33.58	56.33
20	10.0	29.54	14.13	45.06	29.95	1420.4	34.46	55.46
21	10.5	30.97	15.03	45.06	29.95	1327.4	35.43	54.34
22	11.0	32.39	15.96	45.06	29.94	1235.7	36.52	52.96
23	11.5	33.80	16.92	45.06	29.94	1146.1	37.77	51.21
24	12.0	35.20	17.92	45.07	29.94	1059.3	39.22	49.02
25	12.5	36.59	18.96	45.07	29.94	975.3	40.93	46.35
26	13.0	37.97	20.04	45.07	29.93	895.7	43.00	43.04
27	13.5	39.34	21.18	45.07	29.93	822.1	45.63	38.98
28	14.0	40.69	22.36	45.08	29.93	755.7	49.12	34.04
29	14.5	42.02	23.60	45.08	29.93	698.9	54.19	28.19
30	15.0	43.34	24.89	45.08	29.92	654.0	62.50	21.53
31	15.5	44.64	26.26	45.09	29.92	624.0	79.04	14.68
32	16.0	45.92	27.69	45.09	29.92	610.9	117.30	10.03
33	16.5	47.18	29.19	45.09	29.92	616.0	166.25	12.09
34	17.0	48.42	30.78	45.09	29.91	638.9	190.44	18.46
35	17.5	49.62	32.45	45.10	29.91	677.8	201.77	25.35
36	18.0	50.80	34.22	45.10	29.91	729.7	208.48	31.61
37	18.5	51.95	36.08	45.10	29.91	792.7	213.23	36.96
38	19.0	53.06	38.05	45.11	29.90	863.6	217.03	41.42
39	19.5	54.13	40.14	45.11	29.90	941.5	220.33	45.04
40	20.0	55.16	42.34	45.11	29.90	1024.0	223.37	48.01
41	20.5	56.15	44.66	45.11	29.90	1110.6	226.28	50.39
42	21.0	57.08	47.12	45.12	29.89	1200.4	229.15	52.30
43	21.5	57.96	49.71	45.12	29.89	1292.1	232.01	53.85
44	22.0	58.78	52.43	45.12	29.89	1385.7	234.92	55.09
45	22.5	59.53	55.29	45.12	29.89	1481.0	237.88	56.05
46	23.0	60.21	58.28	45.13	29.88	1577.3	240.92	56.80
47	23.5	60.82	61.40	45.13	29.88	1674.7	244.04	57.37
48	24.0	61.35	64.64	45.13	29.88	1772.5	247.24	57.80
49	24.5	61.80	68.00	45.14	29.87	1870.9	250.52	58.09
50	25.0	62.15	71.45	45.14	29.87	1969.6	253.86	58.27
51	25.5	62.41	74.97	45.14	29.87	2068.7	257.25	58.36
52	26.0	62.58	78.55	45.14	29.87	0.0	0.00	0.00
53	26.5	62.65	82.16	45.15	29.86	0.0	0.00	0.00
54	27.0	62.63	85.77	45.15	29.86	0.0	0.00	0.00
55	27.5	62.50	89.37	45.15	29.86	0.0	0.00	0.00
56	28.0	62.28	92.92	45.16	29.86	0.0	0.00	0.00

problem, complete with the intermediate calculations required to evaluate some fairly involved matrix multiplications and inversions. However, two aspects of the program require further elaboration. First, the filter initialization, to which Section B of this chapter alluded; and second, the computation of the Jacobian observer matrix $\underset{\sim}{h}$, which in this case is anything but trivial.

a. Filter Initialization

The method developed in [Ref. 3] has been followed exactly here, thus a two-point initialization is used. Specifically, the northerly and easterly positions calculated from the observations (R, α, β) at time steps 0 and 1 (i.e. the first two nonzero observations) are the initial estimates for x_1 and x_3, and from them the initial velocities are computed, i.e.

$$\hat{x}_1(0) = \underset{\sim}{H}_1^{-1}\left(R(0), \alpha(0), \beta(0)\right),$$

$$\hat{x}_3(0) = \underset{\sim}{H}_3^{-1}\left(R(0), \alpha(0), \beta(0)\right),$$

$$\hat{x}_1(1) = \underset{\sim}{H}_1^{-1}\left(R(1), \alpha(1), \beta(1)\right),$$

$$\hat{x}_3(1) = \underset{\sim}{H}_3^{-1}\left(R(1), \alpha(1), \beta(1)\right),$$

and

$$\hat{x}_2(1) = \frac{\hat{x}_1(1) - \hat{x}_1(0)}{T},$$

$$\hat{x}_4(1) = \frac{\hat{x}_3(1) - \hat{x}_3(0)}{T}. \qquad (5.21)$$

From these calculations, it can readily be shown that an initial estimate of the covariance might be

$$\underset{\sim}{P}(1|1) = \begin{bmatrix} \sigma_N^2 & \sigma_N^2/T & 0 & 0 \\ \sigma_N^2/T & 2\sigma_N^2/T^2 & 0 & 0 \\ 0 & 0 & \sigma_E^2 & \sigma_E^2/T \\ 0 & 0 & \sigma_E^2/T & 2\sigma_E^2/T^2 \end{bmatrix}. \qquad (5.22)$$

The details of this calculation, which involve taking the expected value of the error vector squared as discussed in Section B above, appear in [Ref. 3]. While it could be argued that other methods of initial covariance estimation are available, this method should suffice for the purposes of this analysis.

This completes the initialization of the filter, and from time step "2" (third nonzero observation) onward, the filter runs according to the algorithm of equations 5.16 through 5.20 .

b. Observer Function Matrix

The observer function $\underset{\sim}{h}$ is defined for all times k as

$$\underset{\sim}{H}(k) = \begin{bmatrix} \frac{\partial R}{\partial x_1} & \frac{\partial R}{\partial x_2} & \frac{\partial R}{\partial x_3} & \frac{\partial R}{\partial x_4} \\ \frac{\partial \alpha}{\partial x_1} & \frac{\partial \alpha}{\partial x_2} & \frac{\partial \alpha}{\partial x_3} & \frac{\partial \alpha}{\partial x_4} \\ \frac{\partial \beta}{\partial x_1} & \frac{\partial \beta}{\partial x_2} & \frac{\partial \beta}{\partial x_3} & \frac{\partial \beta}{\partial x_4} \end{bmatrix}. \qquad (5.23)$$

Computation of the matrix elements in the computer program (Appendix B) is performed in accordance with the following derivation. Consider first the following set of equations from Chapters II and III that summarizes the computation of (R, α, β) from $\underset{\sim}{x}$ (surface target case):

$$L_T = \frac{x_1}{r_0},$$

$$\lambda_3 = \frac{x_3}{r_0 \cos L_T},$$

$$\varkappa = \lambda_T - \lambda_S,$$

$$\cos\rho = \sin L_T \sin L_S + \cos L_T \cos L_S \cos\varkappa,$$

$$R^2 = r_0^2 + (r_0 + h_S)^2 - 2r_0(r_0 + h_S)\cos\rho,$$

$$\sin\alpha = \cos L_T \sin\varkappa / \sin\rho, \qquad (5.24)$$

$$\sin\beta = r_0 \sin\rho / R.$$

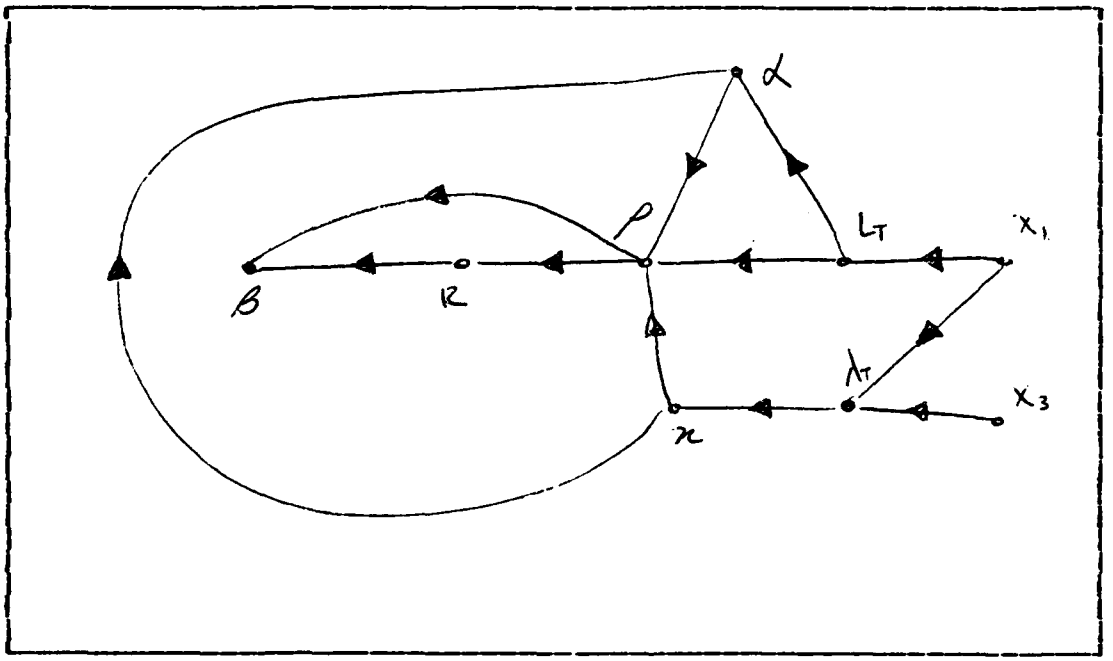

Figure 5.3 Functional Relationships Between The State and Observation Vectors

Obviously, some fairly involved chain-rule differentiation will be required to compute the partial derivatives in the $\underset{\sim}{h}$

matrix of equation 5.23 . Figure 5.3 summarizes the functional relationships between (R, α, β) and $\underline{x}$. By the chain rule then

$$\frac{\partial R}{\partial x_1} = \frac{\partial R}{\partial \rho}\left[\frac{\partial \rho}{\partial L_T}\frac{\partial L_T}{\partial x_1} + \frac{\partial \rho}{\partial r}\frac{\partial r}{\partial \lambda_T}\frac{\partial \lambda_T}{\partial x_1}\right],$$

$$\frac{\partial R}{\partial x_2} = 0,$$

$$\frac{\partial R}{\partial x_3} = \frac{\partial R}{\partial \rho}\frac{\partial \rho}{\partial r}\frac{\partial r}{\partial \lambda_T}\frac{\partial \lambda_T}{\partial x_3},$$

$$\frac{\partial R}{\partial x_4} = 0, \tag{5.25}$$

$$\frac{\partial \alpha}{\partial x_1} = \frac{\partial \alpha}{\partial L_T}\frac{\partial L_T}{\partial x_1} + \frac{\partial \alpha}{\partial \rho}\left[\frac{\partial \rho}{\partial L_T}\frac{\partial L_T}{\partial x_1} + \frac{\partial \rho}{\partial r}\frac{\partial r}{\partial \lambda_T}\frac{\partial \lambda_T}{\partial x_1}\right] + \frac{\partial \alpha}{\partial r}\frac{\partial r}{\partial \lambda_T}\frac{\partial \lambda_T}{\partial x_1},$$

$$\frac{\partial \alpha}{\partial x_2} = 0,$$

$$\frac{\partial \alpha}{\partial x_3} = \left[\frac{\partial \alpha}{\partial \rho}\frac{\partial \rho}{\partial r} + \frac{\partial \alpha}{\partial r}\right]\frac{\partial r}{\partial \lambda_T}\frac{\partial \lambda_T}{\partial x_3},$$

$$\frac{\partial \alpha}{\partial x_4} = 0, \tag{5.26}$$

$$\frac{\partial \beta}{\partial x_1} = \left[\frac{\partial \beta}{\partial R}\frac{\partial R}{\partial \rho} + \frac{\partial \beta}{\partial \rho}\right]\left[\frac{\partial \rho}{\partial L_T}\frac{\partial L_T}{\partial x_1} + \frac{\partial \rho}{\partial r}\frac{\partial r}{\partial \lambda_T}\frac{\partial \lambda_T}{\partial x_1}\right],$$

$$\frac{\partial \beta}{\partial x_2} = 0,$$

$$\frac{\partial \beta}{\partial x_3} = \left[\frac{\partial \beta}{\partial R}\frac{\partial R}{\partial \rho} + \frac{\partial \beta}{\partial \rho}\right]\frac{\partial \rho}{\partial r}\frac{\partial r}{\partial \lambda_T}\frac{\partial \lambda_T}{\partial x_3},$$

$$\frac{\partial \beta}{\partial x_4} = 0. \tag{5.27}$$

All that remains is to perform the required partial differentiations on equations 5.24 for substitution as appropriate in equations 5.25 through 5.27 so that

$$\frac{\partial L_T}{\partial x_1} = 1/r_{o_1}$$

$$\frac{\partial \lambda_T}{\partial x_1} = x_3 \sin L_T / r_o^2 \cos^2 L_{T_1}$$

$$\frac{\partial \lambda_T}{\partial x_3} = 1/r_o \cos L_{T_1}$$

$$\frac{\partial \chi}{\partial \lambda_T} = 1,$$

$$\frac{\partial \rho}{\partial L_T} = \left[\sin L_T \cos L_S \cos\chi - \cos L_T \sin L_S\right] / \sin\rho,$$

$$\frac{\partial \rho}{\partial \chi} = \cos L_T \cos L_S \sin\chi / \sin\rho,$$

$$\frac{\partial R}{\partial \rho} = r_o r_s \sin\rho / R,$$

$$\frac{\partial \alpha}{\partial L_T} = -\sin L_T \sin\chi / \sin\rho \cos\alpha,$$

$$\frac{\partial \alpha}{\partial \chi} = \cos L_T \cos\chi / \sin\rho \cos\alpha,$$

$$\frac{\partial \alpha}{\partial \rho} = -\cos L_T \sin\chi \cos\alpha / \sin^2\rho \cos\alpha,$$

$$\frac{\partial \beta}{\partial R} = -r_o \sin\rho / R^2 \cos\beta,$$

$$\frac{\partial \beta}{\partial \rho} = r_o \cos\rho / R \cos\beta. \qquad (5.28)$$

It is left to the computer to calculate numerically the partial derivatives described by equations 5.28, and then substitute those values into equations 5.25 through 5.27 to evaluate the $\underset{\sim}{h}$ matrix terms. Sequentially, these computations take place after the state and covariance estimates are calculated, and before the filter gains are computed for each iteration k, using $\underline{\hat{x}}(k|k-1)$ in all cases. This completes the observer function derivations.

D. DISCUSSION OF EKF TRACKING RESULTS

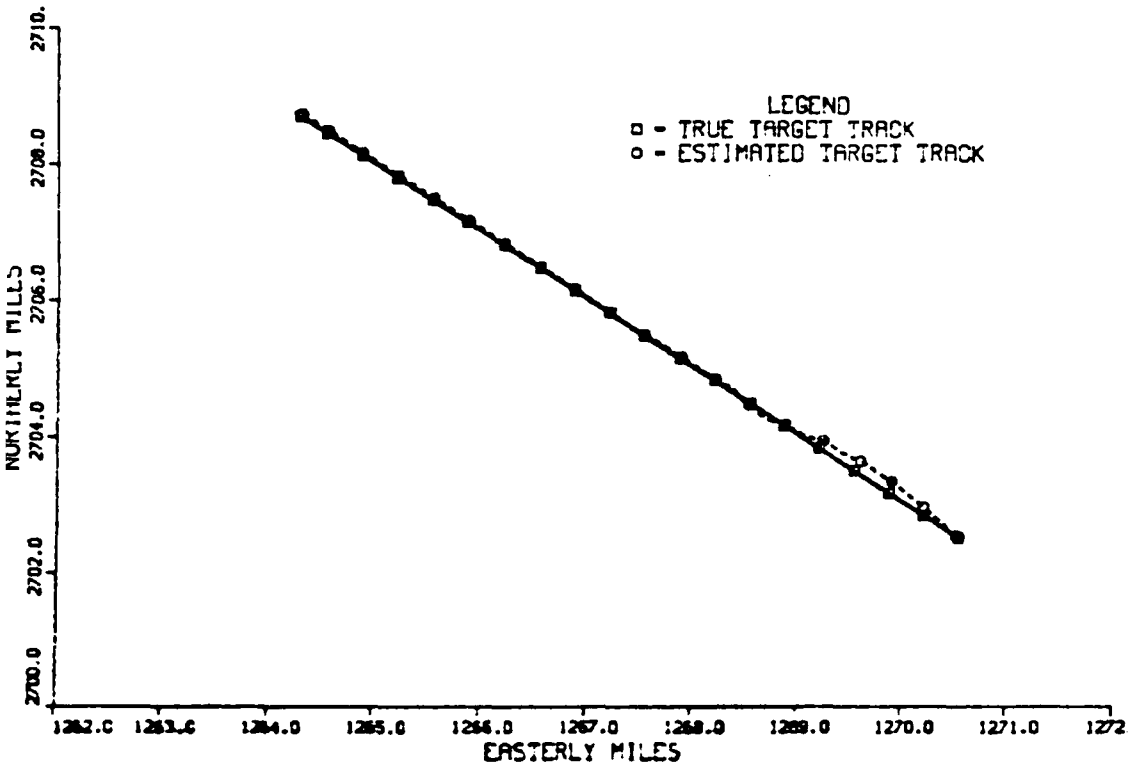

Figure 5.4 True and Estimated Target Track From Range, Alpha, and Beta

Using the DISSPLA graphics subroutines at the program's end, several sets of curves were generated. Of general interest is the tracker's accuracy when R, α, and β are all available, as opposed to R and α only, or α and β only (passive tracking, potentially). The series of graphs that comprise Figures 5.4 through 5.6 show the filter's performance for a single pass of the satellite.

From these three graphs, it appears that the filter estimate does converge to the true target trajectory in all three cases, and that the filter estimate is more accurate when all three variables are present than when only two are available. A single run of a random process has a minimal

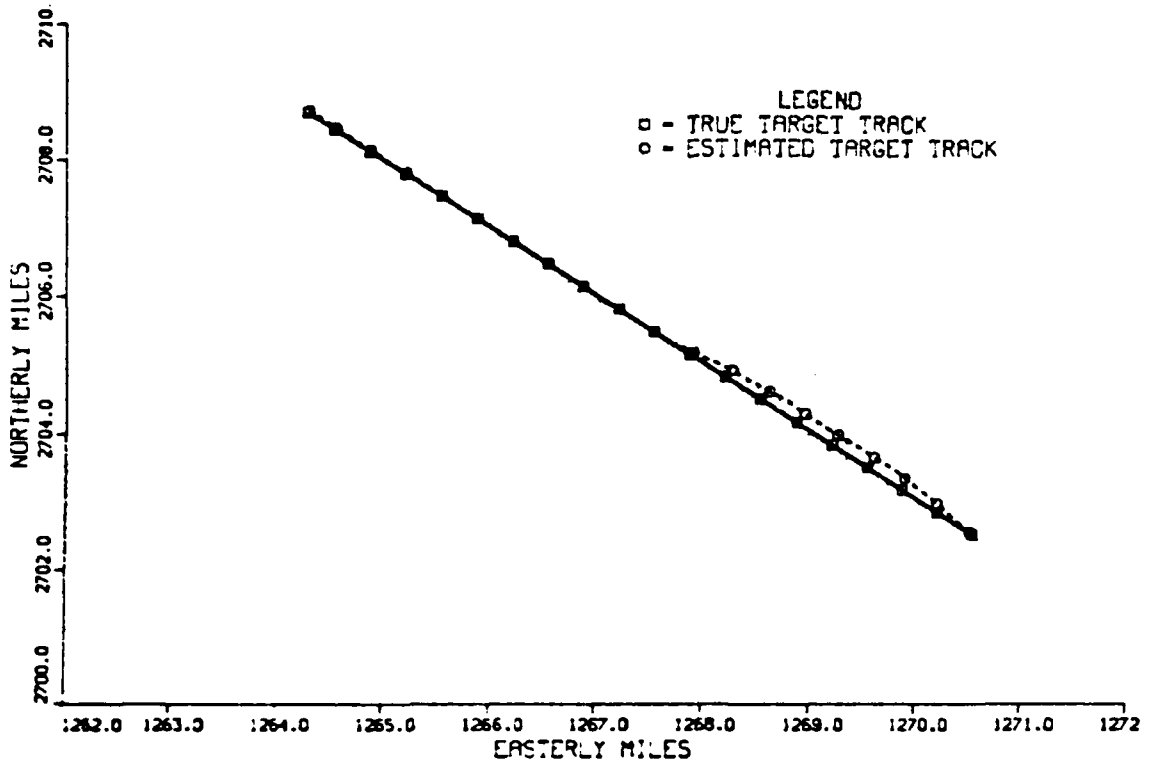

Figure 5.5 True and Estimated Target Track From Range and Alpha Only

amount of statistical significance, however; thus repeated trials of the filter's tracking will be required. In [Ref. 3], Bar-Shalom discusses in several instances the need for multiple sequential testing of any filter based on stochastic principles; the statistical average of these "Monte Carlo runs" then begins to have some significance, increasing in value in direct correlation to the number of runs considered.

First, however, a criterion must be established for error comparison. Bar-Shalom's suggestion is the use of a state-squared error function, defined for eack k as

$$SSE(k) = \underset{\sim}{\tilde{x}}(k)\, \underset{\sim}{P}^{-1}(k|k)\, \underset{\sim}{\tilde{x}}^{T}(k).$$

Application of this criterion to this filter (not shown here) indicates that while the filter is able to track the

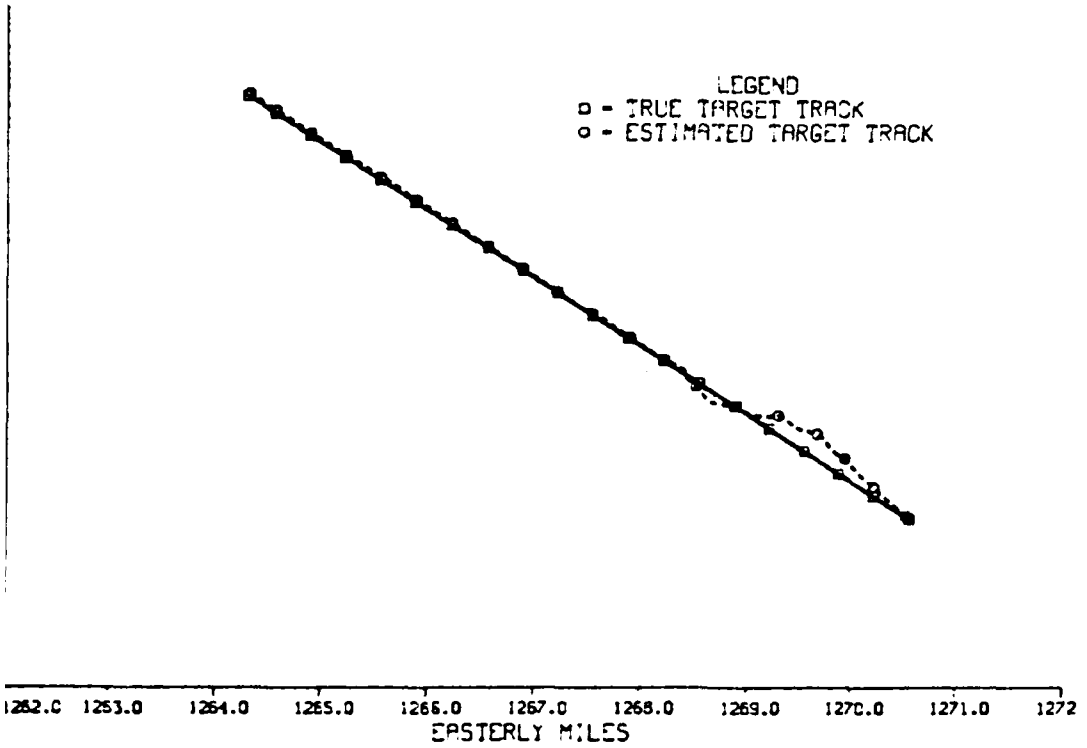

Figure 5.6 True and Estimated Target Track From Alpha and Beta Only

rget in all cases, there is room for improvement in its rformance. Specifically, the quality of the filter operaon can be gauged by how statistically well the SSE values t within a χ^2_N confidence interval, where

N = (number of runs) X (error vector dimension).

this case, when a 95% confidence interval (i.e. the gion within which 95% of the SSE values should fall based the χ^2_{80} probability distribution) is considered, less an half of the SSE values fall within it for any of the ree cases under consideration. Speculation as to how the lter's performance can be improved is reserved for Chapter ; in the meantime, however, a simplified criterion can be ployed here to attempt a rough evaluation of the relative fectiveness of the three different modes of filter eration.

AD-A156 139 TARGET OBSERVABILITY FOR SATELLITE-BASED SENSORS(U) 2/2
NAVAL POSTGRADUATE SCHOOL MONTERREY CA R E BOND MAR 85

UNCLASSIFIED F/G 17/7 NL

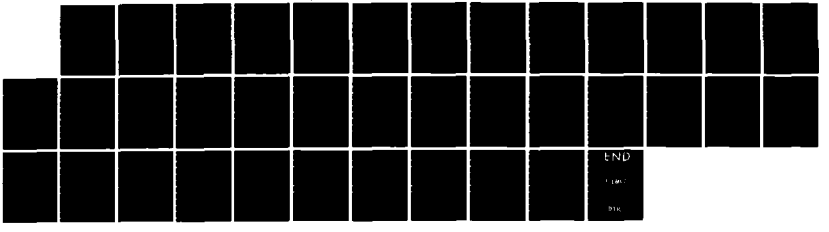

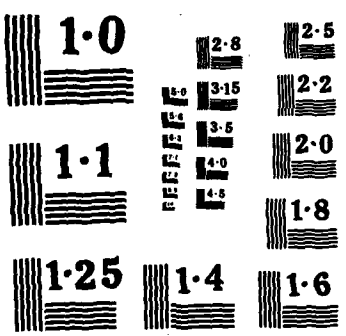

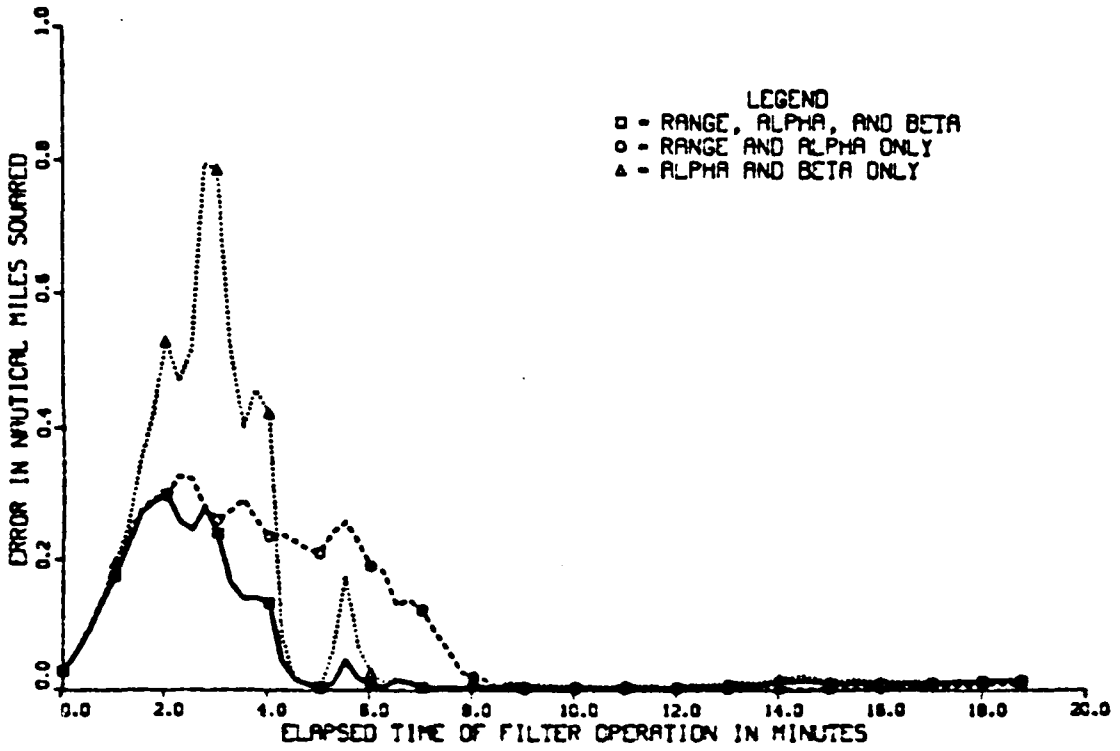

Figure 5.7 Simplified Error Criterion vs Time For a Single Trial of the Filter

A simplified error criterion that suggests itself might be

$$SSSE(k) = \tilde{X}_1^2 + \tilde{X}_3^2 + T^2\left(\tilde{X}_2^2 + \tilde{X}_4^2\right) \quad nm_s^2$$

where the time step functions as a scaling factor to roughly equate the significance of the position and velocity errors. Figure 5.7 shows the application of this criterion to the single run.

Once again, the results seem to validate the hypothesis that the filter works better for all three variables than for two, but this is still information gained from only a single trial. Now that the error criterion has been established, however, the Monte Carlo runs can be considered.

The number of runs is chosen to be 20, and the first application of the repeated trials was to smooth out the

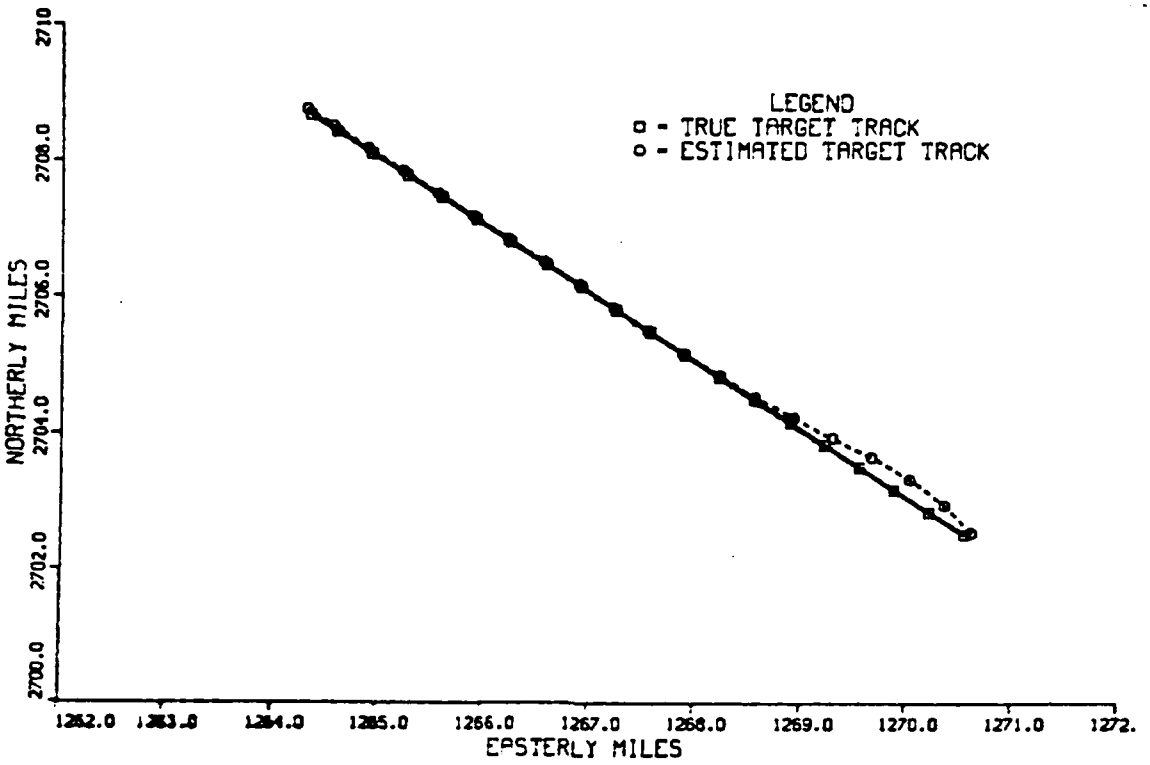

Figure 5.8 True and Estimated Target Track From Range, Alpha, and Beta For Twenty Monte Carlo Runs

estimated trajectories in Figures 5.4 through 5.6; the result was the series of Figures 5.8 through 5.10 . The initial perceptions of the filter's ability to track the target appear to have been borne out, that is, the estimate does converge to the true track in the general case, and the filter tracks better when all three variables of observation are available. However, the initial error in the estimated track proved not to be an anomaly of the particular trial, but showed up repeatedly throughout the Monte Carlo runs. This suggests an imbedded error in the initialization process for the filter, possibly in the initial covariance estimate; this would also help to explain the filter's failure to place the SSE values in the χ^2_{α} confidence interval. Examination of Figure 5.11, which shows the

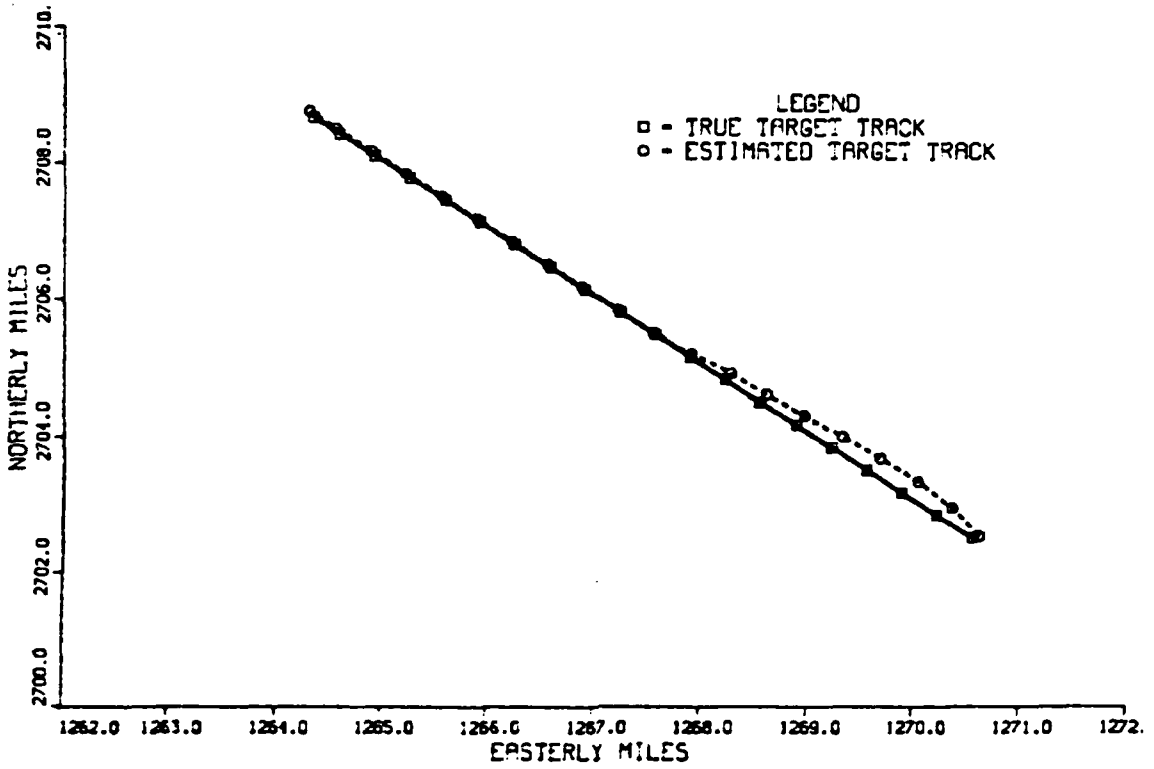

Figure 5.9 True and Estimated Target Track From Range and Alpha Only For Twenty Monte Carlo Runs

simplified error criterion for the 20 runs, also tends to validate the results of the single trial, and further supports the supposition that the filter correctly tracks the target in each case, although there is some initial error. Finally, Figures 5.12 and 5.13 were drawn to take another closer look at the quality of the filter estimates over 20 runs. It now becomes obvious that a primary source of error is in the initial velocity estimates. Also, the filter's slow (30 time steps or 7.5 minutes) convergence to the true velocities indicates that some error in the initial covariance estimate is indeed present. Ironically, because one initial velocity estimate is low and the other is high, the filter's initial estimate of the target's speed is fairly accurate; it is the estimate of target course that is

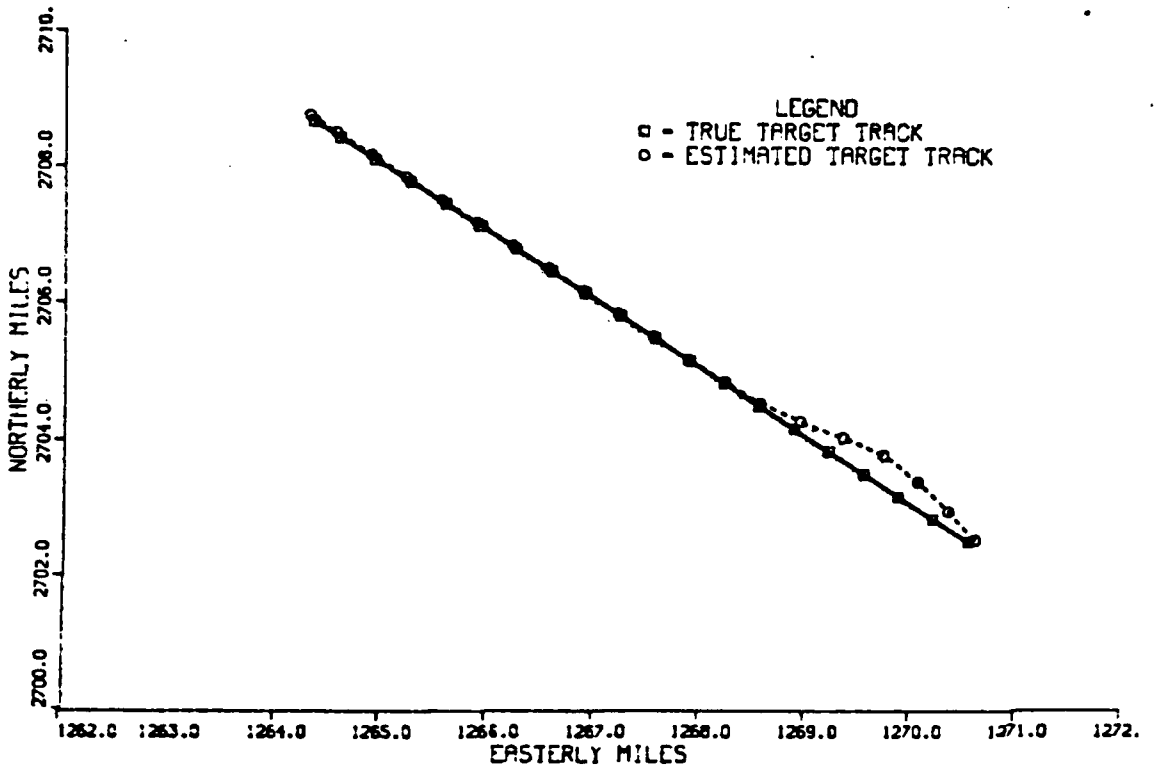

Figure 5.10 True and Estimated Target Track From Alpha and Beta Only For Twenty Monte Carlo Runs

initially in significant error. This could well be a function of the geometry of the nonlinearities of the problem, indicating a potential pitfall of assuming that white noise will remain white after undergoing several nonlinear transformations. Tracking targets moving in other directions might well shed light on the veracity of this supposition.

To summarize briefly, although the filter's initialization might be improved, it nonetheless demonstrates an ability to track the target in all three modes of operation. It provides evidence that the target track is more accurate when all three variables of observation are available as opposed to only two, but that operating in the $\alpha - \beta$ mode does not really represent a significant degradation over the R-α mode. This is an important result because it allows for

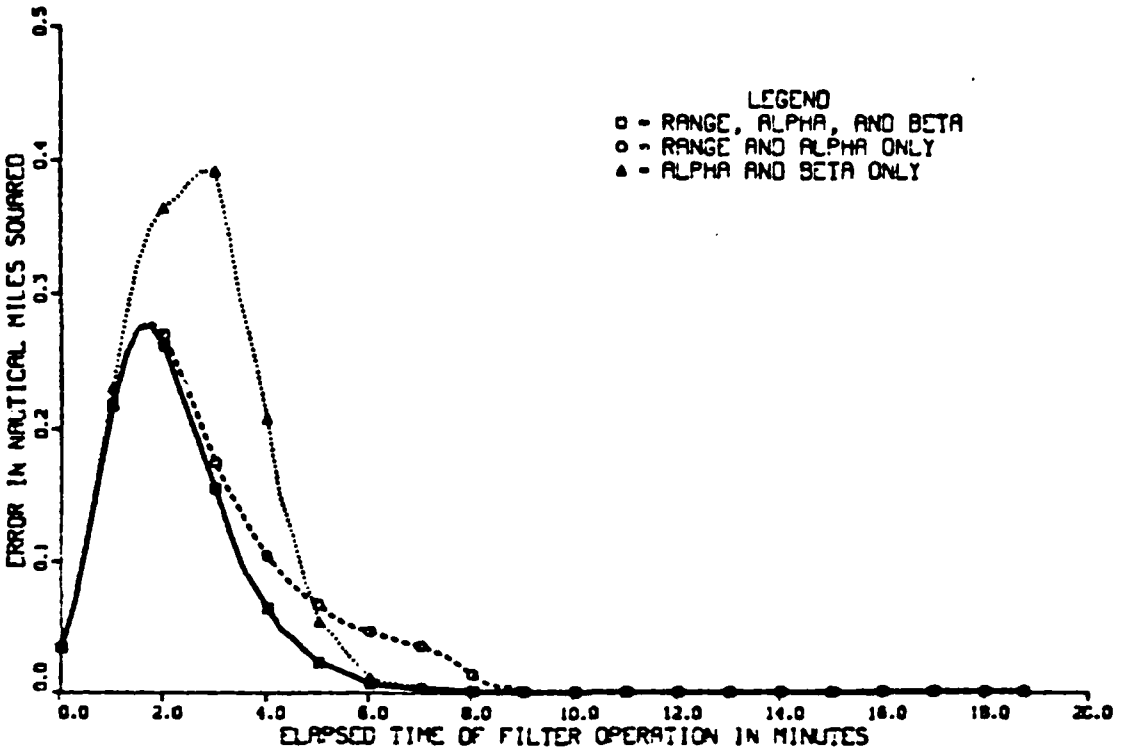

Figure 5.11 Simplified Error Criterion vs Time For Twenty Monte Carlo Runs

the possibility of passive target tracking. The supposedly unobservable R-β mode of operation is not attempted because the solution of the equations that comprise the filter algorithm without R or β is difficult but feasible, but without using α it becomes impossible. Verification of the unobservability of the target tracked by range and altitude angle only thus requires a different filter.

This completes the discussion of the results of the EKF tracking a surface target, and concludes the analytical portion of this thesis.

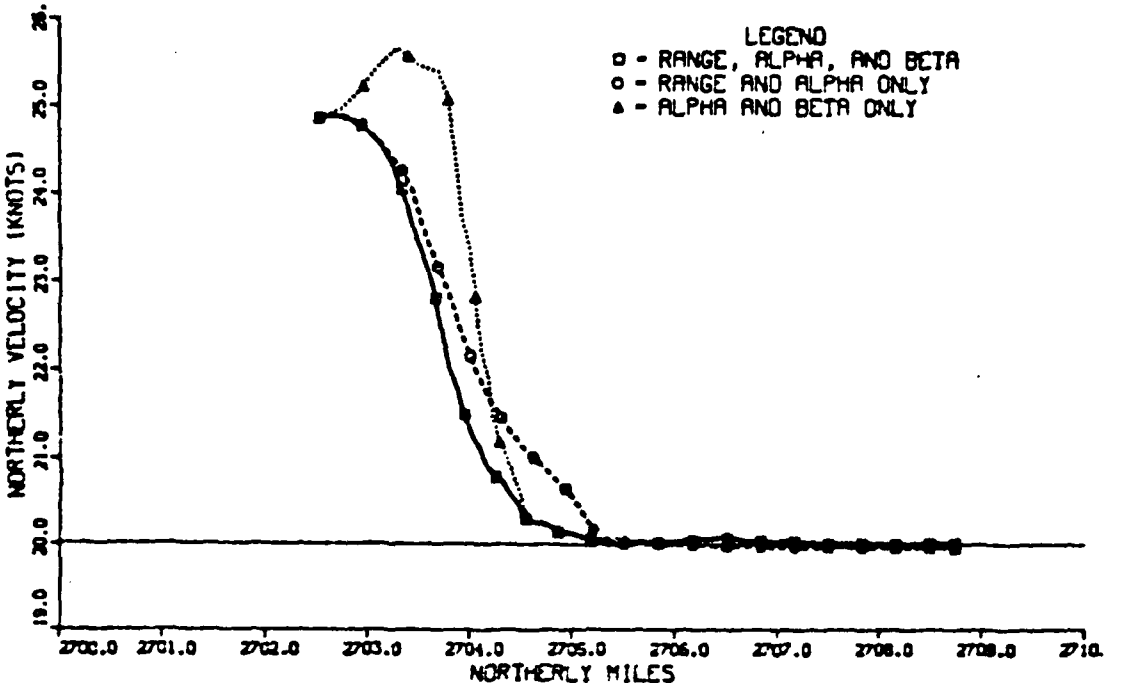

Figure 5.12 Northerly Position vs Velocity
For Twenty Monte Carlo Runs

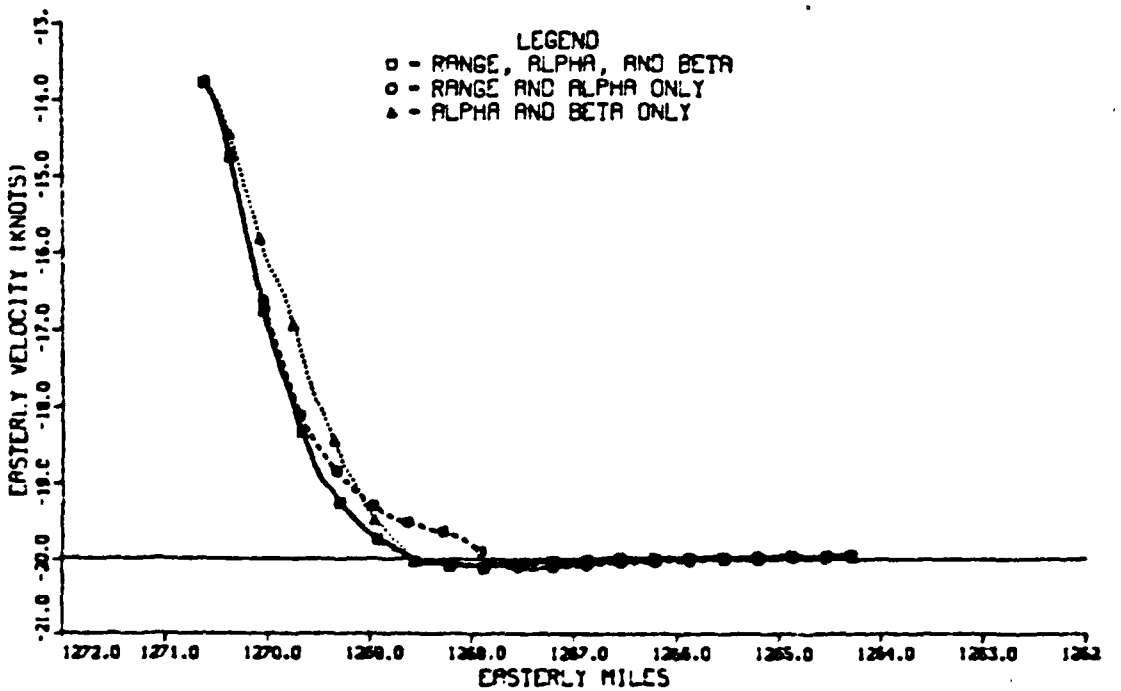

Figure 5.13 Easterly Position vs Velocity
For Twenty Monte Carlo Runs

VI. CONCLUSIONS AND RECOMMENDATIONS FOR FURTHER WORK

During the evolution of this thesis, it has become very clear why the observability of nonlinear systems has historically been an unsolved problem, at least in the most general case, and inroads have been made only gradually by a relatively few individuals. The algebra involved in applying any mathematical form of analysis to a nonlinear system is frequently so prohibitive as to make such procedures of questionable value. Consequently, the observability analysis of a nonlinear system is frequently based as much on intuition as demonstrable mathematical proof. Thus while the statement of this problem--observability analysis for a satellite tracking an earth-bound target--is reasonably simple, it quickly becomes obvious its formulation is not. Specifically, every reference available pertaining to either the satellite-target dynamics or nonlinear observability uses a different notation, and there are very clearly defined crossover points in the information available. Most sources either discuss the satellite's orbit in the language of physics, describe target observations in a purely empirical sense, or discuss nonlinear observability as applied to a general state space. Consequently, one of the major objectives of this thesis becomes the synthesis of as much available information as possible on the entire problem, and the formulation of a pertinent and coherent state vector model. For the sake of their universal recognition, latitude and longitude are retained as the earth's surface coordinates, although much debate has taken place on the subject of alternative coordinate systems that might pertain. Certainly, one would hope that there exists another reference frame wherein the

mathematical observability analysis of Chapter IV could be simplified such that the transformation to rectangular coordinates would not be required. Similarly, the calculations required to implement the filter algorithm of Chapter V might also be streamlined. Because there is potential for continued exploration of these and other aspects of this problem, the suggestions for further work made below are no less important than the specific conclusions that can be drawn from this research effort.

A. CONCLUSIONS

As is so frequently the case, the original intent of this research was overly ambitious in attempting to solve both the complex nonlinear observability and target tracking problems. The results presented here, however, do systematically show the interrelationship of these problems, such as through the computation of the Jacobian matrices for the perturbation analysis, for the EKF, and for the observability analysis. This points out the need for an efficient algorithm for high-order Jacobian evaluations.

The analysis presented here forms a good base for continued research on tracking satellite deployment geometry and desired receiver information. The parametric description of the satellite dynamics pertinent to this problem involves a great deal of information not necessarily familiar to most engineers. This research proved interesting, and is well documented in the literature. There is a wealth of diverse information available in sources such as [Ref. 5] and [Ref. 6]. The intent here, however, is to integrate this information into a coherent overview of the mechanics of an orbiting satellite and its observation of a target moving on or near the Earth's surface, providing enough information to fully define the problem without drowning it in minutia.

Next the physical system is redefined in terms of the state vector space more familiar to Electrical Engineers. Also, the analysis establishes the computational procedure for translation from observed satellite data to earth surface coordinates. Appropriate coordinate selection here is obviously crucial to the observability analysis. Any method of locating position or describing motion on a sphere, however, requires a radial vector and two angles, which is precisely what is defined by latitude, longitude, and altitude (i.e. the radial vector from the Earth's center). The further conversion from latitude and longitude to northerly and easterly distance is made in an effort to at least partially linearize the problem; the merit of this decision is proven by simulation, wherein the constant velocity target is modeled very simply in these coordinates. Had latiude and longitude been retained in the plant coordinates, even this simple case would have required a highly nonlinear description.

With regards to target observability, the simpler cases considered first are intended to provide some intuition about the problem. From the linearized case, it is determined that having the position variables available for two or more observations is equivalent to observing both position and velocity during a single look. From the case of the nonlinear model of the stationary target, it becomes obvious that the coordinates derived in the earlier chapters are not especially well-suited to this method of observability analysis. Thus another transformation is performed, this time from the spherical space into a rectangular one. In the process, it is discovered that a stationary target's position can be fixed with two or more looks at a single variable of observation, which might prove of great utility if it is desired to locate passively a land-based radar transmitter or communications station. When the moving,

airborne, general-case target is ultimately considered, it is shown that such targets prove unobservable when only a single parameter of observation is available. When the variables of observation are considered in combination, however, the target becomes observable in virtually every case that includes at least one position variable. The insight developed during the mathematical derivation of the coordinates suggests that the R-β combinations should prove the exception to this rule, and lead to an unobservable system whether considering complete state or just position observability. Demonstrating unobservability conclusively by this method, however, would require the evaluation of some 130,000 determinants; thus applying the analytical method to demonstrate this result is of questionable practicality. While a complete nonlinear observability analysis then is almost impossible, the analytical method does provide further insight into relevant aspects of observability for the problem. One particularly important result of the analysis is the α-only tracking of the maneuvering surface target, and the α-β tracking of the general target, both very useful if a passive sensor is of tactical advantage. As a footnote, the greater sensitivity of the observer matrices to fluctuations in β than to R or α is discussed briefly; further development of this topic is certainly possible, although time did not permit it here.

The first-cut attempt at a tracking filter design serves to validate many of the concepts and intuitions brought to light during the observability analysis, including the feasibility of α-β tracking, and the greater accuracy possible when employing all the variables of observation. The inherent problems of the EKF in general and this version in particular lead one to conclude that this is not the optimum method for tracking a target. Fortunately, other methods are available, including the Truncated Second Order

Filter (TSOF) and the Gaussian Second Order Filter (GSOF), both discussed in [Ref. 9]. Their greater utility should not, however, take away from the fact that this EKF does generate an estimate that converges to the target's actual track in all three phases of its operation, at least for the small number of cases considered here. It also proves that the coordinates developed in Chapters II and III to describe the problem, while not particularly well-suited to the observability analysis of Chapter IV, work demonstrably well in engineering application.

B. RECOMMENDATIONS FOR FURTHER WORK

During the development of this thesis, it became obvious that to discuss completely all aspects of this problem at this time would not be possible; thus these recommendations for further work are made. A final word on the subject of coordinate selection: for every equation that appears in Appendix A as part of the Jacobian observer matrix calculations, at least half again as many equations were derived during abortive attempts to apply this method of nonlinear observability to the problem in other coordinate systems, including latitude-longitude-altitude, ρ-η, and R-χ-β as the plant (i.e. system) coordinates. None of these provide any simpler mathematical results; in fact, they all prove even more complicated to employ. Perhaps by redefining the problem in terms of a new set of coordinates not discussed in this thesis the observability analysis could become more streamlined and/or definitively conclusive, but no such coordinate system has revealed itself thus far.

Next the question of the tracking filter should be addressed. Had more time been available, this report would have attempted to improve the filter performance, either by eradicating the inherent errors apparent in the state vector

and covariance matrix initializations, or else using a more sophisticated filter such as the TSOF or GSOF. Further, a two-stage nonlinear filter has recently been proposed which shows superior tracking performance to any of these; its specifications and performance are discussed in [Ref. 10] and [Ref. 12]. The employment of these or other more complicated filters might well afford the opportunity to verify the feasibility of an α-only track of the maneuvering surface target or the purported unobservability of the R-β track. The goal in this thesis, however, is not actually to design the optimum tracking filter, but to demonstrate the possibility of doing so. The EKF is a relatively simple algorithm, and thus is useful here; even so, there is room for further analysis of its performance. Other methods of initialization might be considered, particularly for the covariance martix; also, the tracking of other targets, such as a maneuvering surface target or an air target with its six-dimensional state vector, might be attempted. An analysis of its sensitivity could be conducted, varying both the system and the observer noises in turn; this would hopefully validate the declaration in Chapter IV that the system should be more sensitive to fluctuations in β than those in R or α. All of these variations on the theme of filter operation could of course also be undertaken for the alternative filters.

No mention has been made thus far of multiple targets or multiple observers, but of course the situation explored in this thesis is the simplest possible, that is, a single target being observed by a single satellite with a perfect probability of observation when in view. In actuality, of course, the problem is far more complicated, as the consideration of multiple targets and multiple observers immediately introduces the probability of false target detection; of improper correlation of targets to successive or

Differentiating once with respect to time,

$$\dot{\beta} = \frac{h(n\dot{n}+e\dot{e}) - \dot{h}(n^2+e^2)}{(n^2+e^2+h^2)(n^2+e^2)^{1/2}},$$

or $$Q\dot{\beta} = h(n\dot{n}+e\dot{e}) - \dot{h}(n^2+e^2), \quad Q = (n^2+e^2+h^2)(n^2+e^2)^{1/2}$$

The next five time derivatives are taken as before, and then the partial derivatives with respect to n, $\dot{n}$, e, $\dot{e}$, h, and $\dot{h}$. Eliminating all the intermediate steps which would follow in exactly the same sequence as in the previous section, the resultant observer matrices are

$$\underline{J}_5 = \frac{1}{Q^6}\begin{bmatrix}
nh & 0 & eh & 0 & -n^2-e^2 & 0 \\
\dot{n}h-2\dot{n}\dot{h}+\psi_n & nh & \dot{e}h-2\dot{e}\dot{h}+\psi_e & eh & n\dot{n}+e\dot{e}+\psi_h & -n^2-e^2 \\
a_N h-\ddot{n}\dot{h} & 2\dot{n}h-n\dot{h} & a_E h-\ddot{e}\dot{h} & 2\dot{e}h-e\dot{h} & na_N+ea_E & -n\dot{n}-e\dot{e} \\
-2\dot{n}a_N+\ddot{\psi}_n & +\psi_n & -2\dot{e}a_N+\ddot{\psi}_e & +\psi_e & +\dot{n}^2+\dot{e}^2+\psi_h & +\psi_h \\
-3\dot{n}a_N+\dddot{\psi}_n & 3na_N-3\dot{n}a_N & -3\dot{e}a_N+\dddot{\psi}_e & -3\dot{e}a_N+3ha_E & 3\dot{n}a_N+3\dot{e}a_E & 2\dot{\psi}_h \\
 & +2\dot{\psi}_n & & +2\dot{\psi}_e & +\ddot{\psi}_h & \\
-3a_N a_N+\psi^{iv}_n & 3\dot{n}a_N-3na_N & -3a_E a_N+\dddot{\psi}_e & 3ha_E-3\dot{e}a_N & 3a_N^2+3a_E^2 & 3\dot{n}a_N+3\dot{e}a_E \\
 & +3\ddot{\psi}_n & & +3\ddot{\psi}_e & +\ddot{\psi}_h & +3\dddot{\psi}_h \\
\psi^{iv}_n & -6a_N a_N+4\dddot{\psi}_n & \psi^{iv}_e & -6a_E a_N+4\dddot{\psi}_e & \psi^{iv}_h & 6a_N^2+6a_E^2 \\
 & & & & & +4\dot{\psi}_h
\end{bmatrix},$$

$$\underline{J}_6 = \frac{1}{Q^6}\begin{bmatrix}
-\dot{n}h-2n\dot{h} & nh & \dot{e}h-2e\dot{h} & eh & n\dot{n}+e\dot{e}+\psi_h & -n^2-e^2 \\
+\psi_n & & +\psi_e & & & \\
a_N h-\dot{n}\dot{h} & 2\dot{n}h-n\dot{h} & a_E h-\dot{e}\dot{h} & 2\dot{e}h-e\dot{h} & na_N+ea_E & -n\dot{n}-e\dot{e}+\psi_h \\
-2\dot{n}a_N+\ddot{\psi}_n & +\psi_n & -2\dot{e}a_N+\ddot{\psi}_e & +\psi_e & +\dot{n}^2+\dot{e}^2+\psi_h & \\
-3a_N\dot{n}+\dddot{\psi}_n & 3\dot{n}a_N-3na_N & -3\dot{e}a_N+\dddot{\psi}_e & -3\dot{e}a_N+3ha_E & 3\dot{n}a_N+3\dot{e}a_E & 2\dot{\psi}_h \\
 & +2\dot{\psi}_n & & +2\dot{\psi}_e & +\ddot{\psi}_h & \\
-3a_N a_N+\psi^{iv}_n & 3\dot{n}a_N-3na_N & -3a_N a_N+\dddot{\psi}_e & 3ha_E-3\dot{e}a_N & 3a_N^2+3a_E^2 & 3\dot{n}a_N+3\dot{e}a_E \\
 & +3\ddot{\psi}_n & & +3\ddot{\psi}_e & +\dddot{\psi}_h & +3\ddot{\psi}_h \\
\psi^{iv}_n & -6a_N a_N+4\dddot{\psi}_n & \psi^{iv}_e & -6a_E a_N+4\dddot{\psi}_e & \psi^{iv}_h & 6a_N\dot{a}_N+6a_E\dot{a}_E \\
 & & & & & +4\dot{\psi}_h \\
\psi^{v}_n & 5\psi^{iv}_n & \psi^{v}_e & 5\psi^{iv}_e & \psi^{v}_h & 5\psi^{iv}_h
\end{bmatrix}.$$

$$\underset{\sim}{J}_a = \frac{1}{\Sigma^6}\begin{bmatrix} \dot{e}+\chi_n & -e & -\dot{n}+\chi_e & n & 0 & 0 \\ a_e+\dot{\chi}_n & \chi_n & -a_n+\dot{\chi}_e & \chi_e & 0 & 0 \\ \ddot{\chi}_n & a_e+2\dot{\chi}_n & \ddot{\chi}_e & -a_n+2\dot{\chi}_e & 0 & 0 \\ \dddot{\chi}_n & 3\ddot{\chi}_n & \dddot{\chi}_e & 3\ddot{\chi}_e & 0 & 0 \\ \chi^{iv}_n & 4\dddot{\chi}_n & \chi^{iv}_e & 4\dddot{\chi}_e & 0 & 0 \\ \chi^{v}_n & 5\chi^{iv}_n & \chi^{v}_e & 5\chi^{iv}_e & 0 & 0 \end{bmatrix},$$

where

$$\chi_{n,e} = -\Sigma_{n,e}\,\dot{\alpha},$$

$$\dot{\chi}_{n,e} = -\Sigma_{n,e}\,\ddot{\alpha} - \dot{\Sigma}_{n,e}\,\dot{\alpha},$$

$$\ddot{\chi}_{n,e} = -\Sigma_{n,e}\,\dddot{\alpha} - 2\dot{\Sigma}_{n,e}\,\ddot{\alpha} - \ddot{\Sigma}_{n,e}\,\dot{\alpha},$$

$$\dddot{\chi}_{n,e} = -\Sigma_{n,e}\,\alpha^{iv} - 3\dot{\Sigma}_{n,e}\,\dddot{\alpha} - 3\ddot{\Sigma}_{n,e}\,\ddot{\alpha},$$

$$\chi^{iv}_{n,e} = -\Sigma_{n,e}\,\alpha^{v} - 4\dot{\Sigma}_{n,e}\,\alpha^{iv} - 6\ddot{\Sigma}_{n,e}\,\dddot{\alpha},$$

$$\chi^{v}_{n,e} = -\Sigma_{n,e}\,\alpha^{vi} - 5\dot{\Sigma}_{n,e}\,\alpha^{v} - 10\ddot{\Sigma}_{n,e}\,\alpha^{iv}.$$

C. OBSERVER MATRICES FOR ALTITUDE BEARING AND ALTITUDE BEARING RATE

The derivation of the $\underset{\sim}{J}_\beta$ and $\underset{\sim}{J}_{\dot\beta}$ matrices for tha altitude bearing variables β and $\dot\beta$ is the lengthiest of all, but using the lessons learned in the previous two sections, it should prove no more difficult. In this coordinate system,

$$\beta = \cos^{-1} h/R,$$

Obviously, all the partial derivatives with respect to h will be zero.

This leads to the formation of the $\underset{\sim}{J}_3$ and $\underset{\sim}{J}_4$ matrices

$$\underset{\sim}{J}_3 = \begin{bmatrix} \alpha_n & \alpha_i & \alpha_e & \alpha_c & 0 & 0 \\ \dot{\alpha}_n & \dot{\alpha}_i & \dot{\alpha}_e & \dot{\alpha}_c & 0 & 0 \\ \ddot{\alpha}_n & \ddot{\alpha}_i & \ddot{\alpha}_e & \ddot{\alpha}_e & 0 & 0 \\ \dddot{\alpha}_n & \dddot{\alpha}_i & \dddot{\alpha}_e & \dddot{\alpha}_e & 0 & 0 \\ \alpha_n^{iv} & \alpha_i^{iv} & \alpha_e^{iv} & \alpha_e^{iv} & 0 & 0 \\ \alpha_n^{v} & \alpha_i^{v} & \alpha_e^{v} & \alpha_e^{v} & 0 & 0 \end{bmatrix}; \quad \underset{\sim}{J}_4 = \begin{bmatrix} \dot{\alpha}_n & \dot{\alpha}_i & \dot{\alpha}_e & \dot{\alpha}_i & 0 & 0 \\ \ddot{\alpha}_n & \ddot{\alpha}_i & \ddot{\alpha}_e & \ddot{\alpha}_e & 0 & 0 \\ \dddot{\alpha}_n & \dddot{\alpha}_i & \dddot{\alpha}_e & \dddot{\alpha}_e & 0 & 0 \\ \alpha_n^{iv} & \alpha_i^{iv} & \alpha_e^{iv} & \alpha_e^{iv} & 0 & 0 \\ \alpha_n^{v} & \alpha_i^{v} & \alpha_e^{v} & \alpha_e^{v} & 0 & 0 \\ \alpha_n^{vi} & \alpha_i^{vi} & \alpha_e^{vi} & \alpha_e^{vi} & 0 & 0 \end{bmatrix},$$

which are simplified by the same sort of row-reducing method employed in the $\underset{\sim}{J}_1$ and $\underset{\sim}{J}_2$ matrices. This time, however, all the terms do not cancel simply, and the result is

$$\underset{\sim}{J}_3 = \frac{1}{\Sigma^6} \begin{bmatrix} -e & 0 & n & 0 & 0 & 0 \\ \dot{e}+\chi_n & -e & -\dot{n}+\chi_e & n & 0 & 0 \\ a_e+\ddot{\chi}_n & \chi_n & -a_n+\dot{\chi}_e & \chi_e & 0 & 0 \\ \dddot{\chi}_n & a_e+2\dot{\chi}_n & \ddot{\chi}_e & -a_n+2\dot{\chi}_e & 0 & 0 \\ \chi_n^{iii} & 3\ddot{\chi}_n & \chi_e^{iii} & 3\ddot{\chi}_e & 0 & 0 \\ \chi_n^{iv} & 4\dddot{\chi}_n & \chi_e^{iv} & 4\dddot{\chi}_e & 0 & 0 \end{bmatrix};$$

$$\dot{\alpha}_e = \frac{1}{\Sigma}\left(-\dot{n} - \Sigma_e \dot{\lambda}\right),$$

$$\ddot{\alpha}_e = \frac{1}{\Sigma}\left(-a_w - \Sigma_e \ddot{\lambda} - \dot{\Sigma}\dot{\lambda}_e - \dot{\Sigma}_e \dot{\lambda}\right),$$

$$\dddot{\alpha}_e = \frac{1}{\Sigma}\left(-\Sigma_e \dddot{\lambda} - 2\dot{\Sigma}\ddot{\lambda}_e - 2\dot{\Sigma}_e \ddot{\lambda} - \ddot{\Sigma}\dot{\lambda}_e - \ddot{\Sigma}_e \dot{\lambda}\right),$$

$$\alpha^{iv}_e = \frac{1}{\Sigma}\left(-\Sigma_e \lambda^{iv} - 3\dot{\Sigma}\dddot{\lambda}_e - 3\dot{\Sigma}_e \ddot{\lambda} - 3\ddot{\Sigma}\ddot{\lambda}_e - 3\ddot{\Sigma}_e \dot{\lambda} - \dddot{\Sigma}\lambda_e\right),$$

$$\alpha^{v}_e = \frac{1}{\Sigma}\left(-\Sigma_e \lambda^{v} - 4\dot{\Sigma}\lambda^{iv}_e - 4\dot{\Sigma}_e \dddot{\lambda} - 6\ddot{\Sigma}\ddot{\lambda}_e - 6\ddot{\Sigma}_e \ddot{\lambda} - 4\dddot{\Sigma}\dot{\lambda}_e - \Sigma^{iv}\lambda_e\right),$$

$$\alpha^{vi}_e = \frac{1}{\Sigma}\left(-\Sigma_e \lambda^{vi} - 5\dot{\Sigma}\lambda^{v}_e - 5\dot{\Sigma}_e \lambda^{iv} - 10\ddot{\Sigma}\dddot{\lambda}_e - 10\ddot{\Sigma}_e \dddot{\lambda} - 10\dddot{\Sigma}\ddot{\lambda}_e - 5\Sigma^{iv}\dot{\lambda}_e\right);$$

$$\alpha_{\dot{e}} = 0,$$

$$\dot{\alpha}_{\dot{e}} = n/\Sigma,$$

$$\ddot{\alpha}_{\dot{e}} = \frac{1}{\Sigma}\left(-\dot{\Sigma}\dot{\lambda}_{\dot{e}} - \dot{\Sigma}_{\dot{e}}\dot{\lambda}\right),$$

$$\dddot{\alpha}_{\dot{e}} = \frac{1}{\Sigma}\left(-a_w - 2\dot{\Sigma}\ddot{\lambda}_{\dot{e}} - 2\dot{\Sigma}_{\dot{e}}\ddot{\lambda} - \ddot{\Sigma}\dot{\lambda}_{\dot{e}} - \ddot{\Sigma}_{\dot{e}}\dot{\lambda}\right),$$

$$\alpha^{iv}_{\dot{e}} = \frac{1}{\Sigma}\left(-3\dot{\Sigma}\dddot{\lambda}_{\dot{e}} - 3\dot{\Sigma}_{\dot{e}}\ddot{\lambda} - 3\ddot{\Sigma}\dot{\lambda}_{\dot{e}} - 3\ddot{\Sigma}_{\dot{e}}\dot{\lambda} - \dddot{\Sigma}\lambda_{\dot{e}} - \dddot{\Sigma}_{\dot{e}}\lambda\right),$$

$$\alpha^{v}_{\dot{e}} = \frac{1}{\Sigma}\left(-4\dot{\Sigma}\lambda^{iv}_{\dot{e}} - 4\dot{\Sigma}_{\dot{e}}\dddot{\lambda} - 6\ddot{\Sigma}\ddot{\lambda}_{\dot{e}} - 6\ddot{\Sigma}_{\dot{e}}\ddot{\lambda} - 4\dddot{\Sigma}\dot{\lambda}_{\dot{e}} - 4\dddot{\Sigma}_{\dot{e}}\dot{\lambda} - \Sigma^{iv}\lambda_{\dot{e}}\right),$$

$$\alpha^{vi}_{\dot{e}} = \frac{1}{\Sigma}\left(-5\dot{\Sigma}\lambda^{v}_{\dot{e}} - 5\dot{\Sigma}_{\dot{e}}\lambda^{iv} - 10\ddot{\Sigma}\dddot{\lambda}_{\dot{e}} - 10\ddot{\Sigma}_{\dot{e}}\dddot{\lambda} - 10\dddot{\Sigma}\ddot{\lambda}_{\dot{e}} - 10\dddot{\Sigma}_{\dot{e}}\ddot{\lambda} - 5\Sigma^{iv}\dot{\lambda}_{\dot{e}}\right),$$

where $\Sigma = n^2 + e^2$, $\Sigma_e = 2e$, $\Sigma_{\dot{e}} = 0$,

$\dot{\Sigma} = 2n\dot{n} + 2e\dot{e}$, $\dot{\Sigma}_e = 2\dot{e}$, $\dot{\Sigma}_{\dot{e}} = 2e$,

$\ddot{\Sigma} = 2\dot{n}^2 + 2na_w + 2\dot{e}^2 + 2ea_e$, $\ddot{\Sigma}_e = 2a_e$, $\ddot{\Sigma}_{\dot{e}} = 4\dot{e}$,

$\dddot{\Sigma} = 6\dot{n}a_w + 6\dot{e}a_e$, $\dddot{\Sigma}_e = 0$, $\dddot{\Sigma}_{\dot{e}} = 6a_e$,

$\Sigma^{iv} = 6a_w^2 + 6a_e^2$, $\Sigma^{iv}_e = 0$, $\Sigma^{iv}_{\dot{e}} = 0$,

$\Sigma^{v} = 0$.

Taking the partial derivative of each of the first seven equations with respect to $\dot{n}$ follows the same pattern; solving again for the highest order derivative,

$$\alpha_{\dot{n}} = 0,$$

$$\dot{\alpha}_{\dot{n}} = -e/\Sigma,$$

$$\ddot{\alpha}_{\dot{n}} = \frac{1}{\Sigma}\left(-\dot{\Sigma}\dot{\lambda}_{\dot{n}} - \dot{\Sigma}_{\dot{n}}\dot{\lambda}\right),$$

$$\dddot{\alpha}_{\dot{n}} = \frac{1}{\Sigma}\left(a_e - 2\dot{\Sigma}\ddot{\lambda}_{\dot{n}} - 2\dot{\Sigma}_{\dot{n}}\ddot{\lambda} - \ddot{\Sigma}\dot{\lambda}_{\dot{n}} - \ddot{\Sigma}_{\dot{n}}\dot{\lambda}\right),$$

$$\alpha^{iv}_{\dot{n}} = \frac{1}{\Sigma}\left(-3\dot{\Sigma}\dddot{\lambda}_{\dot{n}} - 3\dot{\Sigma}_{\dot{n}}\ddot{\lambda} - 3\ddot{\Sigma}_{\dot{n}}\ddot{\lambda} - 3\ddot{\Sigma}\ddot{\lambda}_{\dot{n}} - \dddot{\Sigma}\dot{\lambda}_{\dot{n}} - \dddot{\Sigma}_{\dot{n}}\dot{\lambda}\right),$$

$$\alpha^{v}_{\dot{n}} = \frac{1}{\Sigma}\left(-4\dot{\Sigma}\alpha^{iv}_{\dot{n}} - 4\dot{\Sigma}_{\dot{n}}\dddot{\lambda} - 6\ddot{\Sigma}_{\dot{n}}\ddot{\lambda} - 6\ddot{\Sigma}\ddot{\lambda}_{\dot{n}} - 4\dddot{\Sigma}\dddot{\lambda}_{\dot{n}} - 4\dddot{\Sigma}_{\dot{n}}\ddot{\lambda} - \Sigma^{iv}\dot{\lambda}_{\dot{n}}\right),$$

$$\alpha^{vi}_{\dot{n}} = \frac{1}{\Sigma}\left(-5\dot{\Sigma}\alpha^{v}_{\dot{n}} - 5\dot{\Sigma}_{\dot{n}}\dddot{\lambda} - 10\ddot{\Sigma}_{\dot{n}}\ddot{\lambda} - 10\ddot{\Sigma}\dddot{\lambda}_{\dot{n}} - 10\dddot{\Sigma}_{\dot{n}}\ddot{\lambda} - 10\dddot{\Sigma}\ddot{\lambda}_{\dot{n}} - 5\Sigma^{iv}\dot{\lambda}_{\dot{n}}\right);$$

where $\Sigma = n^2 + e^2$, $\Sigma_{\dot{n}} = 0$

$$\dot{\Sigma} = 2n\dot{n} + 2e\dot{e}, \quad \dot{\Sigma}_{\dot{n}} = 2n$$

$$\ddot{\Sigma} = 2na_N + 2\dot{n}^2 + 2ea_E + 2\dot{e}^2, \quad \ddot{\Sigma}_{\dot{n}} = 4\dot{n},$$

$$\dddot{\Sigma} = 6\dot{n}a_N + 6\dot{e}a_E, \quad \dddot{\Sigma}_{\dot{n}} = 6a_N$$

$$\Sigma^{iv} = 6a_N^2 + 6a_E^2, \quad \Sigma^{iv}_{\dot{n}} = 0$$

$$\Sigma^{v} = 0.$$

The differentiations with respect to e and $\dot{e}$ follow the identical pattern, with the exception that the (n, n, a_N) terms are replaced by $(e, \dot{e}, a_E)$ terms of opposite sign, so

$$\alpha_e = n/\Sigma,$$

$$\dddot{\Sigma}_n \dot{\alpha} + \ddot{\Sigma}\dot{\alpha}_n + 3\ddot{\Sigma}_n \ddot{\alpha} + 3\ddot{\Sigma}\ddot{\alpha}_n + 3\dot{\Sigma}_n \dddot{\alpha} + 3\dot{\Sigma}\dddot{\alpha}_n + \Sigma_n \alpha^{iv} + \Sigma \alpha^{iv}_n = 0,$$

$$\Sigma^{iv}_n \dot{\alpha} + \Sigma^{iv}\dot{\alpha}_n + 4\dddot{\Sigma}_n \ddot{\alpha} + 4\ddot{\Sigma}\ddot{\alpha}_n + 6\ddot{\Sigma}_n \dddot{\alpha} + 6\ddot{\Sigma}\dddot{\alpha}_n + 4\dot{\Sigma}_n \alpha^{iv} + 4\dot{\Sigma}\alpha^{iv}_n + \Sigma_n \alpha^{v} + \Sigma \alpha^{v}_n = 0,$$

$$5\Sigma^{iv}_n \dot{\alpha} + 5\Sigma^{iv}\dot{\alpha}_n + 10\dddot{\Sigma}_n \ddot{\alpha} + 10\ddot{\Sigma}\dddot{\alpha}_n + 10\ddot{\Sigma}_n \alpha^{iv} + 10\ddot{\Sigma}\alpha^{iv}_n + 5\dot{\Sigma}_n \alpha^{v} + 5\dot{\Sigma}\alpha^{v}_n + \Sigma_n \alpha^{vi} + \Sigma \alpha^{vi}_n = 0;$$

where $\Sigma = n^2 + e^2$, $\Sigma_n = 2n$,

$\dot{\Sigma} = 2n\dot{n} + 2e\dot{e}$, $\dot{\Sigma}_n = 2\dot{n}$,

$\ddot{\Sigma} = 2na_n + 2\dot{n}^2 + 2ea_e + 2\dot{e}^2$, $\ddot{\Sigma}_n = 2a_n$,

$\dddot{\Sigma} = 6\dot{n}a_n + 6\dot{e}a_e$, $\dddot{\Sigma}_n = 0$,

$\Sigma^{iv} = 6a_n^2 + 6a_e^2$, $\Sigma^{iv}_n = 0$,

$\Sigma^{v} = 0$.

Solving for the highest order derivatives,

$$\alpha_n = -e/\Sigma,$$

$$\dot{\alpha}_n = \frac{1}{\Sigma}\left(\dot{e} - \Sigma_n \dot{\alpha}\right),$$

$$\ddot{\alpha}_n = \frac{1}{\Sigma}\left(a_n - \Sigma_n \ddot{\alpha} - \dot{\Sigma}\dot{\alpha}_n - \dot{\Sigma}_n \dot{\alpha}\right),$$

$$\dddot{\alpha}_n = \frac{1}{\Sigma}\left(-\Sigma_n \dddot{\alpha} - 2\dot{\Sigma}\ddot{\alpha}_n - 2\dot{\Sigma}_n \ddot{\alpha} - \ddot{\Sigma}\dot{\alpha}_n - \ddot{\Sigma}_n \dot{\alpha}\right),$$

$$\alpha^{iv}_n = \frac{1}{\Sigma}\left(-\Sigma_n \alpha^{iv} - 3\dot{\Sigma}\dddot{\alpha}_n - 3\dot{\Sigma}_n \dddot{\alpha} - 3\ddot{\Sigma}\ddot{\alpha}_n - 3\ddot{\Sigma}_n \ddot{\alpha} - \dddot{\Sigma}\dot{\alpha}_n\right),$$

$$\alpha^{v}_n = \frac{1}{\Sigma}\left(-\Sigma_n \alpha^{v} - 4\dot{\Sigma}\alpha^{iv}_n - 4\dot{\Sigma}_n \alpha^{iv} - 6\ddot{\Sigma}\dddot{\alpha}_n - 6\ddot{\Sigma}_n \dddot{\alpha} - 4\dddot{\Sigma}\ddot{\alpha}_n - \Sigma^{iv}\dot{\alpha}_n\right),$$

$$\alpha^{vi}_n = \frac{1}{\Sigma}\left(-\Sigma_n \alpha^{vi} - 5\dot{\Sigma}\alpha^{v}_n - 5\dot{\Sigma}_n \alpha^{v} - 10\ddot{\Sigma}\alpha^{iv}_n - 10\ddot{\Sigma}_n \alpha^{iv} - 10\dddot{\Sigma}\dddot{\alpha}_n - 5\Sigma^{iv}\ddot{\alpha}_n\right).$$

where $\Sigma = n^2 + e^2$,

$\dot{\Sigma} = 2n\dot{n} + 2e\dot{e}$,

$\ddot{\Sigma} = 2\dot{n}^2 + 2na_N + 2\dot{e}^2 + 2ea_E$,

$\dddot{\Sigma} = 6\dot{n}a_N + 6\dot{e}a_E$,

$\Sigma^{iv} = 6a_N^2 + 6a_E^2$,

$\Sigma^{v} = 0$.

Solving for the highest order derivative in each equation, one obtains

$$\dot{\alpha} = \frac{1}{\Sigma}\left(n\dot{e} - e\dot{n}\right),$$

$$\ddot{\alpha} = \frac{1}{\Sigma}\left(na_E - ea_N - \dot{\Sigma}\dot{\alpha}\right),$$

$$\dddot{\alpha} = \frac{1}{\Sigma}\left(\dot{n}a_E - \dot{e}a_N - \ddot{\Sigma}\dot{\alpha} - 2\dot{\Sigma}\ddot{\alpha}\right),$$

$$\alpha^{iv} = \frac{1}{\Sigma}\left(-\dddot{\Sigma}\dot{\alpha} - 3\ddot{\Sigma}\ddot{\alpha} - 3\dot{\Sigma}\dddot{\alpha}\right),$$

$$\alpha^{v} = \frac{1}{\Sigma}\left(-\Sigma^{iv}\dot{\alpha} - 4\dddot{\Sigma}\ddot{\alpha} - 6\ddot{\Sigma}\dddot{\alpha} - 4\dot{\Sigma}\alpha^{iv}\right),$$

$$\alpha^{vi} = \frac{1}{\Sigma}\left(-5\Sigma^{iv}\dot{\alpha} - 10\dddot{\Sigma}\ddot{\alpha} - 10\ddot{\Sigma}\alpha^{iv} - 5\dot{\Sigma}\alpha^{v}\right).$$

Taking the partial derivative of each of the first seven equations with respect to n,

$$\Sigma\alpha_n = -e,$$

$$\Sigma_n\dot{\alpha} + \Sigma\dot{\alpha}_n = \dot{e},$$

$$\dot{\Sigma}_n\dot{\alpha} + \dot{\Sigma}\dot{\alpha}_n + \Sigma_n\ddot{\alpha} + \Sigma\ddot{\alpha}_n = a_E,$$

$$\ddot{\Sigma}_n\dot{\alpha} + \ddot{\Sigma}\dot{\alpha}_n + 2\dot{\Sigma}_n\ddot{\alpha} + 2\dot{\Sigma}\ddot{\alpha}_n + \Sigma_n\dddot{\alpha} + \Sigma\dddot{\alpha}_n = 0,$$

$$\underset{\sim}{J}_2 = \frac{3R^{VI}}{R^5}\begin{bmatrix} \dot{n} & n & \dot{e} & e & \dot{h} & h \\ a_N & 2\dot{n} & a_E & 2\dot{e} & a_H & 2\dot{h} \\ 0 & a_N & 0 & a_E & 0 & a_H \\ 0 & 0 & 0 & 0 & 0 & 0 \\ 0 & 0 & 0 & 0 & 0 & 0 \\ n & 0 & e & 0 & h & 0 \end{bmatrix}.$$

B. OBSERVER MATRICES FOR AZIMUTHAL BEARING AND AZIMUTHAL BEARING RATE

The derivation of the Jacobian observer matrices for the azimuthal bearing variables α and $\dot{\alpha}$ follows the method of the previous section, except that the result is not quite so algebraically nice. Consider first the definition of in this coordinate system:

$$\alpha = \text{TAN}^{-1} e/n .$$

Differentiating once with respect to time,

$$\dot{\alpha} = \frac{n\dot{e} - e\dot{n}}{n^2+e^2},$$

or

$$\Sigma\dot{\alpha} = n\dot{e} - e\dot{n}, \quad \Sigma = n^2+e^2.$$

Differentiating five more times with respect to time,

$$\Sigma\ddot{\alpha} + \dot{\Sigma}\dot{\alpha} = na_E - ea_N$$

$$\Sigma\dddot{\alpha} + 2\dot{\Sigma}\ddot{\alpha} + \ddot{\Sigma}\dot{\alpha} = \dot{n}a_E - \dot{e}a_N$$

$$\Sigma\ddot{\alpha}^{IV} + 3\ddot{\Sigma}\ddot{\alpha} + 3\dot{\Sigma}\dddot{\alpha} + \dddot{\Sigma}\dot{\alpha} = 0,$$

$$\Sigma^{V}\dot{\alpha} + 4\dddot{\Sigma}\ddot{\alpha} + 6\ddot{\Sigma}\dddot{\alpha} + 4\dot{\Sigma}\alpha^{IV} + \Sigma\alpha^{V} = 0,$$

$$\Sigma^{V}\dot{\alpha} + 5\Sigma^{IV}\ddot{\alpha} + 10\dddot{\Sigma}\dddot{\alpha} + 10\ddot{\Sigma}\alpha^{IV} + 5\dot{\Sigma}\alpha^{V} + \Sigma\alpha^{VI} = 0,$$

The resulting matrix is

$$\underset{\sim}{J}_1 = \frac{3}{R^4}\begin{bmatrix} n & 0 & e & 0 & h & 0 \\ \dot{n} & n & \dot{e} & e & \dot{h} & h \\ a_N & 2\dot{n} & a_E & 2\dot{e} & a_H & 2\dot{h} \\ 0 & a_N & 0 & a_E & 0 & a_H \\ 0 & 0 & 0 & 0 & 0 & 0 \\ 0 & 0 & 0 & 0 & 0 & 0 \end{bmatrix}.$$

All the terms for the $\dot{R}$ matrix $\underset{\sim}{J}_2$ have already been determined; they come from the same sets of equations just derived, only the first is left off and the last is added on, i.e.

$$\underset{\sim}{J}_2 = \begin{bmatrix} \dot{R}_n & \dot{R}_{\dot{n}} & R_e & \dot{R}_{\dot{e}} & R_h & \dot{R}_{\dot{h}} \\ \ddot{R}_n & \ddot{R}_{\dot{n}} & \ddot{R}_e & \ddot{R}_{\dot{e}} & \ddot{R}_h & \ddot{R}_{\dot{h}} \\ \dddot{R}_n & \dddot{R}_{\dot{n}} & \dddot{R}_e & \dddot{R}_{\dot{e}} & \dddot{R}_h & \dddot{R}_{\dot{h}} \\ R^{iv}_n & R^{iv}_{\dot{n}} & R^{iv}_e & R^{iv}_{\dot{e}} & R^{iv}_h & R^{iv}_{\dot{h}} \\ R^{v}_n & R^{v}_{\dot{n}} & R^{v}_e & R^{v}_{\dot{e}} & R^{v}_h & R^{v}_{\dot{h}} \\ R^{vi}_n & R^{vi}_{\dot{n}} & R^{vi}_e & R^{vi}_{\dot{e}} & R^{vi}_h & R^{vi}_{\dot{h}} \end{bmatrix}.$$

By the same method of row reduction just employed, this matrix will reduce to

and $\dot{n}$; combining those results will lead to the first observer matrix $\underset{\sim}{J}_1$ for the R observation:

$$\underset{\sim}{J}_1 = \begin{bmatrix} R_n & 0 & R_e & 0 & R_h & 0 \\ \dot{R}_n & \dot{R}_{\dot{n}} & \dot{R}_e & \dot{R}_{\dot{e}} & \dot{R}_h & \dot{R}_{\dot{h}} \\ \ddot{R}_n & \ddot{R}_{\dot{n}} & \ddot{R}_e & \ddot{R}_{\dot{e}} & \ddot{R}_h & \ddot{R}_{\dot{h}} \\ \dddot{R}_n & \dddot{R}_{\dot{n}} & \dddot{R}_e & \dddot{R}_{\dot{e}} & \dddot{R}_h & \dddot{R}_{\dot{h}} \\ R^{iv}_n & R^{iv}_{\dot{n}} & R^{iv}_e & R^{iv}_{\dot{e}} & R^{iv}_h & R^{iv}_{\dot{h}} \\ R^{v}_n & R^{v}_{\dot{n}} & R^{v}_e & R^{v}_{\dot{e}} & R^{v}_h & R^{v}_{\dot{h}} \end{bmatrix}.$$

Note that the last equation of each set of seven partial derivatives was not required at this time; they will become necessary in the case of $\dot{R}$. The lower rows of this matrix are linear combinations of the rows above them; to simplify the matrix for the purpose of evaluating its determinant and testing it for positive or negative definiteness, it must be row-reduced by subtracting each of the higher rows (multiplied by the proper constant) from the lower rows as follows:

$$\text{Row } 6 - \frac{R^{v}}{R}\,\text{Row}1 - \frac{5R^{iv}}{R}\,\text{Row}2 - \frac{10\dddot{R}}{R}\,\text{Row}3 - \frac{10\ddot{R}}{R}\,\text{Row}4 - \frac{5\dot{R}}{R}\,\text{Row}5\,;$$

$$\text{Row}5 - \frac{R^{iv}}{R}\,\text{Row}1 - \frac{4\dddot{R}}{R}\,\text{Row}2 - \frac{6\ddot{R}}{R}\,\text{Row}3 - \frac{4\dot{R}}{R}\,\text{Row}4\,;$$

$$\text{Row}4 - \frac{\dddot{R}}{R}\,\text{Row}1 - \frac{3\ddot{R}}{R}\,\text{Row}2 - \frac{3\dot{R}}{R}\,\text{Row}3\,;$$

$$\text{Row}3 - \frac{\ddot{R}}{R}\,\text{Row}1 - \frac{2\dot{R}}{R}\,\text{Row}2\,;$$

$$\text{Row}2 - \frac{\dot{R}}{R}\,\text{Row}1\,.$$

Taking the partial derivatives of the first set of equations with respect to $\dot{n}$,

$$R R_{\dot{n}} = 0,$$

$$R \ddot{R}_{\dot{n}} + R_{\dot{n}} \dot{R} = n,$$

$$R \dddot{R}_{\dot{n}} + R_{\dot{n}} \ddot{R} + 2\dot{R} \ddot{R}_{\dot{n}} = 2\dot{n},$$

$$R \ddddot{R}_{\dot{n}} + R_{\dot{n}} \dddot{R} + 3\dot{R} \dddot{R}_{\dot{n}} + 3\ddot{R}_{\dot{n}} \ddot{R} = 3a_N,$$

$$R R^{v}_{\dot{n}} + R_{\dot{n}} R^{iv} + 4\dot{R} \ddddot{R}_{\dot{n}} + 4\dddot{R}_{\dot{n}} \dot{R} + 6\ddot{R} \ddot{R}_{\dot{n}} = 0,$$

$$R R^{vi}_{\dot{n}} + R_{\dot{n}} R^{v} + 5\dot{R} R^{v}_{\dot{n}} + 5\ddot{R}_{\dot{n}} R^{iv} + 10\dddot{R} \dddot{R}_{\dot{n}} + 10\ddot{R}_{\dot{n}} \ddot{R} = 0,$$

$$R R^{vii}_{\dot{n}} + R_{\dot{n}} R^{vi} + 6\dot{R} R^{vi}_{\dot{n}} + 6\ddot{R}_{\dot{n}} R^{v} + 15\ddot{R} R^{iv}_{\dot{n}} + 15\dddot{R}_{\dot{n}} R^{iv} + 20\dddot{R} \dddot{R}_{\dot{n}} = 0.$$

Solve for the highest order partial derivatives as before.

$$R_{\dot{n}} = 0,$$

$$\dot{R}_{\dot{n}} = n/R,$$

$$\ddot{R}_{\dot{n}} = \frac{2}{R}\left(\dot{n} - \dot{R} \ddot{R}_{\dot{n}}\right),$$

$$\dddot{R}_{\dot{n}} = \frac{3}{R}\left(a_N - \ddot{R} \ddot{R}_{\dot{n}} - \dot{R} \ddot{R}_{\dot{n}}\right),$$

$$R^{iv}_{\dot{n}} = \frac{1}{R}\left(-4\dddot{R} \dot{R}_{\dot{n}} - 6\ddot{R} \ddot{R}_{\dot{n}} - 4\dot{R} \dddot{R}_{\dot{n}}\right),$$

$$R^{v}_{\dot{n}} = \frac{1}{R}\left(-5R^{iv} \dot{R}_{\dot{n}} - 10\dddot{R} \ddot{R}_{\dot{n}} - 10\dddot{R}_{\dot{n}} \ddot{R} - 5\dot{R} R^{iv}_{\dot{n}}\right),$$

$$R^{vi}_{\dot{n}} = \frac{1}{R}\left(-6R^{v} \dot{R}_{\dot{n}} - 15R^{iv} \ddot{R}_{\dot{n}} - 20\dddot{R}_{\dot{n}} \ddot{R} - 15\ddot{R} R^{iv}_{\dot{n}} - 6\dot{R} R^{v}_{\dot{n}}\right).$$

Obviously, partial differentiation with respect to e and $\dot{e}$ and h and $\dot{h}$ will fcllow the pattern just established for n

Taking the partial derivative of each of the above equations with respect to n,

$$R\frac{\partial R}{\partial n} = n,$$

$$R\frac{\partial \dot{R}}{\partial n} + \frac{\partial R}{\partial n}\dot{R} = \dot{n},$$

$$R\frac{\partial \ddot{R}}{\partial n} + \frac{\partial R}{\partial n}\ddot{R} + 2\dot{R}\frac{\partial \dot{R}}{\partial n} = a_N,$$

$$R\frac{\partial \dddot{R}}{\partial n} + \frac{\partial R}{\partial n}\dddot{R} + 3\frac{\partial \dot{R}}{\partial n}\ddot{R} + 3\dot{R}\frac{\partial \ddot{R}}{\partial n} = 0,$$

$$R\frac{\partial R^{iv}}{\partial n} + \frac{\partial R}{\partial n}R^{iv} + 4\dot{R}\frac{\partial \dddot{R}}{\partial n} + 4\frac{\partial \dot{R}}{\partial n}\dddot{R} + 6\ddot{R}\frac{\partial \ddot{R}}{\partial n} = 0,$$

$$R\frac{\partial R^{v}}{\partial n} + \frac{\partial R}{\partial n}R^{v} + 5\dot{R}\frac{\partial R^{iv}}{\partial n} + 5\frac{\partial \dot{R}}{\partial n}R^{iv} + 10\ddot{R}\frac{\partial \dddot{R}}{\partial n} + 10\frac{\partial \ddot{R}}{\partial n}\dddot{R} = 0,$$

$$R\frac{\partial R^{vi}}{\partial n} + \frac{\partial R}{\partial n}R^{vi} + 6\dot{R}\frac{\partial R^{v}}{\partial n} + 6\frac{\partial \dot{R}}{\partial n}R^{v} + 15\ddot{R}\frac{\partial R^{iv}}{\partial n} + 15\frac{\partial \ddot{R}}{\partial n}R^{iv} + 20\dddot{R}\frac{\partial \ddot{R}}{\partial n} = 0.$$

Solving for the highest order derivative in each equation,

$$\frac{\partial R}{\partial n} = R_n = n/R,$$

$$\frac{\partial \dot{R}}{\partial n} = \dot{R}_n = \frac{1}{R}(n - \dot{R}R_n),$$

$$\frac{\partial \ddot{R}}{\partial n} = \ddot{R}_n = \frac{1}{R}(a_N - \ddot{R}R_n - 2\dot{R}\dot{R}_n),$$

$$\frac{\partial \dddot{R}}{\partial n} = \dddot{R}_n = \frac{1}{R}(-\dddot{R}R_n - 3\ddot{R}\dot{R}_n - 3\dot{R}\ddot{R}_n),$$

$$\frac{\partial R^{iv}}{\partial n} = R^{iv}_n = \frac{1}{R}(-R^{iv}R_n - 4\dddot{R}\dot{R}_n - 6\ddot{R}\ddot{R}_n - 4\dot{R}\dddot{R}_n)$$

$$\frac{\partial R^{v}}{\partial n} = R^{v}_n = \frac{1}{R}(-R^{v}R_n - 5R^{iv}\dot{R}_n - 10\dddot{R}\ddot{R}_n - 10\ddot{R}\dddot{R}_n - 5\dot{R}R^{iv}_n)$$

$$\frac{\partial R^{vi}}{\partial n} = R^{vi}_n = \frac{1}{R}(-R^{vi}R_n - 6R^{v}\dot{R}_n - 15R^{iv}\ddot{R}_n - 20\dddot{R}\dddot{R}_n - 15\ddot{R}R^{iv}_n - 6\dot{R}R^{v}_n).$$

APPENDIX A
DERIVATION OF OBSERVATION MATRICES

The following series of derivations follows the pattern established in Chapter 4 Section B for establishing the terms in the Jacobian observer matrices for the general case target. The accelerations are assumed to be piecewise constant (i.e. constant for each time step of a discrete observer); thus third and higher order derivatives of the position variables will be zero. The derivations are grouped by two's into R and $\dot{R}$, α and $\dot{\alpha}$, and β and $\dot{\beta}$ for the reason that many of the terms in their matrices are the same.

A. OBSERVER MATRICES FOR RANGE AND RANGE RATE

Consider first that in the rectangular coordinate system,

$$R^2 = n^2 + e^2 + h^2.$$

Differentiating this equation implicitly six times with respect to time,

$$R\dot{R} = n\dot{n} + e\dot{e} + h\dot{h},$$

$$R\ddot{R} + \dot{R}^2 = n a_N + \dot{n}^2 + e a_E + \dot{e}^2 + h a_H + \dot{h}^2,$$

$$R\dddot{R} + 3\dot{R}\ddot{R} = 3\dot{n} a_N + 3\dot{e} a_E + 3\dot{h} a_H,$$

$$R R^{IV} + 4\dot{R}\dddot{R} + 3\ddot{R}^2 = 3a_N^2 + 3a_E^2 + 3a_H^2,$$

$$R R^{V} + 5\dot{R} R^{IV} + 10\ddot{R}\dddot{R} = 0,$$

$$R R^{VI} + 6\dot{R} R^{V} + 15\ddot{R} R^{IV} + 10\dddot{R}^2 = 0.$$

simultaneous observations; and of missing detection altogether. By viewing the entire process start-to-finish as stochastic rather than deterministic, the problem ultimately achieves a true real-world significance. In [Ref. 3], Bar-Shalom has pulled together a wide variety of resources to analyze just this sort of situation in the general sense; the application of the principles discussed there for this particular problem would arguably generate several more reports as involved as this one.

On a higher level, the theoretical implications of the applicability (or limitations thereof) of the method of [Ref. 1] to this problem and others of equal difficulty might be discussed. Previous employment of this method has shown the utility of such observability testing in determining the lack of observability of the bearing-only target (BOT) for typical earth-borne radar and sonar applications. The complicated geometry of this problem has not yet yielded such complete conclusions; the potential exists, however. Another topic that might be explored further is the pervasive nature of the Jacobian matrix, which appears as part of the observability analysis; in the development of the nonlinear observer here and elsewhere, i.e. [Ref. 10], [Ref. 11], and [Ref. 12]; and again in the computation of the observer functions for the filter. Finally, the continuing effort must be made to resolve all these results, current and future, with the empirical evidence available of track observability and maintainability, taking into account both the capabilities of the sensor and the wiles of the target.

where

$$\psi_{n,e,h} = -\mathcal{Q}_{ne,h}\,\dot{\beta},$$

$$\dot{\psi}_{n,e,h} = -\mathcal{Q}_{n,e,h}\,\ddot{\beta} - \dot{\mathcal{Q}}_{n,e,h}\,\dot{\beta},$$

$$\ddot{\psi}_{n,e,h} = -\mathcal{Q}_{n,e,h}\,\dddot{\beta} - 2\dot{\mathcal{Q}}_{n,e,h}\,\ddot{\beta} - \ddot{\mathcal{Q}}_{n,e,h}\,\dot{\beta},$$

$$\dddot{\psi}_{n,e,h} = -\mathcal{Q}_{n,e,h}\,\beta^{iv} - 3\dot{\mathcal{Q}}_{n,e,h}\,\dddot{\beta} - 3\ddot{\mathcal{Q}}_{n,e,h}\,\ddot{\beta} - \dddot{\mathcal{Q}}_{n,e,h}\,\dot{\beta},$$

$$\psi^{iv}_{n,e,h} = -\mathcal{Q}_{n,e,h}\,\beta^{v} - 4\dot{\mathcal{Q}}_{n,e,h}\,\beta^{iv} - 6\ddot{\mathcal{Q}}_{n,e,h}\,\dddot{\beta} - 4\dddot{\mathcal{Q}}_{n,e,h}\,\ddot{\beta} - \mathcal{Q}^{iv}_{n,e,h}\,\dot{\beta},$$

$$\psi^{v}_{n,e,h} = -\mathcal{Q}_{n,e,h}\,\beta^{vi} - 5\dot{\mathcal{Q}}_{n,e,h}\,\beta^{v} - 10\ddot{\mathcal{Q}}_{n,e,h}\,\beta^{iv} - 10\dddot{\mathcal{Q}}_{n,e,h}\,\dddot{\beta} - 5\mathcal{Q}^{iv}_{n,e,h}\,\ddot{\beta} - \mathcal{Q}^{v}_{n,e,h}\,\dot{\beta}.$$

APPENDIX B

PROGRAM LISTING FOR THE SATELLITE-TARGET SIMULATION AND THE EKF IMPLEMENTATION

```
C       DECLARE ALL VARIABLES
          INTEGER I,J,K,FLAG1,FLAG2,COUNT1,COUNT2,L,M,N,INK
          REAL DT,PI,A0,DPHI,OMEGA,PHI,DENOM,DLATS,DLONGS
          REAL R0,RHOMAX,RHO,RS,NU,LATHAT,WN1,WN2,GGNOF,RS2
          REAL LATS(121),LONGS(121),TIME(121),LATT(121),AS2
          REAL RANGE(121),ALPHA(121),BETA(121),ASIG,BSIG,S4
          REAL X1(121),X2(121),X3(121),X4(121),PE(121),PN4
          REAL XHAT1(121),XHAT2(121),XHAT3(121),XHAT4(121)
          REAL P1(121),P3(121),P4(121),P9(121),PA(121),ESIG
          REAL XNHAT1,XNHAT2,XNHAT3,XNHAT4,PN1,INNOVA,RSIG
          REAL PN9,PNA,PNB,PNC,PND,PNE,G8,S7,S8,INNOVR,NSIG
          REAL PNF,RHOHAT,ALHAT,EHAT,BEHAT,DLADX1,DRHDLA,GC
          REAL DRHDNU,DNUDX1,DRALRH,DRHDX1,DRADX1,DNUDX3,Q2
          REAL DALDRH,DALDNU,DALDX1,DALDX3,DBEDRA,DBEDRH,Q3
          REAL H1,H2,H3,H4,A,B,C,DET,R1,R2,R3,R4,G1,G2,HS2
          REAL Q4,Q5,Q6,R5,R6,R7,R8,R9,RA,RB,RC,H5,H6,D,E,F
          REAL XG1(121),YG1(121),YG2(121),YG3(121),SSE(121)
          REAL XAVE1(121),XAVE2(121),XAVE3(121),XAVE4(121)
          REAL LONHAT,LONGT(121),PN3,S5,PF(121),PD(121),ES2
          REAL PB(121),PC(121),INNOVB,S1,S2,S3,G9,GA,GB,E1
          REAL NUHAT,DALDX3,DALDIA,DBEDX1,DBEDX3,XG2(121)
          REAL SSEBAR(121),E2,E3,E4,G3,G4,G5,G6,G7,Q1
          DOUBLE PRECISION DSEED

C       CONSTANTS
                                FLAG1=0
                                FLAG2=0
                                DT=.25
                                PI=3.1415926
                                A0=1.1065387
                                DPHI=PI/53.7248
                                OMEGA=PI/720.
                                R0=3438.
                                RS=4038.
                                RHOMAX=ACOS(R0/RS)
                                ASIG=PI/108000.
                                BSIG=PI/108000.
                                ESIG=.002
                                NSIG=.002
                                RSIG=.1
                                AS2=ASIG**2
                                BS2=BSIG**2
                                ES2=ESIG**2
                                NS2=NSIG**2
                                RS2=RSIG**2

C       OUTER OUTER LOOP FOR ALTERNATIVE OBSERVATIONS
          DO 86 INK=1,3
            DSEED=123486579.

C       OUTER LOOP FOR MONTE CARIO RUNS
          DO 92 I=1,121
            XAVE1(I)=0.
            XAVE2(I)=0.
            XAVE3(I)=0.
            XAVE4(I)=0.
            SSEBAR(I)=0.
 92       CONTINUE
```

```
      DO 94 N=1,20
C     INITIALIZE TIME, POSITIONS, MEASUREMENTS
                        TIME(1)=0.
                        LATS(1)=0.
                        LONGS(1)=0.
                        LATT(1)=45.*PI/180.
                        LONGT(1)=30.*PI/180.
                        RANGE(1)=0.
                        ALPHA(1)=0.
                        BETA(1)=0.
                        X1(1)=R0*LATT(1)
                        X2(1)=.3333333
                        X3(1)=R0*COS(LATT(1))*LONGT(1)
                        X4(1)=-.3333333
C     LOOP TO UPDATE TIME, POSITIONS, MEASUREMENTS
                      DO 10 I=2,121
                        K=I-1
                        TIME(I)=DT*FLOAT(K)
C     SATELLITE POSITION
          PHI=DPHI*TIME(I)
          DENOM=COS(PHI)**2+(CCS(A0)*SIN(PHI))**2
          DLONGS=DPHI*COS(A0)/DENOM-OMEGA
          DLATS=DPHI*SIN(A0)*CCS(PHI)/DENOM**.5
          LATS(I)=LATS(K)+DT*DIATS
          LONGS(I)=LONGS(K)+DT*DLONGS
C     TARGET POSITICN
          WN1=NSIG*GGNQF(DSEED)
          WN2=ESIG*GGNQF(DSEED)
          X1(I)=X1(K)+DT*X2(K)+DT**2*WN1/2.
          X2(I)=X2(K)+DT*WN1
          X3(I)=X3(K)+DT*X4(K)+DT**2*WN2/2.
          X4(I)=X4(K)+DT*WN2
          LATT(I)=X1(I)/R0
          LONGT(I)=X3(I)/(R0*CCS(LATT(I)))
C     MEASUREMENTS
          NU=LONGT(I)-LONGS(I)
          RHO=ACOS(SIN(LATT(I))*SIN(LATS(I))+COS(LATT(I))
     +          *COS(LATS(I))*COS(NU))
          IF (RHO.LE.RHOMAX) GC TO 30
            IF ((FLAG1.NE.1).OR.(FLAG2.NE.0)) GO TC 60
              COUNT2=K
              FLAG2=1

 60           RANGE(I)=0.
              ALPHA(I)=0.
              BETA(I)=0.
              GO TO 10

 30           IF (FLAG1.EQ.0) COUNT1=I
                FLAG1=1
              RANGE(I)=(R0**2+RS**2-2.*R0*RS*COS(RHO))**.5
     +                +RSIG*GGNQF(DSEED)
              ALPHA(I)=ASIN(COS(LATT(I))*SIN(NU)/SIN(RHO))
     +                +ASIG*GGNQF(DSEED)
                IF (LATT(I).LT.LATS(I)) ALPHA(I)=PI-ALPHA(I)
              BETA(I)=ASIN(R0*SIN(RHO)/RANGE(I))
     +                +BSIG*GGNQF(DSEED)

 10         CONTINUE
            M=COUNT2-COUNT1+1
C     ESTIMATION
C     TARGET NOT YET IN SIGHT
```

```
                              J=COUNT1-1
                              DO 40 I=1,J
                                XHAT1(I)=0.
                                XHAT2(I)=0.
                                XHAT3(I)=0.
                                XHAT4(I)=0.
 40       CONTINUE

C         TWO-POINT INITIALIZATION OF THE EKF
           J=COUNT1+1
           DO 80 I=COUNT1,J
             RHO=ASIN(RANGE(I)*SIN(BETA(I))/R0)
             LATHAT=ASIN(SIN(LATS(I))*COS(RHO)+COS(LATS(I))
     +                *SIN(RHO)*COS(ALPHA(I)))
             NU=ACOS((COS(RHO)-SIN(LATHAT)*SIN(LATS(I)))/
     +                (COS(LATHAT)*COS(LATS(I))))
               IF (ALPHA(I).GE.PI) NU=-NU
             LONHAT=LONGS(I)+NU
             XHAT1(I)=R0*LATHAT
             XHAT2(I)=0.
             XHAT3(I)=R0*COS(LATHAT)*LONHAT
             XHAT4(I)=0.

 80       CONTINUE
             XHAT2(J)=(XHAT1(J)-XHAT1(COUNT1))/DT
             XHAT4(J)=(XHAT3(J)-XHAT3(COUNT1))/DT
                              P1(J)=NS2
                              PD(J)=NS2/DT
                              P4(J)=2.*NS2/DT**2
                              P3(J)=ES2
                              PF(J)=ES2/DT
                              P9(J)=2.*ES2/DT**2
                              PA(J)=0.
                              PB(J)=0.
                              PC(J)=0.
                              PE(J)=0.

C         UPDATE THE EKF
                              J=J+1
                              DO 50 I=J,COUNT2
                                K=I-1

C         STATE AND COVARIANCE ESTIMATES
                                XNHAT1=XHAT1(K)+DT*XHAT2(K)
                                XNHAT2=XHAT2(K)
                                XNHAT3=XHAT3(K)+DT*XHAT4(K)
                                XNHAT4=XHAT4(K)
             PN1=P1(K)+2.*DT*PD(K)+DT**2*P4(K)+NS2*DT**4/4.
             PND=PD(K)+DT*P4(K)+NS2*DT**3/2.
             PN4=P4(K)+NS2*DT**2
             PN3=P3(K)+2.*DT*PF(K)+DT**2*P9(K)+ES2*DT**4/4.
             PNF=PF(K)+DT*P9(K)+ES2*DT**3/2.
             PN9=P9(K)+ES2*DT**2
             PNB=PB(K)+DT*(PE(K)+PA(K))+DT**2*PC(K)
             PNA=PA(K)+DT*PC(K)
             PNE=PE(K)+DT*PC(K)
             PNC=PC(K)

C         OBSERVER FUNCTIONS
             LATHAT=XNHAT1/R0
             LONHAT=XNHAT3/(R0*COS(LATHAT))
             NUHAT=LONHAT-LONGS(I)
             RHOHAT=ACOS(SIN(LATHAT)*SIN(LATS(I))+COS(LATHAT)
     +                *COS(LATS(I))*COS(NUHAT))
             RHAT=(R0**2+RS**2-2.*R0*RS*COS(RHOHAT))**.5
             ALHAT=ASIN(COS(LATHAT)*SIN(NUHAT)/SIN(RHOHAT))
               IF (LATHAT.LT.LATS(I)) ALHAT=PI-ALHAT
             BEHAT=ASIN(R0*SIN(RHOHAT)/RHAT)
             DLADX1=1./R0
```

```
      DRHDLA=(SIN(LATHAT)*COS(LATS(I))*COS(NUHAT)-
     +       COS(LATHAT)*SIN(LATS(I)))/SIN(RHOHAT)
      DRHDNU=COS(LATHAT)*COS(LATS(I))*SIN(NUHAT)/
     +       SIN(RHOHAT)
      DNUDX1=XNHAT3*SIN(LATHAT)/(R0*COS(LATHAT))**2
      DRHDX1=DRHDLA*DLADX1+DRHDNU*DNUDX1
      DRADRH=R0*RS*SIN(RHOHAT)/RHAT
      DNUDX3=1./(R0*COS(LATHAT))
      DRADX1=DRADRH*DRHDX1
      DRADX3=DRADRH*DRHDNU*DNUDX3
      DALDLA=-SIN(LATHAT)*SIN(NUHAT)/(COS(ALHAT)
     +       *SIN(RHOHAT))
      DALDRH=-COS(LATHAT)*SIN(NUHAT)*COS(RHOHAT)/
     +       (COS(ALHAT)*SIN(RHOHAT)**2)
      DALDNU=COS(LATHAT)*COS(NUHAT)/(COS(ALHAT)
     +       *SIN(RHOHAT))
      DALDX1=DALDLA*DLADX1+DALDRH*DRHDX1+DALDNU*DNUDX1
      DALDX3=(DALDRH*DRHDNU+DALDNU)*DNUDX3
      DBEDRA=-R0*SIN(RHOHAT)/(RHAT**2*COS(BEHAT))
      DBEDRH=R0*COS(RHOHAT)/(RHAT*COS(BEHAT))
      DBEDX1=DBEDRA*DRADX1+DBEDRH*DRHDX1
      DBEDX3=DBEDRA*DRADX3+DBEDRH*DRHDNU*DNUDX3
      H1=DRADX1
      H2=DALDX1
      H3=DBEDX1
      H4=DRADX3
      H5=DALDX3
      H6=DBEDX3
        IF (INK.EQ.2) H3=0.
        IF (INK.EQ.2) H6=0.
        IF (INK.EQ.3) H1=0.
        IF (INK.EQ.3) H4=0.

C     EKF GAINS
      A=RS2+PN1*H1**2+2.*PNB*H1*H4+PN3*H4**2
      B=PN1*H1*H2+PNB*(H1*H5+H2*H4)+PN3*H4*H5
      C=AS2+PN1*H2**2+2.*PNB*H2*H5+PN3*H5**2
      D=PN1*H1*H3+PNB*(H1*E6+H3*H4)+PN3*H4*H6
      E=PN1*H2*H3+PNB*(H2*H6+H3*H5)+PN3*H5*H6
      F=BS2+PN1*H3**2+2.*PNB*H3*H6+PN3*H6**2
      DET=A*C*F+2.*B*E*D-C*D**2-F*B**2-A*E**2
                        Q1=(C*F-E**2)/DET
                        Q2=(D*E-B*F)/DET
                        Q3=(A*F-D**2)/DET
                        Q4=(B*E-C*D)/DET
                        Q5=(E*D-A*E)/DET
                        Q6=(A*C-B**2)/DET
                        R1=H1*PN1+H4*PNB
                        R2=H2*PN1+H5*PNB
                        R3=H3*PN1+H6*PNB
                        R4=E1*PND+H4*PNE
                        R5=H2*PND+H5*PNE
                        R6=E3*PND+H6*PNE
                        R7=H1*PNB+H4*PN3
                        R8=E2*PNB+H5*PN3
                        R9=H3*PNB+H6*PN3
                        RA=E1*PNA+H4*PNF
                        RB=H2*PNA+H5*PNF
                        RC=E3*PNA+H6*PNF
                        G1=R1*Q1+R2*Q2+R3*Q4
                        G2=R1*Q2+R2*Q3+R3*Q5
                        G3=R1*Q4+R2*Q5+R3*Q6
                        G4=R4*Q1+R5*Q2+R6*Q4
                        G5=R4*Q2+R5*Q3+R6*Q5
                        G6=R4*Q4+R5*Q5+R6*Q6
                        G7=R7*Q1+R8*Q2+R9*Q4
                        G8=R7*Q2+R8*Q3+R9*Q5
                        G9=R7*Q4+R8*Q5+R9*Q6
                        GA=RA*Q1+RB*Q2+RC*Q4
```

```
                              GB=RA*Q2+RB*Q3+RC*Q5
                              GC=RA*Q4+RB*Q5+RC*Q6

C       STATE AND COVARIANCE UPDATES
            INNOVA=ALPHA(I)-ALHAT
            INNOVB=BETA(I)-BEHAT
            INNOVR=RANGE(I)-RHAT
            XHAT1(I)=XNHAT1+G1*INNOVR+G2*INNOVA+G3*INNOVB
            XHAT2(I)=XNHAT2+G4*INNOVR+G5*INNOVA+G6*INNOVB
            XHAT3(I)=XNHAT3+G7*INNOVR+G8*INNOVA+G9*INNOVB
            XHAT4(I)=XNHAT4+GA*INNOVR+GB*INNOVA+GC*INNOVB
                              S1=1.-G1*H1-G2*H2-G3*H3
                              S2=-G1*H4-G2*H5-G3*H6
                              S3=-G4*H1-G5*H2-G6*H3
                              S4=-G4*H4-G5*H5-G6*H6
                              S5=-G7*H1-G8*H2-G9*H3
                              S6=1.-G7*H4-G8*H5-G9*H6
                              S7=-GA*H1-GB*H2-GC*H3
                              S8=-GA*H4-GB*H5-GC*H6
                              P1(I)=S1*PN1+S2*PNB
                              PD(I)=S1*PND+S2*PNE
                              P4(I)=S3*PND+S4*PNE+PN4
                              P3(I)=S5*PNB+S6*PN3
                              PF(I)=S5*PNA+S6*PNF
                              P9(I)=S7*PNA+S8*PNF+PN9
                              PA(I)=S1*PNA+S2*PNF
                              PB(I)=S1*PNB+S2*PN3
                              PC(I)=S3*PNA+S4*PNF+PNC
                              PE(I)=S5*PND+S6*PNE

C       AVERAGED PERFORMANCE AND SQUARED ERROR FUNCTIONS
            XAVE1(I)=XAVE1(I)+XHAT1(I)/20.
            XAVE2(I)=XAVE2(I)+XHAT2(I)*3.
            XAVE3(I)=XAVE3(I)+XHAT3(I)/20.
            XAVE4(I)=XAVE4(I)+XHAT4(I)*3.
            E1=X1(I)-XHAT1(I)
            E2=X2(I)-XHAT2(I)
            E3=X3(I)-XHAT3(I)
            E4=X4(I)-XHAT4(I)
            SSE(I)=(E2**2+E4**2)*DT**2+E1**2+E3**2
            SSEBAR(I)=SSEBAR(I)+SSE(I)/20.
 50       CONTINUE

C       TARGET OUT OF SIGHT
                              J=COUNT2+1
                              DO 70 I=J,121
                                 K=I-1
                                 XHAT1(I)=XHAT1(K)+DT*XHAT2(K)
                                 XHAT2(I)=XHAT2(K)
                                 XHAT3(I)=XHAT3(K)+DT*XHAT4(K)
                                 XHAT4(I)=XHAT4(K)
 70                           CONTINUE
 94       CONTINUE

C       GRAPHICS
                             J=COUNT1+2
                             K=M-2
                             DO 90 I=J,COUNT2
                               L=I-J+1
                               IF (INK.NE.1) GO TO 84
                                 XG1(L)=XAVE3(I)
                                 YG1(L)=XAVE4(I)
                                 GO TO 90
 84                            IF (INK.NE.2) GO TO 82
                                 XG2(L)=XAVE3(I)
                                 YG2(L)=XAVE4(I)
                                 GO TO 90
 82                            XG3(L)=XAVE3(I)
                               YG3(I)=XAVE4(I)
```

```
90          CONTINUE
86        CONTINUE

          CALL LRGBUF
          CALL TEK618
          CALL PAGE(11.,8.5)
          CALL NOBRDR
          CALL AREA2D(8.5,6)
          CALL XNAME('EASTERLY MILES$',100)
          CALL YNAME('EASTERLY VELOCITY (KNOTS)$',100)
          CALL GRAF(1262.,1.,1272.,-21.,1.,-13.)
          CALL LINES('RANGE, ALPHA, AND BETA$',IPAK,1)
          CALL LINES('RANGE AND ALPHA ONLY$',IPAK,2)
          CALL LINES('ALPHA AND BETA ONLY$',IPAK,3)
          XW=XLEGND(IPAK,3)
          YW=YLEGND(IPAK,3)
          XL=8.5-2.5-XW-.1
          YL=6.-.5-YW-.1
          CALL THKCRV(.02)
          CALL CURVE(XG1,YG1,K,4)
          CALL DASH
          CALL CURVE(XG2,YG2,K,4)
          CALL RESET('DASH')
          CALL DOT
          CALL CURVE(XG3,YG3,K,4)
          CALL RESET('DOT')
          CALL RLVEC(1262.,-20.,1272.,-20.,0000)
          CALL LEGEND(IPAK,3,XL,YL)
          CALL ENDPL(0)
          CALL DONEPL
                              STOP
                              END
```

LIST OF REFERENCES

1. Hwang, C.S. and R.R. Mohler, "Nonlinear Observability and Mixed Coordinate Bearing-Only Signal Processing", Proc. 23rd IEEE Conf. Decision and Control, Las Vegas, 1984.

2. Kirk, D.E., Optimal Control Theory, Prentice-Hall, Englewood Cliffs, N.J., 1970.

3. Bar-Shalom, Y., Multi-Target Tracking, Academic Press, New York, to appear.

4. Fowles, G.R., Analytical Mechanics, Holt, Rinehart, and Winston, New York, 1977.

5. Eisele, J.A. and K. Nichols, Orbital Mechanics of General Coverage Satellites, U.S. Naval Research Laboratory, Washington D.C., 1976.

6. Eisele, J.A., Astrodynamics, Rockets, Satellites, and Space Travel, National Book Company, Washington D.C., 1967.

7. Hwang, C.S., and R.R. Mohler, Observability and Information in Nonlinear Processing, to appear.

8. Kirk, D.E., Optimal Estimation: An Introduction to the Theory and Applications, Naval Postgraduate School Class Notes, 1975.

9. Maybeck, P.S., Stochastic Models, Estimation and Control (Vol. 3), Academic Press, New York, 1982.

10. Kolodziej, W.J., and R.R. Mohler, "State Estimation and Control of Conditionally Linear Systems", SIAM J. Control and Opt., Vol. 23, to appear 1985.

11. Hsu, C.S., and R.R. Mohler, "Design of Bilinear Observers and Estimators", in Applied Digital Control, (S. Tzafestas, ed.), North Holland, Amsterdam, to appear 1985.

12. Halamani, T.A., R.R. Mohler, and W.J. Kolodziej, "A Two-Step Bilinear Filtering Operation", IEEE Trans. on ASSP, 1984.

BIBLIOGRAPHY

Bate, R.R., D.D. Mueller, and J.E. White, Fundamentals of Astrodynamics, Dover Publications, New York, 1971.

Burdick, D.L., Probability Analysis of the Performance of Radar Satellite Correlation Algorithms, Naval Ocean Systems Center, San Diego, 1983.

Cline, J.K., and D.C. Toretta, "Aircraft Track Initiation with Space-Based Radar", IEEE EASCON Conference, 1983.

Halawani, T.U., W.J. Kolodziej, and R.R. Mohler, "On a Suboptimal Nonlinear Filter", Proc. 22nd IEEE Conf. Decision and Control, San Antonio, 1983.

INITIAL DISTRIBUTION LIST

		No. Copies
1.	Defense Technical Information Center Cameron Station Alexandria, Virginia 22314	2
2.	Superintendent ATTN: Library, Code 0142 Naval Postgraduate School Monterey, California 93943	2
3.	Department Chairman, Code 62 Dept. of Electrical and Computer Engineering Naval Postgraduate School Monterey, California 93943	1
4.	Professor Ronald R. Mohler, Code 62Mz Dept. of Electrical and Computer Engineering Naval Postgraduate School Monterey, California 93943	2
5.	Professor Paul H. Moose, Code 62Me Dept. of Electrical and Computer Engineering Naval Postgraduate School Monterey, California 93943	1
6.	Professor Yaakov Bar-Shalom Department of Electrical Engineering University of Connecticut Storrs, Connecticut 06268	1
7.	Captain Leon Wardle, USN Naval Electronics Systems Command Headquarters Washington, DC 20360	1
8.	Lieutenant Shelley Mort, USN, SMC 1291 Dept. of Electrical and Computer Engineering Naval Postgraduate School Monterey, California 93943	1
9.	Lieutenant Robert E. Lee Bond, USN 144 Yellowstone Drive Pittsburgh, Pennsylvania 15235	3

END

FILMED

8-85

DTIC